An Adsorption Based Cooling Solution for Electronics used in Thermally Harsh Environments

A dissertation
Presented to
The Academic Faculty

by

Ashish Sinha

In Partial Fulfillment
of the Requirements for the Degree
'Doctor of Philosophy' in the
George W Woodruff School of Mechanical Engineering

Georgia Institute of Technology, Atlanta

December 2010

An Adsorption Based Cooling Solution for Electronics used in Thermally Harsh Environments

Approved by:

Dr. Yogendra Joshi, Advisor
School of Mechanical Engineering
Georgia Institute of Technology

Dr. Sankar Nair
School of Chemical and Biomolecular Engineering
Georgia Institute of Technology

Dr. Srinivas Garimella
School of Mechanical Engineering
Georgia Institute of Technology

Dr. Sotira Z. Yiacoumi
School of Civil and Environmental Engineering
Georgia Institute of Technology

Dr. Mostafa Ghiaasiaan
School of Mechanical Engineering
Georgia Institute of Technology

Date Approved: 27th August 2010

To
My younger brother
Vineet Sinha (tukku babu)

(Who helped me by all means)

And
My wife
Pragya Akhouri

(Who married me overlooking my career uncertainties)

Acknowledgements

I received immense support form a few people without whom my work would not have been possible. Among them, first of all, I want to acknowledge Dr Yogendra Joshi (my advisor) for his support and guidance throughout my graduate studies. Next, I would like to acknowledge the support received from Dr Bruce H Storm [currently with Kenda Capitals, formerly with Halliburton Energy Services] for providing valuable industrial insight and numerous discussions regarding the roadmap and scope of the project. Acknowledgements are also due to members of my thesis reading committee [Dr Srinivas Garimella, Dr Sankar Nair, Dr Seyed M Ghiaasiaan, Dr Sotira Yiacoumi] for valuable feedback at the PhD proposal stage. This helped me focus on a few important aspects that simplified my research work as well as made it more comprehensive.

My sincere acknowledgements are also reserved for the staff at ME Machine shop and Georgia Tech Research Institute (GTRI). John Graham, Nathan Flieg, John Pittman and Chat Huynh (all at ME Machine shop) helped me in fabricating parts for my experimental set up. Dennis Brown at GTRI was helpful in brazing steel and copper parts of the adsorption bed. He also generously took care of any subsequent leakage problems that would occur within a few weeks of the brazing.

Help in terms of technical inputs and lab hardware from past and present members of my research group has been critical to my research work. In this regard, I would like to acknowledge Juan-Carlos Jakaboski, Dr David Gerlach, Shivesh Suman, Dr YoonJo Kim, Dr Qihong Nie, Dr Yunhyeok Im, Carter Dietz, Dr Aniruddha Pal, Robert Wadell, Scott Wilson, Shankar Narayanan and Vivek Sahu.

During the course of my graduate studies, I have had the good fortunes of having some wonderful researchers as my office mates. Their professionalism has been an inspiration. Acknowledgements to Dr Thomas Beechem, Dr Roderick Jackson, Mark Gleva and Dr Jeff Rambo.

The encouragement and support I received from a few friends at Georgia Tech often helped me de-stress myself. Special note of thanks to Shubham Saxena, Subrahmanyam Kalyanasundaram, Kamlesh Nair, Sumit Mishra and Varun for providing me with good company.

Finally, I would like to acknowledge the immense support I received from my parents (papa and mummy) and my younger brother. They have seen me through lots of difficult situations and patiently waited for me to earn my doctorate degree. They always had words of encouragement for me and wished me luck every time they found me in a challenging situation.

Table of Contents

List of Tables

List of Figures

List of Symbols

COP	Coefficient of Performance
cp	Specific Heat Capacity (J kg^{-1} K^{-1})
G	Geometric Factor of the TE device. Ratio of area to length of a TE junction. (m)
ΔH	Heat of adsorption (J)
h	Enthalpy (J kg^{-1})
I	Current (Ampere)
M, m	Mass (Kg)
N	Number of thermo-electric junctions in a TE device.
num	Number of TE devices sandwiched between adsorbent beds
P, p	Pressure (milibars, 1 bar = 100 kPa)
Pow	Power (Watts)
Q	Heat (j)
q_c, q_h	Rate of heat transfer (Watts) associated with cold and hot face of TE device respectively
R	Universal gas constant (J kg^{-1} K^{-1})
R_{th}	Thermal Resistance (K W^{-1})
T	Temperature- (K)
t	Time
U	Product of convective heat transfer coefficient and surface area (W K^{-1})
V	Vapor mass
Volt	Voltage (V)
w	Water content (mass/ mass)
i	Inert mass ratio (= inert thermal mass/ active thermal mass)

Greek symbols

Ω	Electrical resistance (Ohms)
λ	Thermal mass (J K^{-1}); also a dimensionless quantity in chapter 7

Subscripts

ads	Adsorption
b	Pertaining to adsorbent beds
cond, c	Condenser
c1	Pertaining to cold face of Thermoelectric device
des	Desorption
evap, e	Evaporator
f	Fluid
g	Gas
h1	Pertaining to hot face of Thermoelectric device
i, j	Pertaining to bed 'i' and 'j'
i_te	Referring to interface between bed 'i' and thermoelectric device
j_te	Referring to interface between bed 'j' and thermoelectric device
p_ads,p_des	Primary adsorption and primary desorption
r	Recovery
s_ads,s_des	Secondary adsorption and secondary desorption
TE, te	Thermoelectric
TEA, tea	Thermoelectric Adsorption
v	Vapor
z	Zeolite

Summary

Industries such as automobiles, oil exploration, military hardware, etc often deal with harsh environment (temperatures 150 ^{0}C- 200 ^{0}C), which makes it difficult to use conventional electronics for tasks such as performance monitoring, and data acquisition. Commercial-off-the-shelf electronics can survive up to 125 ^{0}C, hence the electronics currently used are pre-screened for the desired temperature and assembled with or without cooling systems that are limited in cooling capacity and/ or need to be reset/ recharged. This offsets cost benefits and hinders continuous operation. While high temperature compatible electronics could provide a solution in future, immediate concerns could be addressed by compact thermal management systems that should work without having to be reset and require less maintenance (human interference during system operation must be ruled out). Also, the system should be scalable to smaller sizes without loss of performance.

In this backdrop this research aims at realization of an adsorption based cooling system for evaporator temperatures in the range of 140 ^{0}C-150 ^{0}C, and heat rejection temperature in the range of 160 ^{0}C-200 ^{0}C. Adsorption cooling systems have few moving parts, and the use of ThermoEelectric (TE) devices to regenerate heat of adsorption in between adsorbent beds enhances the compactness and performance efficiency of the overall 'ThermoElectric-Adsorption' (TEA) system. The work presented identifies the challenges involved and respective technical solutions for high temperature application. Performance deterioration of TE device at high temperatures (> 150 ^{0}C) and its thermal operating limits have been identified as major challenges, and a two-step adsorption cycle proposed to accommodate the thermal needs of the TE device. Methods of operation have

been proposed that enable the system to manage varying thermal load while accommodating TE device thermal operating requirements. An experimental set up was fabricated to demonstrate operation of the TEA cooling system at high temperature. Mathematical system models were also developed to benchmark experimental results.

Also, it is worth noting that TEA cooling system comprises of TE and Adsorption cooling systems. A TE cooler can be a compact thermal management system in its own right. Hence a comparison of the performance of TEA and TE cooling systems has also been presented.

This research will help in achieving a reliable and compact high temperature cooling system that should extend the working envelope of existing conventional electronics.

CHAPTER 1: Introduction

This chapter describes the relevance of electronics in thermally harsh environment and the need for developing thermal management solutions for regions characterized by high temperature (> 150 ^{0}C), mechanical shock and inaccessibility. Motivation for the research undertaken has been set forth and a glimpse of the structure and content of the dissertation document has been described in the last two paragraphs.

1.1 Electronics in thermally harsh environment

In several industries application of electronic equipments/ sensors is desired in regions that can be termed as 'thermally harsh' (temperature above 125 ^{0}C is widely considered as 'harsh', since it is outside the usually acceptable limit for silicon based devices [1]-[3]). Typical applications include sensing and processing of data in combustion chambers, nuclear reactors, turbine exhausts, and oil wells. Fig. 1-1 provides a list of industries with temperature range for respective harsh regions. Fig. 1-2 illustrates the use of electronics in oil drilling operation at depths of the order of thousands of feet. Application of electronics for data acquisition during oil exploration helps mitigate risk factors associated with drilling operations [6]- [11]. Fig. 1-3 and Table 1-1 describe the tasks carried out by various electronic modules. Developments such as gradual shift from hydraulics to 'fly by wire' in aerospace and automotive industries, the need to dig deeper for oil exploration and the constant shift from fossil fuel to electric driven vehicles that require more electronics, have underlined the need to use electronics in thermally harsh environments ([4], [5], [12], [14], [15]).

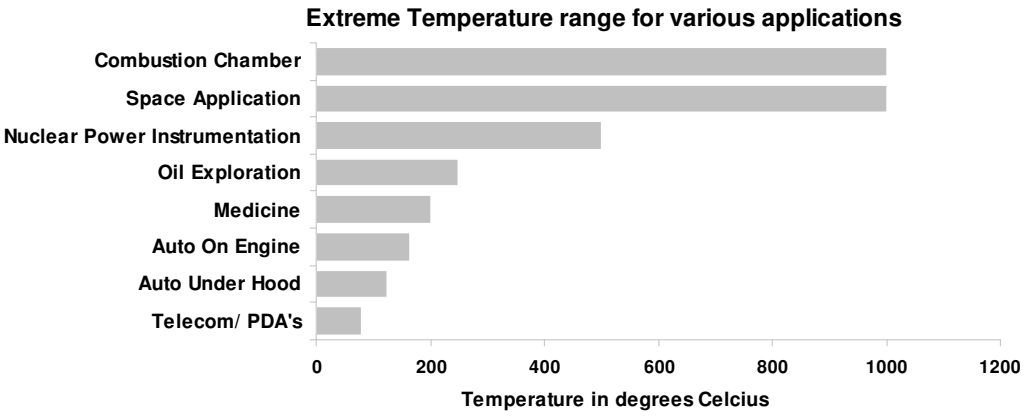

Fig. 1-1 Temperature range for various electronics applications [1]-[2]-[4]

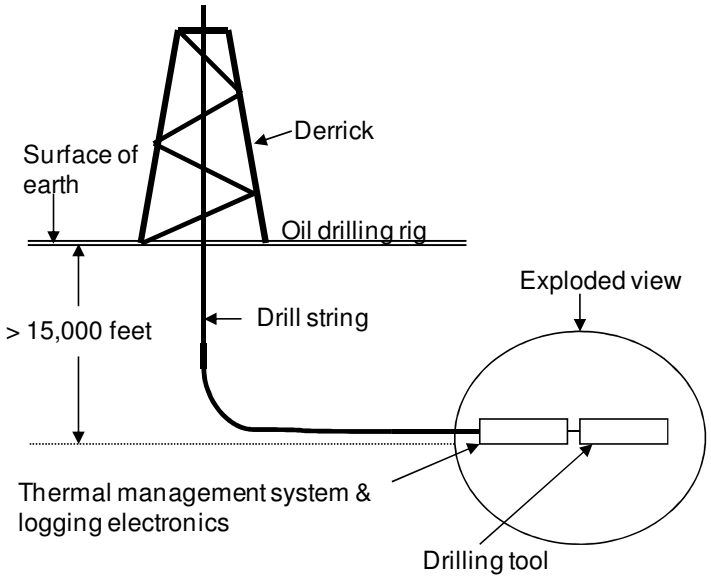

Fig. 1-2 Schematic of oil drilling operation [5]. Heat source (heat dissipating electronics to be cooled) remains in harsh and inaccessible conditions, thus necessitating an accompanying thermal management system.

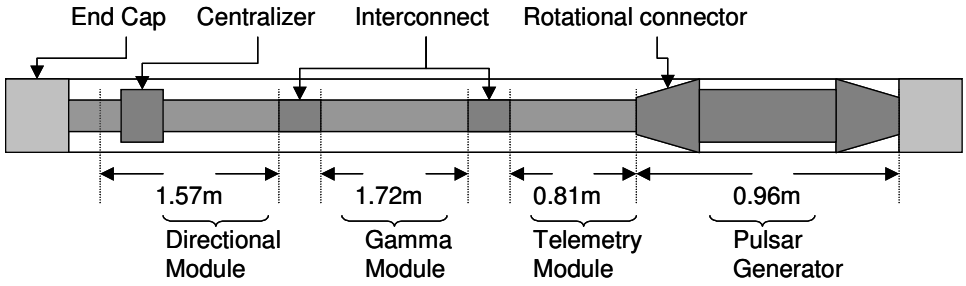

Fig. 1-3 Schematic of a 'Measurement While Drilling' tool used to capture oil well data during the drilling operation. Various modules process data that is transmitted to ground stations using mud pulses ([12], [13]). Diagram not to scale.

Table 1-1 Various modules and their function in a 'Measurement While Drilling' tool ([12], [13], [14]).

Modules	*Function*
Telemetry	Stores data and conditions it for transmission.
Directional	Compares the drill direction with earth's magnetic field
Gamma	Sends out and receives gamma ray signals to capture rock data
Battery	High temperature lithium batteries to power other modules.
Pulse generator	Generates pressure pulses in the out-flowing mud to communicate with ground station.

1.2 Motivation for development of novel thermal management techniques

Silicon based electronics, however, are unsuitable for application in environments where temperatures exceed 125 ^{0}C [4]. Failure modes include change in resistance, current leakage, increased electro-migration of metallized layers, dielectric breakdown, and increased mechanical stress due to thermal expansion and solder meltdown ([4], [16]). Several other materials exist by which electronics chip can be made (ref: Table 1-2), however inadequate packaging technologies come as a major hindrance. Developing packaging technology for hotter environments presents a significant challenge ([4], [18]-[22]). A setback to high temperature electronics research is the lack of concerted effort among various industries due to varying requirements. While a temperature of 125 ^{0}C to 200 ^{0}C may be 'harsh' enough for the auto industry, the geothermal industry encounters temperatures in excess of 250 ^{0}C [4], [23].

Table 1-2 Semiconductor materials for use at various temperature ranges [2], [17].

Semiconductor	*Temperature range in ^{o}C*
Flip Chip Silicon	Room temperature-150
Silicon on Insulator	150-300
Gallium Arsenide	300-350
Silicon Carbide	350-700
Gallium Nitride	700-800
Diamond	800-1100

The easy solution of placing the electronics far from the high temperature environment and connecting it with cables to transducers in hotter regions, often leads to noise pick up and safety issues [24]. Most industries currently work around the non availability of high temperature compatible electronics by prescreening available electronics ([25], [26], [27]) for high temperature survivability and by using custom made electronic modules ([13], [28]-[35]). While replacement of silicon-based components with materials better suited to high temperature environments, such as Silicon Carbide and Gallium Nitride ([2], [36], [37]) can provide a potential long-term solution to this problem, in the interim, localized thermal management can help implement conventional silicon based electronics in a thermally harsh environment [38]. A 66% increase in power dissipation per unit area is projected by 2018, for electronics used in harsh environments [39], thus further stressing on the need for cooling solutions for harsh environment electronics.

While it has been recognized that complex cooling systems will be needed for continuous operation at high temperatures [40], the development of electronics cooling systems that could reliably work at high temperature has been slow. Harsh environment applications require the thermal management system to be resistant to high temperature, shock, and vibrations and be reliable enough to work for long durations without human interference. Also, space is often a premium and the system must be compact enough to fit into electronic enclosures. These requirements could be waived if it were possible to place the cooling system far from the heat source and thermally connect the evaporator with heat source by lengthy heat exchanger fluid loop. An idea on similar lines has been described in US patent 4,248,298 [41], where a cooling fluid is pumped down through a tubing to the electronics that are placed few feet above drilling tool in an oil well, however it is difficult to implement. Also, the extreme inaccessibility of the heat source as in the case of oil drilling

operations (as shown in Fig. 1-2) makes it difficult to place the cooling system far from heat source.

These requirements present unusual challenges for conventional cooling techniques, for instance, the system must have few moving parts for greater reliability in the face of mechanical shocks and inaccessibility. Also, the system must be easy to miniaturize without loss of performance. Vapor compression systems based on mechanical compressors, such as centrifugal and reciprocating, have several moving parts which makes them less desirable in environments prone to shock and vibrations such as oil well. Such systems also suffer from increased irreversibility due to miniaturization ([42], [43], [44], [45]). Passive cooling technologies, such as phase change material heat storage, insulation, evaporative cooling, etc are limited in their ability to maintain electronics temperature below the ambient for a longer duration. *Jakaboski* [46] provides an extensive survey of passive thermal management techniques used in thermally harsh environments. Systems based on phase change heat storage will need to be recharged once phase change process is complete. Similarly systems based on evaporative cooling will need to have a means of replacing the cooling fluid once it has been depleted. These operations are often not feasible in harsh environment. Acoustic cooling systems, though compact, usually rely on a motor and crankshaft mechanism to produce standing waves, thus introducing moving parts and additional frictional heat load that would need to be pumped out along with electronics heat load [47]. The TE cooler offers a promising solution due to its compactness and low maintenance needs, but it proves inefficient for pumping heat through a higher temperature difference [48](temperature difference typically greater than 30 ^{0}C). Adsorption cooling systems have less moving parts, and such systems are scalable (i.e. can be miniaturized without loss of performance ([42], [45])), however, they are often bulky [49] due to the presence of fluid loops and heat

exchangers that are needed to bring about internal heat recovery and regeneration. A comparison of various cooling technologies has been presented by *Jakaboski* [46].

1.3 ThermoElectric Adsorption: A possible solution

In-spite of their individual limitations, a combination of thermoelectric cooler and adsorption system, as suggested by Gordon et al [42], could be made compact to meet the cooling needs with fewer moving parts. The TEA system comprises several TE devices sandwiched in between adsorbent beds. A TE device pumps heat from beds undergoing exothermic processes to beds undergoing endothermic processes, thus bringing about heat regeneration and recovery. This eradicates need for bulky heat exchangers, thus paving way for miniaturization of an adsorption heat pump. Detailed description of the working of such a system has been described in a subsequent section. *Gordon et al* [42] theoretically studied a TEA system for electronics cooling applications (with an evaporator temperature of 30 ^{0}C and a condenser temperature of 40 ^{0}C) and it was shown that the COP could be as high as 1.2. Subsequently *Ng et al* [45] performed experiments on the prototype of the system (for similar temperature conditions as Gordon et al) and obtained a COP of 0.7. The work done by Gordon et al [42] and Ng et al [45] confirm the viability of miniaturized adsorption heat pump with TE device assisted heat regeneration and recovery. Their work makes it attractive to investigate a similar system for high temperature application. A review of available literature on adsorption cooling presents very little information regarding their application for high temperature cooling (evaporator temperature > 150 ^{0}C and condenser temperature > 200 ^{0}C). Fig. 1-4 shows the evaporator, condenser and regeneration temperatures for adsorption based cooling applications available in the literature.

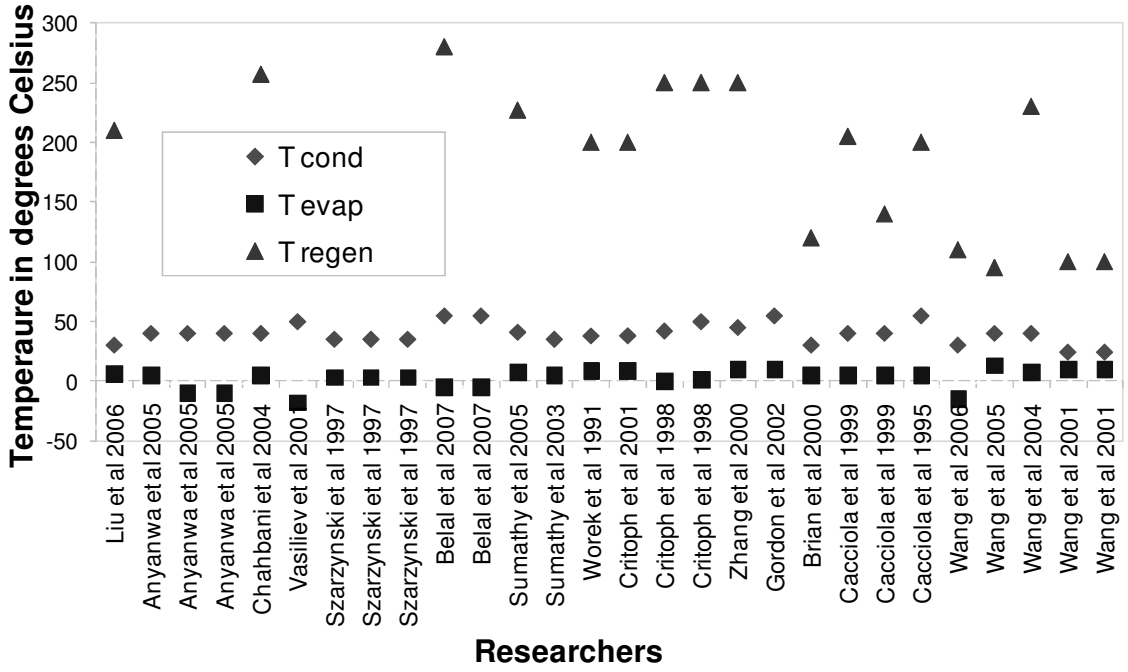

Fig. 1-4 Heat source (evaporator) and heat sink (condenser) temperature considered during research on various adsorption systems as reported in the literature [42], [50]-[67].

1.4 Introduction to structure and content of the dissertation

In the subsequent portions of the text, a detailed explanation of the working of TEA, TE and Adsorption chillers have been provided (CHAPTER 2). In CHAPTER 3 challenges with high temperature application of TEA chiller and ways to mitigate it have been discussed. Since high temperature application requires TE devices to work near their operating thermal limits, ensuring efficient and reliable performance of TE devices has been pointed out as a major challenge. A 'modified' cycle has been suggested (in place of 'conventional' adsorption cycle) to mitigate these challenges. It was discovered that a TEA system tuned to accommodate TE device requirements will only be able to manage a narrow range of cooling loads. Hence ways to make the system flexible to address varying cooling loads are discussed (in CHAPTER 4). CHAPTERs 5 and 6 describe the fabrication of experimental set up, development of mathematical model to mimic the TEA chiller, the

results obtained from experiments and simulations of the model and a comparison of the experimentally obtained and simulated results. The results indicate a moderate COP of 0.2 for the TEA chiller with a 'conventional' adsorption cycle, and a COP of 0.3 for the TEA chiller with a 'modified' adsorption cycle. In view of the low COP, a detailed theoretical analysis was done to maximize chiller performance (CHAPTER 7). This theoretical analysis proposes a novel method of operation that should help obtain COPs of above 1.0 from adsorption chillers. CHAPTER 7 also compares the performance of TE, Adsorption and TEA chillers and demarcates the suitability of TEA chiller vis-à-vis TE chillers. CHAPTER 8 contains concluding remarks. This is followed by several appendices that provide relevant information about the experimental set up.

CHAPTER 2: Thermoelectric, Adsorption and Thermoelectric Adsorption chillers

This chapter describes the working of thermoelectric (TE), adsorption and thermoelectric adsorption (TEA) chillers and also introduces terms like 'heat regeneration and recovery', 'cycle and switching time' etc that will be used in the following parts of this dissertation. The TEA chiller is a novel combination of TE and adsorption chillers. A description of the working of TE and adsorption chillers is essential to describe the working of TEA chillers.

2.1 Thermoelectric (TE) chiller

The (TE) chiller works on the Peltier effect [69]. It comprises rows of positively and negatively doped semi-conductor material such as Bi_2Te_3 (Bismuth Telluride). These rows are connected together by a copper plate as shown in Fig. 2-1. Electrically insulating ceramic surfaces that have good thermal conductivity, sandwich this arrangement. As current flows through the device in a particular direction, one of the junctions gets cold while the other gets hot. Heat is pumped from the cold junction to the hot junction.

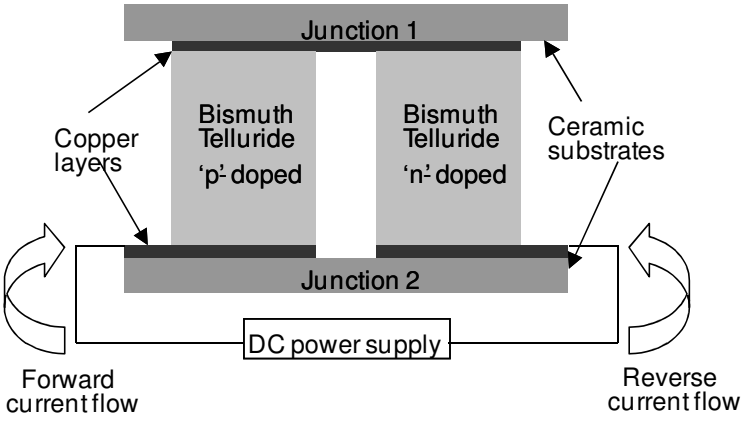

Fig. 2-1 Schematic diagram of a single thermocouple unit in a TE device. Junction 1 is cold during reverse current flow and hot during forward current flow.

The COP of the TE chiller can be expressed as the ratio of heat pumped at the cold side to the total electrical power input into the device. Eq. 2-1 describes the COP.

$$COP_{TE} = q_c / Pow_{TE} \quad \textbf{eq. 2.1}$$

Here q_c denotes the rate at which heat is pumped at the cold face of TE device and Pow_{TE} denotes the rate of electrical power input. Typical values of TE device COP for cooling applications vary from 0.1 to 0.4 [42] . Eq. 2.2 – 2.5 describe the relationship between 'q_c', heat released at the hot side 'q_h', 'Pow_{TE}' and various other parameters of a TE device. These equations can be found in the work by Simons et al [70].

$$q_c = 2N[(\alpha_p - \alpha_n)IT_{c1} - kG_1(T_{h1} - T_{c1}) - 0.5(I^2\rho / G_1)] = (T_c - T_{c1}) / R_{th} \quad \textbf{eq. 2.2}$$

$$Pow_{TE} = (Volt)I = 2N[(\alpha_p - \alpha_n)I(T_{h1} - T_{c1}) + (I^2\rho / G_1)] \quad \textbf{eq. 2.3}$$

$$q_h = Pow_{TE} + q_c \quad \textbf{eq. 2.4}$$

$$q_h = 2N[kG_1T_{c1} + (\alpha_p - \alpha_n)IT_{h1} - kG_1T_{h1} + 0.5I^2\rho / G_1] = (T_{h1} - T_h) / R_{th} \quad \textbf{eq. 2.5}$$

2.2 Adsorption chiller

An adsorption chiller comprises adsorbent beds, condenser, evaporator and fluid loop heat exchangers. Refrigerant vapors from evaporator are adsorbed in the adsorbent bed, pressurized from evaporator to condenser pressure by constant volume heating of the bed, and further desorbed to the condenser. The system usually comprises more than one beds, with two bed being the norm ([52], [42], [45], [56], [57], [67]). Multiple beds facilitate utilization of heat of adsorption and sensible heat that are internal to the system.

An adsorption cycle in a single bed comprises four stages. Adsorption, constant volume-heating, desorption and constant volume-cooling. Refrigerant vapors from evaporator are adsorbed at evaporator pressure during the adsorption phase and further

pressurized to the condenser pressure during the constant volume-heating phase. Once compressed the vapors are desorbed to condenser during the desorption phase. Further during the constant volume cooling that follows, the bed is cooled down to the evaporator pressure and made ready for the next cycle. Since the adsorption cycle comprises of two constant volume and two isobaric processes, it is usually described on a Clapeyron diagram that plots the log of pressure ln(P) in the adsorbent bed against the negative of reciprocal of temperature –(1/T). For ease of illustration, however, a plot of pressure against temperature is also widely used. Fig. 2-2 and Fig. 2-3 shows these different plots.

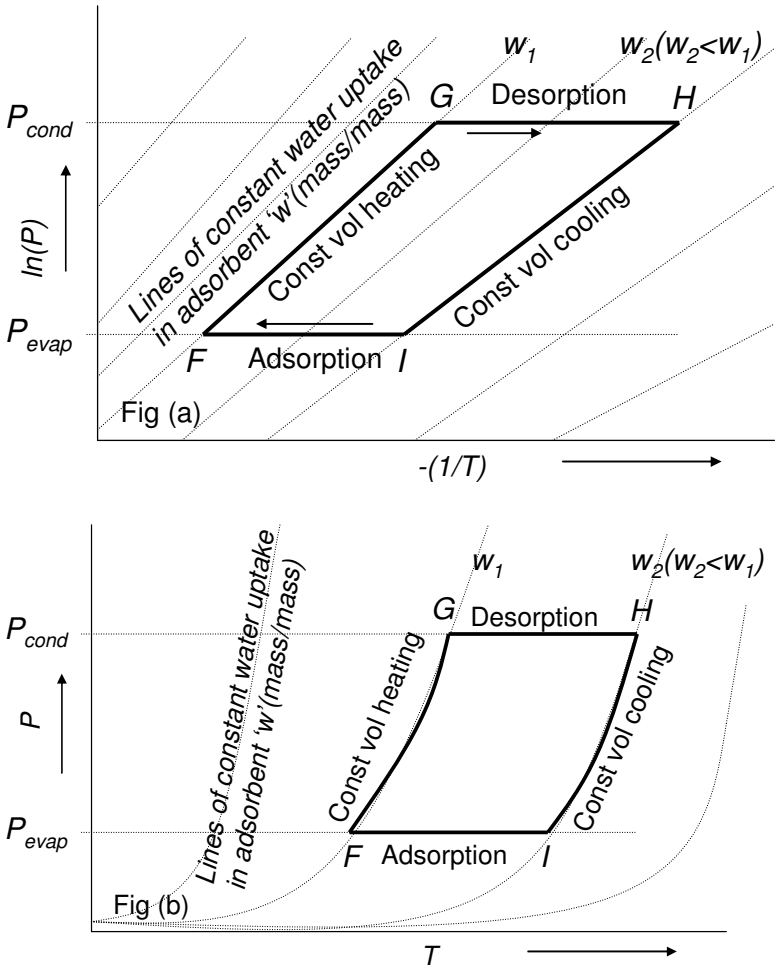

Fig. 2-2 Processes that comprise an adsorption cycle (Adsorption I-F; Constant volume heating F-G; Desorption G-H and Constant volume cooling H-I) shown on a ln(P)-(-1/T) plot (fig a) and P-T plot (fig b).

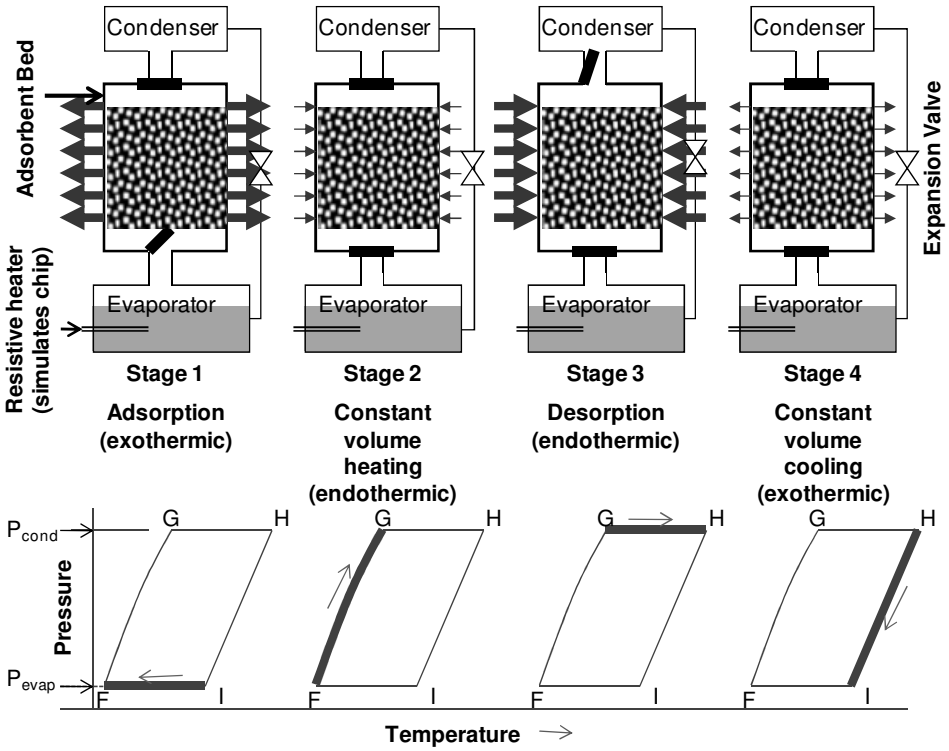

Fig. 2-3 Schematic and thermodynamic illustration of the four stages in adsorption cycle on a P-T diagram. Arrows shown along the edges of the adsorbent beds represent heat coming out OR being introduced into the beds. Thickness of arrow is representative of the magnitude of heat transfer.

In two bed systems, beds operating together, with appropriate phase difference in terms of cycle stages, provide a means of harnessing internal heat in the processes. The heat released during adsorption and constant volume cooling in one of the beds could be used for constant volume heating and desorption in another bed. The schematic of a two-bed adsorption heat pump is shown in Fig. 2-4. Valves 2 and 4 remain open (1 and 3 remain closed) during adsorption in bed 1 and desorption in bed 2. Further, during constant volume heating in bed 1 and constant volume cooling in bed 2, all the valves are closed. This is followed by desorption in bed 1 and adsorption in bed 2, during which valves 1 and 3 remain open and the rest are closed. Finally, bed 1 undergoes constant volume cooling and bed 2 undergoes constant volume heating. All the valves remain closed during this phase.

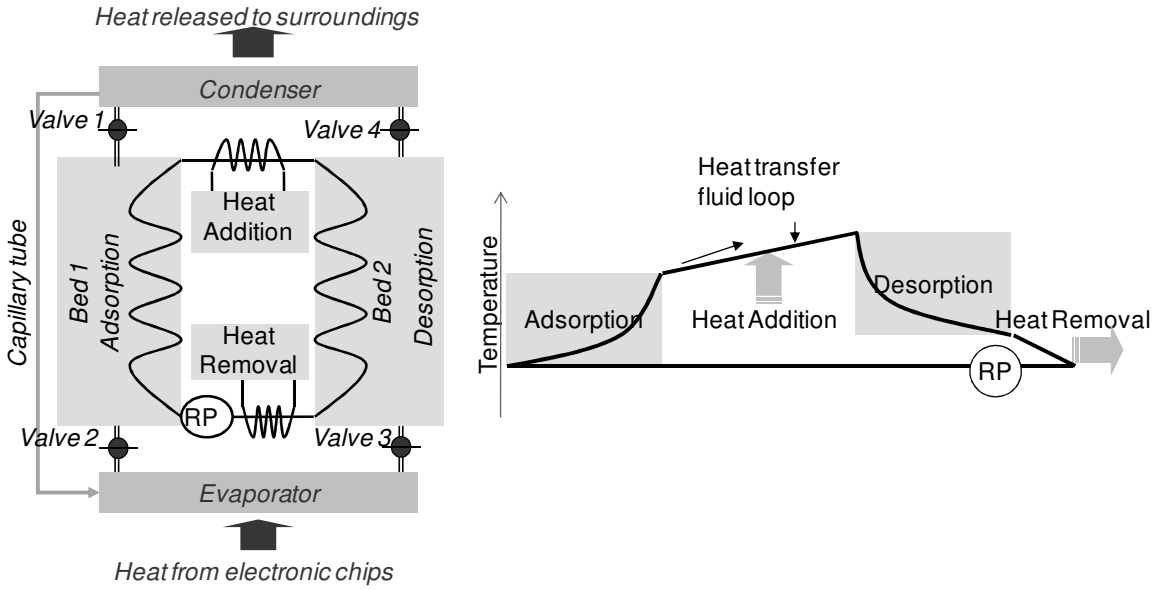

Fig. 2-4 (Left) Schematic of a two-bed adsorption heat pump. Heat recovery and regeneration are driven by a fluid loop – heat exchanger arrangement. (Right): Temperature variations in the heat transfer fluid as it passes through adsorbing bed, regenerative heat addition phase, desorbing bed and heat removal phase. A similar illustration can also be found in the work by Szarzynski et al [67].

Heat released during constant volume cooling is transferred to the bed undergoing constant volume heating by a fluid loop heat exchanger. Since this heat transfer is from a bed at higher temperature to a bed at lower temperature, it is termed '*heat recovery*'. The heat of desorption to the desorbing bed is provided by heating the heat exchanger fluid to regeneration temperature. This is done once the fluid exits the adsorbing bed after collecting heat of adsorption. Once the fluid exits the desorbing bed, it is cooled by a heat sink to a temperature below that of adsorbing bed. This cooling ensures removal of heat of adsorption from the adsorbing bed. A reversible fluid pump is used to reverse the direction of fluid flow as beds flip their role. The process of utilizing heat of adsorption for desorption process is termed '*heat regeneration'* as it involves transfer of heat from a lower temperature bed to a higher temperature bed. The adsorption heat pump is characterized by parameters such as '*cycle time'* and '*switching time'*. With various kinds of adsorption cycles in existence, there is little evidence of agreement in the scientific community about the use of

these terms [62], however, for the purpose of this study, these terms have been considered in accordance with *Gordon* [42] and *Ng et al* [45]. The cycle time is the time between two consecutive adsorption processes. Switching time is the time taken for heat recovery (also, the time taken for beds to switch their roles). This has been illustrated graphically in Fig. 2-5.

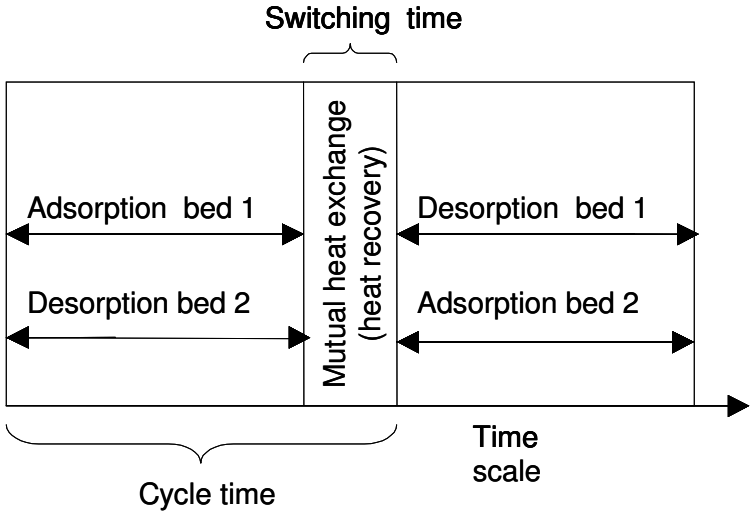

Fig. 2-5 Graphical representation of switching and cycle time. Mutual heat exchange refers to heat recovery during constant volume heating and cooling processes.

The COP of the adsorption system is expressed by equation 2.6 as the ratio of heat load managed at the evaporator in one cycle time (Q_{evap}) to the net heat needed during the processes in the adsorbent beds in one cycle ($= Q_{FG} + Q_{GH} - Q_r$), where Q_{xy} is the heat needed during the process '*x-y*' in the adsorption cycle and Q_r is the heat recovered during the cycle (*Cacciola and Restuccia* 1995). Typical values for the COP of a regenerative adsorption heat pump vary from 0.1 to 0.6 [42].

$$COP_{ads} = \left(\frac{Q_{evap}}{Q_{FG} + Q_{GH} - Q_r} \right) \qquad \textbf{eq. 2.6}$$

2.3 Thermoelectric adsorption (TEA) chiller

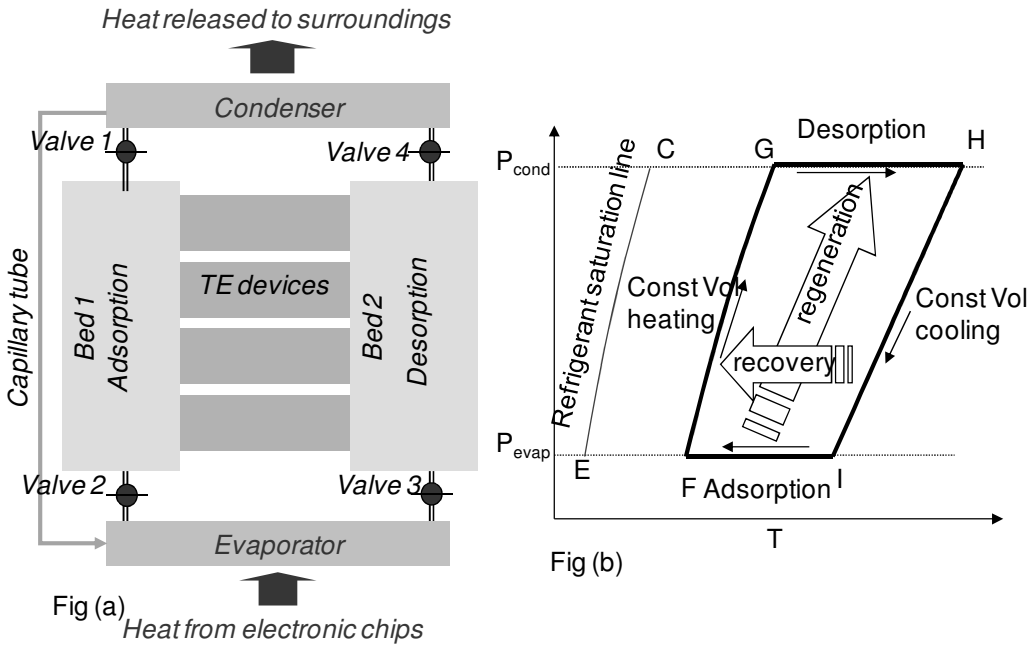

Fig. 2-6 (Left) Schematic of an Adsorption cooling system with heat regeneration and recovery driven by TE devices. (Right) Heat regeneration and recovery shown on a Clausius diagram.

The schematic of the thermoelectric adsorption chiller is shown in Fig. 2-6. A notable difference from Fig. 2-4 is the replacement of fluid loop heat exchanger, heat source, heat sink and reversible pump, with a few compact TE devices. All the processes inside the adsorbent beds and on-off sequence of the valves are the same as in the adsorption cooling system explained in the previous section. The difference lies in the way heat recovery and regeneration are achieved by the use of TE devices. For instance during adsorption in bed 1 and desorption in bed 2, TE devices are supplied electric current, such that it pumps heat of adsorption from bed 1 to bed 2. As beds flip their roles in the next cycle (i.e. desorption in bed 1 and adsorption in bed 2), the voltage polarity across the TE device is flipped to reverse the direction of the heat pump. During constant volume heating and cooling phases, the heat flow from the bed being cooled to the bed being heated does not need an active heat

pumping mechanism, however, the TE device sandwiched in between beds prevents any direct thermal contact. Heat could still flow through the low conductivity of TE device material ('Bismuth Telluride' Bi_2Te_3), but this would take longer time and result in vapor accumulation in evaporator and consequent temperature rise of electronic chips. Hence in order to hasten the heat recovery process, electric power supply is provided to TE device. The (COP) of the TEA chiller is given by the following equation as proposed by *Gordon et al* [42]. Values for the COP of TEA chiller reported by *Gordon et al* and *Ng et al* were 1.2 and 0.7 respectively [42], [45].

$$COP_{TEA} = COP_{ads}(1 + COP_{TE}) \qquad \textbf{eq. 2.7}$$

2.4 Conclusion

The mechanism of working and formulation of performance of the various chillers associated with the TEA chiller has been provided in this chapter. The COP for the TEA chiller apparently seems to be enhanced by a factor greater than unity when compared to the COP of an adsorption chiller. However, as will be seen in subsequent chapters, COP of TEA chiller is reduced by heat losses through adsorbent bed insulation. Chapter 7 provides a detailed comparison of the performance of these three chillers for identical cooling conditions.

CHAPTER 3: High temperature application of Thermoelectric Adsorption chillers

This chapter deals with the various challenges and ways for their mitigation in high temperature application of the TEA chiller. Most challenges relate to the deterioration in performance of TE device with increasing hot side temperature. A 'modified' adsorption cycle has been proposed to reduce hot side temperature as well as temperature variations as compared to the 'conventional' adsorption cycle. The performance of the modified and conventional cycles has been compared for an ambient temperature of 200 ^{0}C and condenser temperature of 220 ^{0}C. Results show similar COPs for the conventional and modified cycles, however, the modified cycle offers better thermal parameters for accommodation of the thermoelectric device.

3.1 Challenges in high temperature application

Referring to the conventional adsorption cycle as shown in Fig. 2-6-right, the following issues would have to be addressed with regard to high temperature application of the TEA chiller.

3.1.1 Highest cycle temperature

The highest cycle temperature (i.e. the regeneration temperature at point H in Fig. 2-6-right, 'T_H') should not exceed the highest temperature that the hot side of TE device can withstand. The regeneration temperature is greater than the condenser temperature. Since the condenser temperature would need to be higher than the ambient temperature of 200 ^{0}C, the regeneration temperature must be controlled to accommodate commercially available TE devices. The HT series TE modules available from Melcor Corp (now a part of Laird Technologies [71]) were able to survive temperatures of up to 225 ^{0}C [72]. Currently

the ThermaTEC^{TM} series high temperature TE modules available from Laird Technologies are rated for an operating temperature of 175 ^{0}C with the solder joint between the thermoelectric material (Bi_2Te_3) and the ceramic material (Al_2O_3) rated up to 271 ^{0}C [73]. The TG series power generator TE modules available from Marlow Industries Inc are rated for a hot side temperature of up to 250 ^{0}C [74].

3.1.2 Thermal swing

The *thermal swing* is defined as $\max(T_H) - \min(T_F)$. Here T_x is the temperature at point '*x*' in Fig. 2-6-right. It is the maximum temperature difference through which thermoelectric device has to pump heat, and it should lie within limits that allow appreciable TE device COP. In order to gauge this limit, a COP plot Fig. 3-1 of TE device HT8-7-30 (available from Laird Technologies [71]) was obtained using equations 2.2-2.4. The plot was obtained for a set of parameters as shown in Table. 3-1. It must be noted that, for this analysis, the heat rejection temperature for the TE device (i.e. the temperature of the desorbing bed) was considered 250 ^{0}C, since it is close to the expected highest regeneration temperature (T_H) of 260 ^{0}C to 270 ^{0}C, and to the operating limit of TE devices. This plot shows that an appreciable TE COP (> 0.4) can be obtained by restricting the thermal swing below 45 ^{0}C. Similarly the COP can be maintained above 0.6 if the thermal swing is restricted below 35 ^{0}C.

The challenges with thermally harsh environment application are further corroborated by the contour plot shown in Fig. 3-2. This plot shows the variation of TE device COP with average of hot and cold face temperatures as well as with the difference between hot and cold face temperatures. The average of hot and cold face temperatures is a

representative of the temperature of application of the TE device. The contour plot was obtained for a 3 Ampere current supply to the TE device. The thermo physical parameters used were same as stated in Table. 3-1. For high temperature applications (i.e. $(T_{hot}+T_{cold})/2$ > 150 ^{0}C) the plot shows a decrease in TE device COP with any increase in temperature of application or the difference between hot and cold face temperatures. An opposite trend is observed for application temperatures less than 150 ^{0}C, which supports the fact that the challenges highlighted in this section are not pronounced for low temperature application of TEA system (as studied by *Gordon et al* [42] and *Ng et al* [45]).

Table. 3-1 Values for the various parameters involved in equations 2.2-2.4. In this table 'T_{avg}' refers to the average of hot and cold face temperatures of the TE device.

Parameter	*Description*	*Value*
I	Current supplied	0.5 A, 1 A, 2 A, 3 A, 4 A, 5 A, 6 A
T_h	Heat rejection temperature	523 K (250 ^{o}C)
T_c	Heat source temperature	473 K (200 ^{0}C) < Tc < 523 K (250 ^{0}C)
$R_{TIM,c}$	Thermal interface resistance between TE cold face and heat source	0.052 K W^{-1}
$R_{TIM,h}$	Thermal interface resistance between TE hot face and heat sink	0.052 K W^{-1}
α_p-α_n	Net Seebeck coefficient of TE material	(-2.025x10^{-9}x$T_{avg}^{\ 2}$ +1.42x10^{-6} T_{avg} -4.49 x 10^{-5}) V K^{-1} (*Gordon et al* [42])
ϱ	Electrical Resistivity of TE material	(4.35x10^{-8} x T_{avg} -2.754x10^{-6}) Ω m (*Gordon et al* [42])
k	Thermal conductivity of TE material	(2.91x10^{-5}x$T_{avg}^{\ 2}$ -0.019x T_{avg} + 4.81) Wm^{-1}K^{-1} (*Gordon et al* [42])
G	Geometric factor of TE device (ratio of area to length of a TE element)	0.171x10^{-2} m
N	Number of thermoelectric elements in one HT-8-7-30 TE device	71

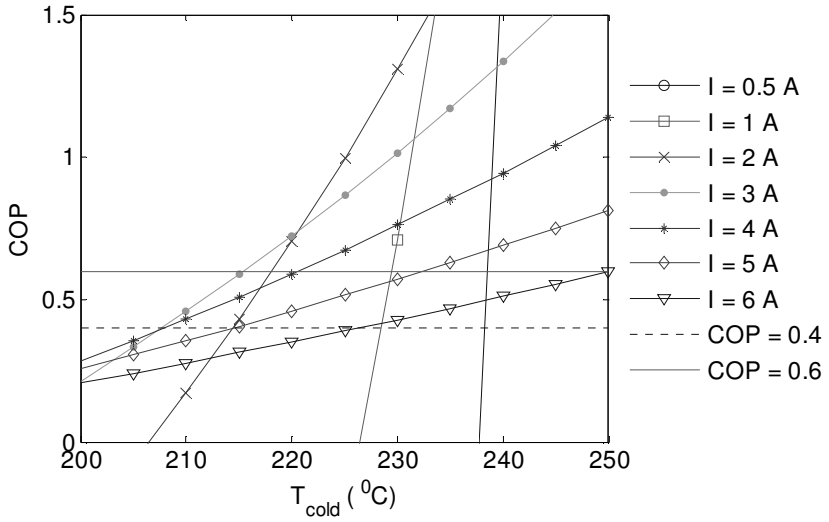

Fig. 3-1 A TE COP greater than 0.4 and 0.6, can only be possible for values of *'T_{cold}'* greater than 205 ^{0}C and 215 ^{0}C respectively (i.e. thermal swing should be less than 45 ^{0}C and 35 ^{0}C respectively). Above plot was obtained for a hat rejection temperature of 250 ^{o}C for the TE device.

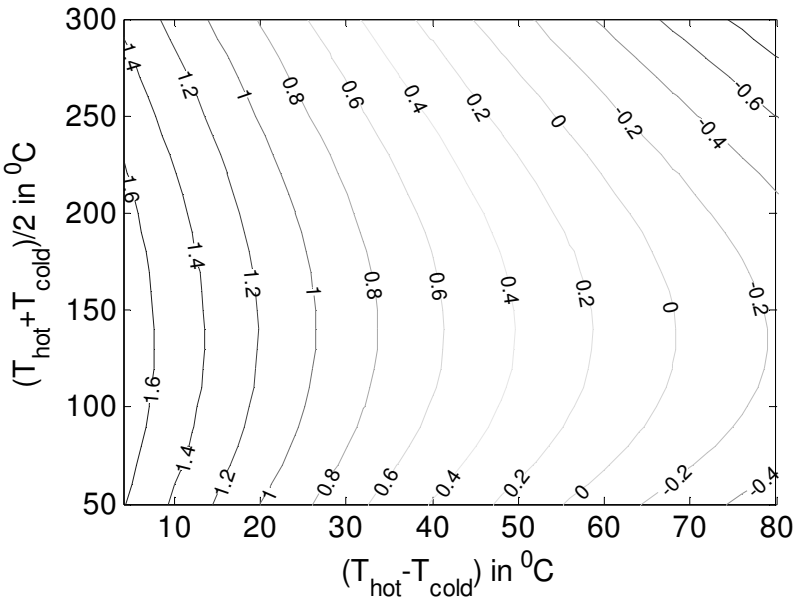

Fig. 3-2 Contour plot for the TE device COP. At low application temperature (< 150 ^{0}C) the COP increases with increasing values of $(T_{hot}+T_{cold})/2$. At application temperature above 150 ^{0}C, the COP decreases with any increase in the values of $(T_{hot}+T_{cold})/2$.

To put the challenges expressed above in quantifiable terms it was necessary to determine the highest temperature and the thermal swing encountered for a typical target cooling condition that comprised an evaporator (heat source) temperature of 150 ^{0}C and a

condenser (heat sink) temperature of 220 ^{0}C. With these conditions, temperature at various cycle points (I, F, G and H in Fig. 2-6-right) were calculated under certain assumptions that ensured cooler temperatures for the adsorption cycle. The temperature at point G (T_G) was assumed equal to the heat sink temperature. Also, the temperature at point I (T_I) was considered equal to T_G, which results in negligible overlap between adsorption and desorption processes on the temperature scale. A negligible overlap (i.e. $T_G = T_I$) ensures that the entire process H-I has a temperature higher than that of process F-G, thus ensuring that transfer of heat from process H-I to process F-G is entirely supported by the temperature difference between them. A positive overlap (i.e. $T_G < T_I$) would result in increased thermal swing, whereas a negative overlap (i.e. $T_G > T_I$) would necessitate active heat pumping by TE device to transfer a part of heat released during process H-I, to process F-G.

With pressure at G and I known (P_G and P_I are equal to saturation pressure of water at condenser and evaporator temperature respectively), the water uptake at G (w_G) and I (w_I) were calculated using equations that describe adsorption characteristics of the adsorbate and adsorbent pair. For this research work Zeoite 13-X-Water was considered as the adsorbent–adsorbate pair due to its recommended use for high regeneration temperature (> 200 °C) in literature [50], [59]. [*Table 3-2 presents a comparison of various adsorbent-adsorbate pairs in the context of regenerative application at temperatures greater than 200 °C. Zeolite 13X-water and Zeolite 4A-Water pair was found to be suitable for application. Zeolite 13X-water pair was chosen due to its higher pore size and hence higher water uptake when compared to zeolite 4A.*] Equations 3.1-3.3 describe the water content in zeolite-13X at various temperatures and pressures. In these equations the

term '*p*' represents absolute adsorbent bed pressure in milibars and term '*T*' represents the bed temperature in Kelvin. $a_{i=0,1,2,3}$ and $b_{i=0,1,2,3}$ are constants whose values are listed below. These were obtained from literature (*Cacciola and Restuccia* [75]; *Cacciola et al* [76]).

Table 3-2 Comparison of various adsorbent-adsorbate pairs for suitability in hig temperature application of TEA system.

Adsorbent-adsorbate pairs	*Primary application*	*Suitability for application at thermally harsh environment*
Silica Gel-Water [50], [54], [77], [87])	Air conditioning, Low temp waste heat recovery, Solar cooling	Silica gel disintegrates above 100 °C in the presence of water.[54][67]
Zeolite 4A-Water ([51], [61], [87])	Air conditioning, Low temp waste heat recovery, Solar cooling	Stable till temperatures greater than 350 °C
Zeolite 4A-Methanol	Deep freeze applications (below 0 °C)	Methanol disintegrates at temperatures greater than 150 °C with zeolite acting as catalyst [54]
Zeoite 4A-Ammonia	Deep freeze applications (below 0 °C)	Ammonia is toxic and can be explosive at high temperatures and pressure [54]
Zeolite 13X-Water ([96])	Air conditioning, Low temp waste heat recovery, Solar cooling	Stable till temperatures greater than 350 °C
Zeolite 13X-Methanol	Deep freeze applications (below 0 °C)	Methanol disintegrates at temperatures greater than 150 °C with zeolite acting as catalyst [54]
Zeolite 13X-Ammonia	Deep freeze applications (below 0 °C)	Ammonia is toxic and can be explosive at high temperatures and pressure [54]
Activated Carbon-Methanol ([51], [55], [61], [63])	Air conditioning, Deep freeze applications (below 0 °C)	Methanol disintegrates at temperatures greater than 150 °C with carbon acting as catalyst [54]
Activated Carbon-Ammonia ([51], [53], [57])	Air conditioning, Deep freeze applications (below 0 °C)	Ammonia is toxic and can be explosive at high temperatures and pressure [54]

$a_0 = 13.4244; a_1 = 110.8540; a_2 = -731.7600; a_3 = 1.64e3$

$b_0 = -7.37e3; b_1 = 6.722e3; b_2 = 5.624e3; b_3 = -3.48e3$

$$\ln(p) = a(w) + b(w)/T \qquad \textbf{eq. 3.1}$$

$$a(w) = a_0 + a_1 w + a_2 w^2 + a_3 w^3 \qquad \textbf{eq. 3.2}$$

$$b(w) = b_0 + b_1 w + b_2 w^2 + b_3 w^3 = \Delta H(w)/R \qquad \textbf{eq. 3.3}$$

Lines for constant water uptake were drawn from G and I towards constant pressure lines of P_E and P_C to get an estimate of T_F and T_H respectively. The value of T_H, the highest temperature, was calculated as 283 ^{0}C while the thermal swing was calculated to be 83 ^{0}C. These values make it difficult to harness efficient performance from thermoelectric devices while operating with a conventional adsorption cycle. Hence the need for a modified cycle that could allow a reduction in these values.

3.2 Modified adsorption cycle

A modified adsorption cycle is proposed to reduce the thermal swing and the highest temperature encountered during the cycle. The proposed cycle breaks the process of adsorption and desorption as well as constant volume heating and cooling into two steps Fig. 3-3, so that primary adsorption (I-F) in bed-1 is accompanied by primary desorption in bed-2 (G-H) and secondary adsorption in bed-1 (I_1-F_1) is accompanied by secondary desorption in bed-2 (G_1-H_1). It must be noted that unlike the conventional cycle, the modified cycle comprises of two condensers and two evaporators, as indicated by points C, C_1, E and E_1 in Fig. 3-3. Condensation at C and C_1 is termed as primary and secondary condensation respectively. Similarly evaporation at E and E_1 is termed as primary and secondary evaporation respectively. The maximum temperature encountered is given by $\max(T_H, T_{H1})$ where T_X is the temperature at point *'x'* on the cycle's Clausius diagram. The thermal swing for the modified cycle is given by $\max(T_H, T_{H1}) - \min(T_F, T_{F1})$. In the context

of a*b*sorption systems, such a cycle is widely used for low temperature waste heat recovery and is termed as the '*half effect*' cycle.

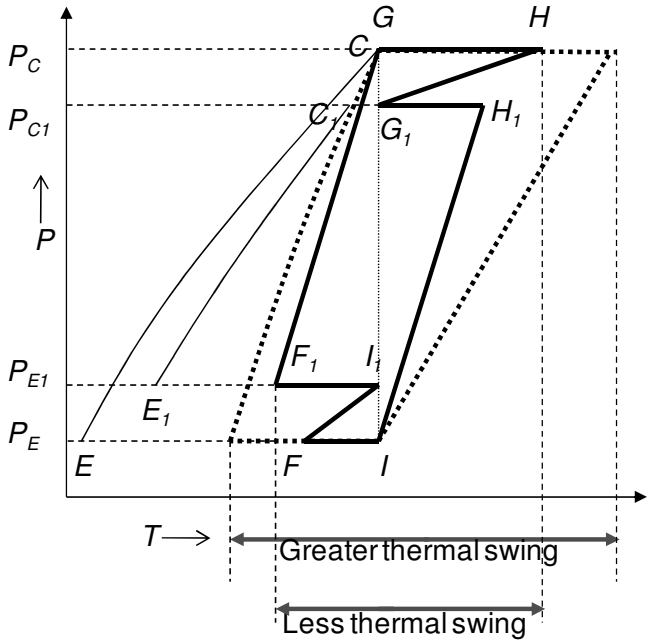

Fig. 3-3 The modified cycle (thick lines) has been shown along with the conventional cycle (broken lines). Points C and G coincide in the diagram indicating $T_C = T_G$. Modified cycle exhibits less thermal swing in comparison to conventional cycle.

In order to compare the advantages of the modified cycle over conventional cycle the temperatures at various points (I, F, G, H, I_1, F_1, G_1 and H_1) on the cycle were determined. Referring to Fig. 3-3, the evaporator temperature (T_E =150 ^{0}C) and condenser temperatures (T_C =220 ^{0}C, T_{C1}=205 ^{0}C) were considered known a-priori. The temperature difference $\Delta T_{GC} (= T_G - T_C)$ is chosen as 0 ^{0}C. To target least thermal swing (as explained in section 3.1.2), any overlap between adsorption and desorption processes is considered negligible, (i.e $T_G = T_{G1} = T_{I1} = T_I$). This is evident from the vertical line that runs through points G, G_1, I_1 and I in Fig. 3-3. With temperature and pressure and G, G_1 and I known, water uptake at G (w_G), G_1 (w_{G1}) and I (w_I) can be determined by using equations 3.1-3.3.

An intersection of constant water uptake line w_I and constant pressure line P_{C1} gives an estimate of T_{H1}. Similarly T_H can be determined by using w_{G1} and P_C. Determination of T_{H1} and T_H easily leads to the determination of w_{H1} and w_H. Since the adsorption process I-F corresponds to the desorption process G-H, $(w_F - w_I)$ must equal $(w_G - w_H)$ which leads to determination of w_F. Since pressure at F is known $(= P_E)$, T_F can be determined by the knowledge of w_F. Further the knowledge of $w_{I1} (= w_F)$ and T_{I1} leads to the estimation of secondary evaporator pressure P_{E1}. Since pressure and water uptake at F_1 $(= P_{E1}$ and w_G respectively) are known, T_{F1} can be determined.

3.3 Comparison with conventional cycle

A graphical illustration of the modified cycle in the backdrop of conventional cycle has been presented in Fig. 3-3. If the temperature at heat source (T_E), heat sink (T_C) and at point G (T_G) are considered the same for both cycles, the equality of T_I, w_G and w_I is ensured, which leads to same total water uptake $(= w_G - w_I)$ for both cycles. However, unlike the conventional cycle, where total water uptake is achieved during one adsorption process, in the case of modified cycle the value of $\Delta T_{IF} = (T_I - T_F)$ provides a control on the extent of contribution of primary and secondary adsorption processes on total water uptake. A high value of ΔT_{IF} leaves less water to be adsorbed during secondary adsorption process.

For a comparison, the values T_E =150 ^{0}C, T_C =220 ^{0}C and T_G =220 ^{0}C are considered for both cycles. For the modified cycle the value of T_{C1} is chosen as 205 ^{0}C. Using procedures already discussed, the temperature and pressure at various cycle points are

calculated. Table. 3-3 shows various parameters points for both cycles. It can be observed that modified cycle leads to a drop in thermal-swing by nearly 20 ^{0}C and a drop in maximum cycle temperature by 13 ^{0}C.

Table. 3-3 Comparison of conventional and modified cycles in terms of temperature and thermal-swing.

	T_F (^{0}C)	T_{F1} (^{0}C)	T_H (^{0}C)	T_{H1} (^{0}C)	Thermal swing (^{0}C)	w_G-w_I
Conventional Cycle	168	NA	283	NA	115	0.022
Modified Cycle	212	174	231	270	96	0.022

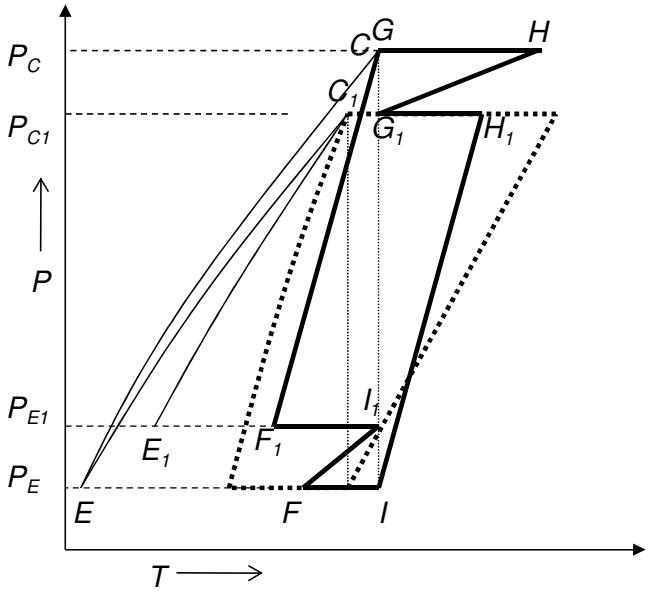

Fig. 3-4 Clausius diagram showing modified (thick line) and conventional (broken line) cycles, such that the temperature and pressure at secondary condenser of modified cycle matches those at condenser of conventional cycle.

The comparison made above considers a condenser temperature of 220 ^{0}C for the conventional cycle which need not be the case. The modified cycle needs a higher primary condensation temperature to make room for the secondary condenser. The same is not necessary for the conventional cycle. Hence another comparison is made where the conditions at condenser of conventional cycle match the conditions at secondary condenser of the modified cycle.

For this condition Fig. 3-4 depicts both cycles on a Clausius diagram. The refrigerant saturation line for primary and secondary condensation of modified cycle is depicted by processes C-E and C_1-E_1 respectively, whereas the process C_1-E depicts the same for conventional cycle. A comparison was made between the two cycles with T_E =150 ^{0}C, T_C =220 ^{0}C, $T_G = T_C$ and T_{C1} =205 ^{0}C. Table. 3-4 shows temperature at various points for both cycles. In this case the thermal-swing is observed to increase by 8 ^{0}C and the highest cycle temperature increases by 18 ^{0}C. These figures are not favorable for modified cycle, however, it must be pointed out that modified cycle manages a cooling load nearly 40% greater than that of conventional cycle under the given conditions of comparison.

Table. 3-4 Comparison of conventional and modified cycles in terms of temperature at various points.

	T_F (^{0}C)	T_{F1} (^{0}C)	T_H (^{0}C)	T_{H1} (^{0}C)	Thermal swing (^{0}C)	w_G-w_I
Conventional Cycle	164	NA	252	NA	88	0.016
Modified Cycle	212	174	231	270	96	0.022

3.4 Performances of various cycles

A clear picture of the advantages involved with modified cycles could only emerge after a comparison of their performance. Towards this end equations formulated by Cacciola et al [76] were used to determine the energy requirements of the various stages of conventional and modified cycles. The energy equations have been shown in Table 3-5.

Each energy equation comprises various energy terms, such as enthalpy of sorption and sensible heating/ cooling of the adsorbent beds and the adsorbate. For a calculation of these terms the zeolite mass and the mass of adsorbent beds would have to be known. Since a typical cooling load for harsh environment electronics (such as oil drilling operation) is in the range of 10 to 20W ([47], [48]), a cooling load of 15W was considered for this analysis.

Assuming the evaporator temperature as 150 °C, and estimate of vapor generation rate at evaporator can be obtained using equation 3.8. it should be noted that 'V' represents vapor mass.

Table 3-5 List of energy equations as a summation of different terms. Q_{xy} represents the energy 'required' (as in case of constant volume heating and desorption processes) or 'given off' (as in case of adsorption and constant volume cooling processes) during a process x-y as shown on Clausius diagram (Figs. 5b, 8, 9 and 11). Here x and y represent the beginning and end points of the process.

Energy 'required'/ 'given-off' during process x-y =	Term 1: Enthalpy of Adsorption +	Term 2: Sensible heating of Zeolite and bed metal mass +	Term 3: Sensible heating of adsorbed water +	Term 4: Sensible heating of vapor in transition from evaporator/ condenser to bed
Q_{xy}= (x,y) = (I,F) or (I_1,F_1)	$m_z \int_{w_x}^{w_y} \Delta H dw$	$m_z(c_{pz}+ic_{pz})(T_x-T_y)$	$m_z c_{pw} \int_{T_y}^{T_x} w(T)dT$	$-m_z \sum_{i=1}^{n=100}(w_i-w_{i-1})c_{pv}(T_E)$ **eq. 3-4** $\left[\frac{1}{2}\left(\frac{b(w_i)}{\ln(P_E)-a(w_i)}+\frac{b(w_{i-1})}{\ln(P_E)-a(w_{i-1})}\right)-T_E\right]$
Q_{xy}= (x,y) = (F,G) or (F,I_1) or (F_1,G)		$m_z(c_{pz}+ic_{pz})(T_y-T_x)$	$m_z(c_{pw}w_F)(T_y-T_x)$	**eq. 3-5**
Q_{xy}= (x,y) = (G,H) or (G_1,H_1)	$m_z \int_{w_y}^{w_x} \Delta H dw$	$m_z(c_{pz}+ic_{pz})(T_y-T_x)$	$m_z c_{pw} \int_{T_x}^{T_y} w(T)dT$	**eq. 3-6**
Q_{xy}= (x,y) = (H,I) or (H,G_1) or (H_1,I)		$m_z(c_{pz}+ic_{pz})(T_x-T_y)$	$m_z(c_{pw}w_I)(T_x-T_y)$	**eq. 3-7**

$$\dot{V} = (cooling\_load)/(h_{g,T_E} - h_{f,T_E}) \qquad \textbf{eq. 3-8}$$

Referring back to Table. 3-3 a conventional cycle will have a water uptake variation ($\Delta w = w_F - w_I$) of 0.022 during the adsorption process. Thus the net amount of vapor adsorbed by Zeolite during adsorption can be expressed as a product of mass of zeolite and water uptake variation, '$M_Z(\Delta w)$.' If we consider a typical cycle time 't_{cycle}' of 10 minutes (as considered by Ng et al [45]) for the adsorption cycle, the amount of vapor to be adsorbed by the zeolite can also be expressed as: '$\dot{V}t_{cycle}$.' Equating the two expressions arrived at in this paragraph, we obtain:

$$M_Z(\Delta w) = \dot{V}t_{cycle} \qquad \textbf{eq. 3-9}$$

Equations 3.8 and 3.9 were used to estimate the mass of zeolite in one adsorbent bed. The value obtained was 185 g. To compare various cycles in terms of their COP and cooling load, equations 3.4-3.7 were used to calculate the energy 'required'/ 'given off' by the various stages of the cycle. The cooling load managed by the cycles was obtained using equations 3.8 and 3.9. The energy terms and cooling load were plugged into equation 2.6 to obtain COP_{ads}. Further a constant value of TE device COP (COP_{TE} = 0.4) was plugged into equation 2.7 to obtain the overall system COP. The basis for chosing COP of TE device has been explained in one of the assumptions listed below. The plots for overall COP were obtained with the evaporator temperature varying from 95 ^{0}C to 195 ^{0}C and the primary condenser temperature kept constant at 220 ^{0}C.

The following assumptions were made during calculations:

1. The spatial distribution of pressure, temperature and water uptake in adsorbent bed was considered uniform [78].
2. The specific heat of zeolite at high temperatures was obtained by extrapolating the data available in literature [79]. A constant value of 1.082 kJ kg^{-1} K^{-1} was assumed for the entire temperature range.
3. The inert mass ratio '*i*' of beds, defined as the ratio of thermal mass of inactive bed material to the thermal mass of zeolite, was considered 0.5. Similar value has been reported in literature *Dawoud* [54] had a value of 0.7, whereas *Critoph* [57] considered a value of 0.49).
4. The heat capacity of adsorbate in adsorbed phase was considered equal to its heat capacity in vapor phase [76].
5. A constant TE device COP (COP_{TE} = 0.4) was considered. This allows a simplistic estimation of the COP of the TEA system. A true estimation of COP_{TE} would require tracking COP_{TE} from a high value (>1) at the initiation of heat regeneration process to a low value (~0.1) at the end of heat regeneration process and then estimating the average. This has not been covered in this chapter (it has been considered in detail in chapter 7). A COP_{TE} of 0.4, however, is an approximation

closer to the average value. For instance COP_{TE} varies from a value close to 1.8 to a value close to 0 as evident from Fig. 3-1, for a current supply of 3 Amperes. Table. 3-3 and Table. 3-4 suggest that most cycles have their thermal swing values in the vicinity of 90 ^{0}C. A COP_{TE} at one half the thermal swing (i.e. 45 ^{0}C) would be 0.4 as observed in Fig. 3-1.

3.5 Results and discussions

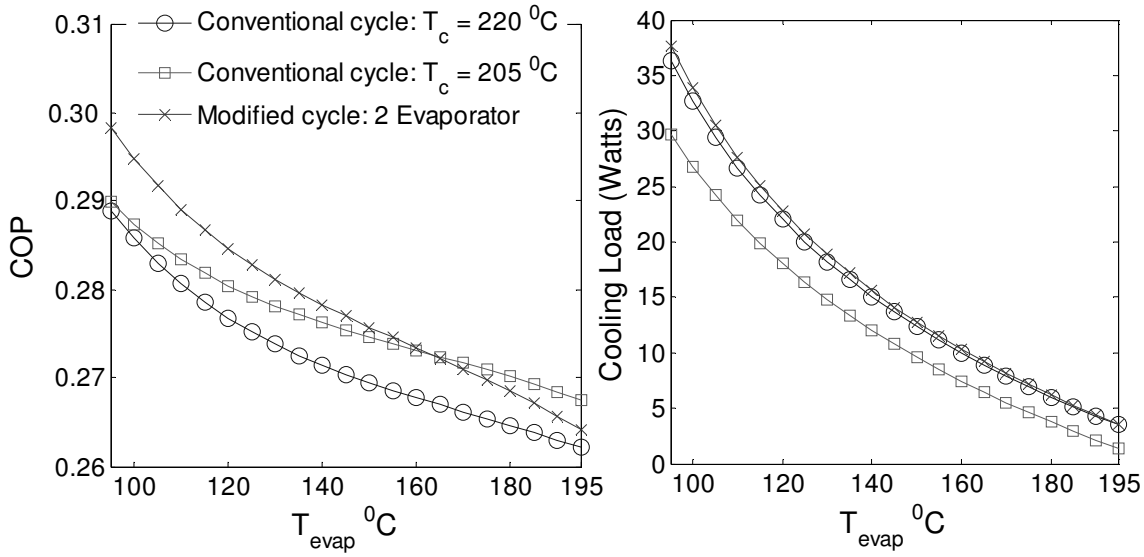

Fig. 3-5 Comparison of various cycles in terms of their coefficient of performance and cooling load.

A MATLAB code was prepared to carry out adsorption cycle calculations. REFPROP (McLinden at al [80]) database was integrated into the code to obtain thermo-physical properties of water. The conventional and modified cycles were compared in terms of their COP, cooling load, thermal swing and highest cycle temperature. Fig. 3-5 and Fig. 3-6 show relevant plots. The plot for COP reflects the performance of the adsorption cycle (COP_{ads}) alone as the COP_{TE} was considered constant during this study.

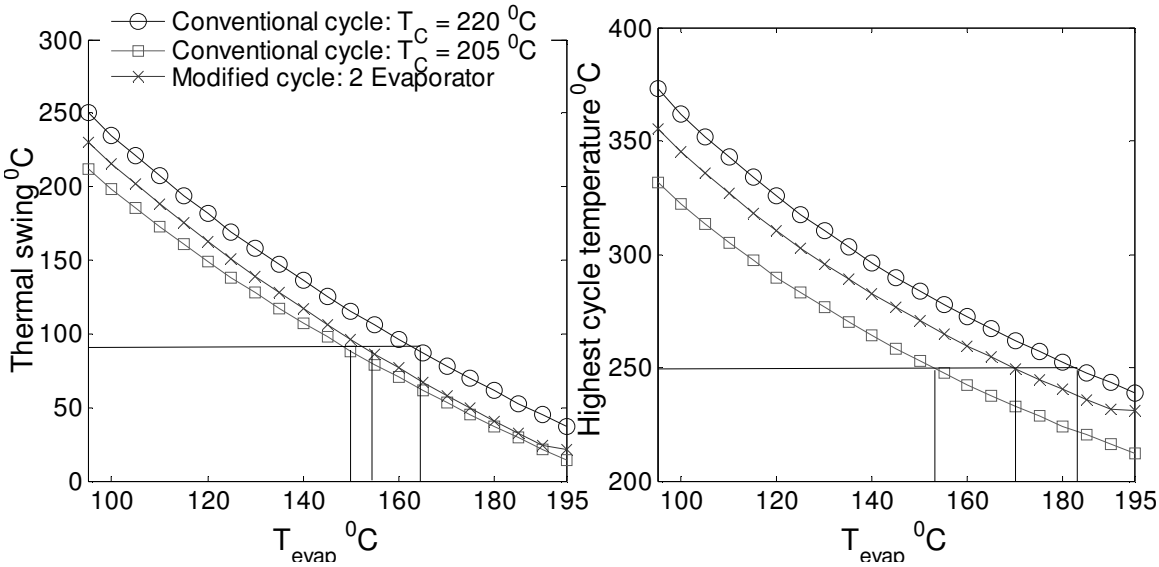

Fig. 3-6 Comparison of various cycles in terms of the thermal swing and highest temperature encountered during the cycle. The horizontal lines show the limits for thermal swing and highest cycle temperature. Limit for thermal swing (~95 ^{0}C) was obtained from values obtained in Table. 3-3 and Table. 3-4, whereas limit for highest cycle temperature (~250 ^{0}C) depends on the operating limit of commercially available TE devices.

Leaving out the conventional cycle with condenser temperature of 205 ^{0}C, all other cycles have same highest condenser temperature of 220 ^{o}C. Among those cycles, the modified cycles perform better than the conventional in terms of COP, cooling load as well as thermal swing and highest cycle temperature. This is on account of improved cooling load, as well as reduced energy requirements due to less thermal swing. Less thermal swing reduces the energy required during cyclic heating of adsorbent beds and contained zeolite. Once we incorporate the results for the conventional cycle with lower condenser temperature (i.e. T_C = 205 ^{0}C), it is observed that lowering the condenser temperature has a healthy effect on thermal swing, highest cycle temperature and the COP. However, the price for these improvements is paid in terms of lower cooling load. Lower cooling capability results from reduced pressure difference between points G and I on the Clausius diagram (P_{C1} in Fig. 3-4 in less than P_C in Fig. 3-3).

The horizontal lines in Fig. 3-6 mark the maximum allowable limit of thermal swing and highest cycle temperature (refer: caption of Fig. 3-6). The corresponding vertical lines mark the temperature to which a particular cycle can be used to cool electronics. A cycle should be used to cool only till an evaporator temperature that satisfies both the thermal swing as well as highest cycle temperature requirements. For instance, the modified cycle will breach the highest temperature limit and allowable thermal swing limit for cooling below 170 ^{0}C and 155 ^{0}C respectively, hence it can only be used to cool till an evaporator temperature of 170 ^{0}C.

The COP (Fig. 3-5) has an unexpected behavior (i.e. it decreases as the heat source temperature approaches the heat sink temperature). This can be explained on the basis that with increasing evaporator temperature, the net water uptake during a single cycle time decreases for both conventional and modified cycles. The total water uptake during a cycle depends on the difference between the pressure extremes that the cycle faces (i.e. pressure difference between points G and I on the Clausius diagram). A reduction in net water uptake $(= w_G - w_I)$ occurs as evaporator pressure gets closer to the condenser pressure. However, the energy requirements do not decrease enough to keep the overall COP increasing. A different trend in COP can be observed if a different criterion is chosen to determine the adsorption cycle. In the present study, the temperatures at G and I were considered equal. One can also chose a constant temperature difference between points I and F or a constant water uptake during adsorption process. Fig. 3-7 shows the COP of the conventional cycle (T_C = 220 ^{0}C) for these criteria.

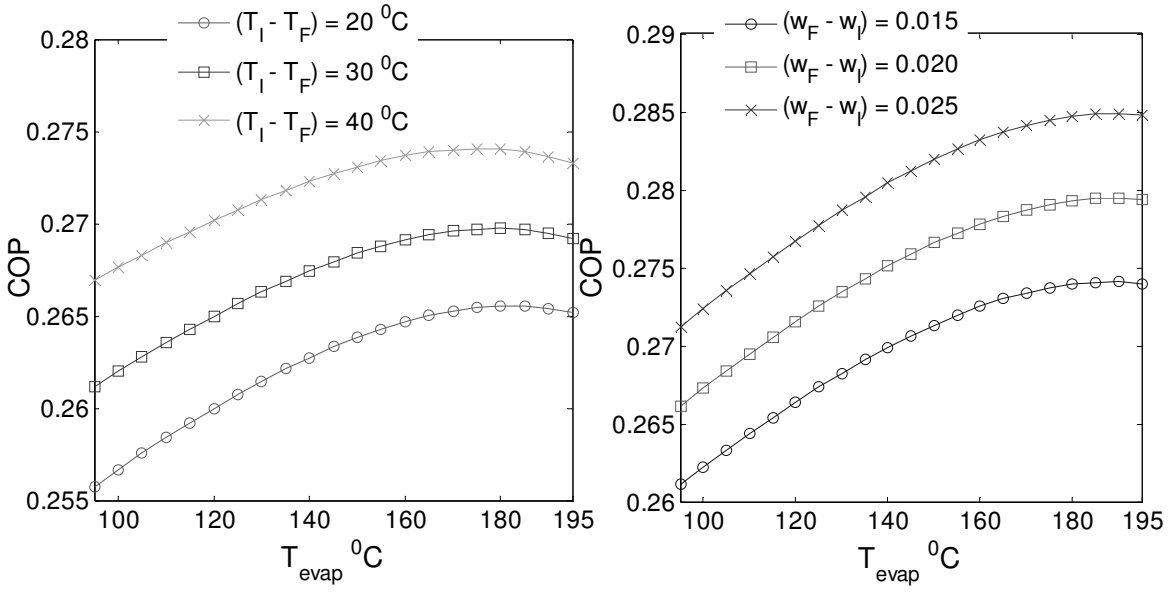

Fig. 3-7 COP for the conventional cycle under two different criteria. (Left): Temperature difference between I and F considered constant. (Right): water uptake during the adsorption process considered constant.

The plot obtained in Fig. 3-7 does confirm to the notion that COP should increase with decreasing difference between evaporator and condenser temperature, however, a close observation of Fig. 3-7 reveals that for a certain evaporator temperature (close to the condenser temperature) a maxima exists for the cycle COP. This happens because the energy requirements for the cyclic heating and cooling of adsorbent beds do not decrease enough to lead to a monotonous rise in COP. In the context of electronics cooling by TEA chiller, enforcing the condition that equates temperatures at G and I will be more useful as it leads to higher COP at evaporator temperatures that are farther apart from condenser temperature (refer: Fig. 3-5-left, and Fig. 3-7).

3.6 Volume considerations for the TEA chiller

While the above section shows the viability of adsorption system on the basis of its performance and thermal behavior, a sizing estimation will be essential to show that the system could be suitable for an electronic enclosure. For this purpose cooling load for

various electronics applications was considered from Ohadi and Qi [38] and the amount of zeolite needed for their thermal management was calculated using equations 3.8 and 3.9. Fig. 3-8 gives an approximate pointer to the volume of the zeolite needed for different cooling requirements.

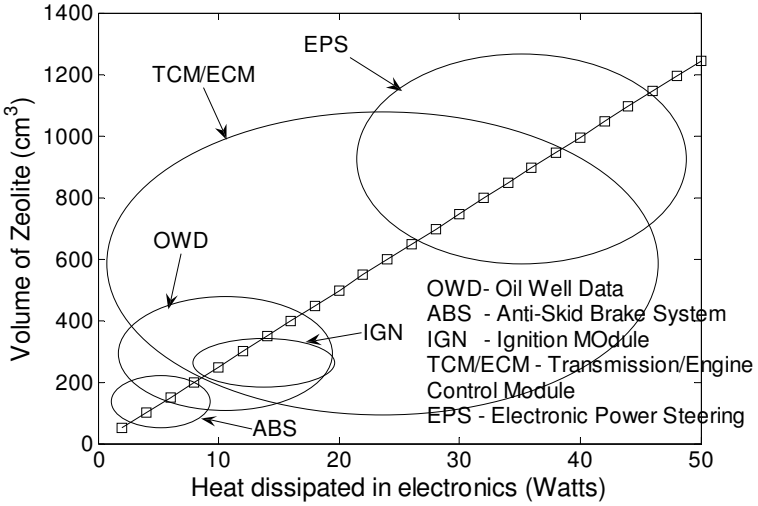

Fig. 3-8 Volume of zeolite needed in a single bed for various electronic cooling applications. (Condenser temperature 220 ^{0}C, Evaporator temperature 150 ^{0}C, cycle time 10 minutes).

It can be observed that a zeolite volume of 1200 cm^3 per bed would satisfy most of the cooling loads. Since adsorption beds contain inert metal mass along with the zeolite, the volume of metal mass must also be included to have a realistic estimate. The volume of metal required was assumed nearly equal to the volume of zeolite used in the beds. Also, considering the fact that at least two beds would be needed for a regenerative system, the complete 'adsorption compressor' may occupy volumes up to 4800 cm^3 (=1200 x 2 x 2). With most of the electronics cooling application (i.e. ABS, IGN and OWD as shown in Fig. 3-8) being taken care of within a volume limit of 600 cm^3 of zeolite for a single bed (2400 cm^3 for the whole 'adsorption compressor'), the adsorption compressor would compare well with some of the conventional mechanical compressors that have been used to make

compact cooling systems for electronics. Table. 3-6 lists few examples of commercially available mechanical compressors that have been made to fit into compact enclosures for electronics cooling (Coggins [81]).

Table. 3-6 Volume of various commercially available mechanical compressors that have been used for electronics cooling (Coggins [81]).

Commercial name of Compressor	*Volume (cm3)*
Danfoss BD35F	2229.3
Danfoss BD50F	2229.3
Danfoss TL4CL	3766.7
Danfoss FR8.4CL	4860.4
Danfoss NF9FX	3671.3

3.7 Conclusion

Incorporation of thermoelectric device in between adsorbent beds makes the cooling system compact and eliminates need for several moving parts such as flow reversal pumps that are otherwise required for fluid flow assisted heat regeneration and recovery. However, a high temperature application poses challenges in the light of thermal operating limits of TE devices. The study presented in this chapter suggests a modified cycle to mitigate such challenges. The modified cycle breaks adsorption and desorption into two steps, thus reducing temperature variations and highest cycle temperature encountered during the adsorption process.

CHAPTER 4: Practical issues with application of TEA chillers in harsh environment

In the previous chapter a comparison of the performances of a modified cycle with conventional cycle was presented. The modified cycle was proposed with a view to reduce highest temperature and temperature variations in the cycle. These measures are necessitated due to the operating limits of the TE device. However, an adsorption cycle tuned to the requirements of TE device has less flexibility in managing varying cooling load from electronics. This chapter identifies several options to solve this problem. It has been shown that varying number of 'active' TE devices in between beds of a TEA chiller is the most promising solution to handle dynamic cooling loads, while still satisfying TE device needs. For simplicity, this chapter deals with the conventional adsorption cycle, however, if one considers modified cycle as a combination of two conventional cycles, the analysis and results can easily be extended to modified cycles also.

4.1 Cooling load Vs thermal operating requirements of the TE device

Given the fact that a target temperature of the harsh environment would be close to 200 ^{0}C and that most commercially available TE devices have their thermal operating limits near 250 ^{0}C, constraints would have to be placed on the hot and cold face temperatures of the TE device. This implies that the adsorption cycle (process $I-F-G-H$) in Fig. 2-6-right would have to be accommodated within a very narrow temperature range, thus leaving little room to vary temperatures at points $F,(T_F)$ and $H,(T_H)$. An adsorption cycle limited in adsorption and desorption temperature may only address a restricted range of cooling loads, thus making the system inflexible in face of varying cooling loads. Below this problem is described in a mathematical framework.

Considering steady state operation where an adsorption cycle manages a certain heat load. The amount of vapor adsorbed in the adsorbent bed '$V_{adsorbed}$' is given by the product of adsorbent (Zeolite) mass and the increase in water uptake 'w' during the adsorption process.

$$V_{adsorbed} = M_z \times (w_F - w_I) \qquad \textbf{eq. 4.1}$$

Since during steady state operation the amount of vapor given by expression 4.1, must be equal to the vapor generated in the evaporator during one cycle time 't_{cycle}'. Hence the vapor generation rate in the evaporator '$\dot{V}_{net,evap}$' is given by:

$$\dot{V}_{net,evap} = V_{net,adsorbed} / t_{cycle} \qquad \textbf{eq. 4.2}$$

Equations 4.1 and 4.2 can also be directly deduced from equation 3.9. It should be noted that in deriving the above set of equations we have assumed steady state condition, hence irrespective of the amount of vapor occupying the open spaces in the evaporator and adsorbent beds, the vapor cycled between evaporator and adsorbent beds will be the net vapor generated in the evaporator.

Independent of equations 4.1 and 4.2, the vapor generation rate in the evaporator can also be obtained by using thermo-physical properties of refrigerant, cooling load and evaporator and condenser temperatures. The net enthalpy gain for an evaporator (in a cycle time 't_{cycle}') is given by the sum of cooling load and the enthalpy of the throttled refrigerant coming in from the condenser. Hence the net vapor generated in one cycle time can be expressed as:

$$V_{net,evap} = \left(\frac{\dot{Q}_{chip} t_{cycle}}{h_{g,evap} - h_{f,evap}} \right) + \left(\frac{\dot{V}_{throttle} (h_{f,cond} - h_{f,evap}) t_{cycle}}{h_{g,evap} - h_{f,evap}} \right) \qquad \textbf{eq. 4.3}$$

Since the mass of refrigerant in the evaporator remains constant over time, the amount of refrigerant coming in through the expansion valve '$\dot{V}_{throttle} \times t_{cycle}$', must equal the refrigerant vapors that are adsorbed during the adsorption process '$V_{net,evap}$' implying:

$$V_{net,evap} = \dot{V}_{throttle} \times t_{cycle} \qquad \textbf{eq. 4.4}$$

Combining equations 4.3 and 4.4 we obtain an equation 4.5 for net vapor generation rate in the evaporator. This is a detailed form of equation 3.8.

$$\dot{V}_{net,evap} = \frac{\dot{V}_{chip}}{(1-e)}; e = \left(\frac{h_{f,cond} - h_{f,evap}}{h_{g,evap} - h_{f,evap}} \right); \dot{V}_{chip} = \left(\frac{\dot{Q}_{chip}}{h_{g,evap} - h_{f,evap}} \right) \qquad \textbf{eq. 4.5}$$

These equations show that there exist two independent ways of arriving at the total vapor generation rate. The first is given by equation 4.2 and the second is given by equation 4.5. For proper thermal management of the cooling load, the vapor generation rate given by these two equations must be equal. Since the evaporator and condenser temperature and the thermo-physical properties of refrigerant are fixed for a given cooling system, the parameters associated with the adsorption cycle (M_z, w_F, w_I and t_{cycle}) must vary in response to a change in '$\dot{Q}_{chip}$', the rate of heat dissipation by the electronics. In the list of adsorption cycle parameters w_F, and $w_I (= w_H)$ are directly dependent on the temperatures at $F(T_F)$ and $H(T_H)$. These temperatures are an indicator of the temperature difference across which TE device needs to pump heat during heat regeneration. These temperatures have limited variability due to thermal requirements of TE device. Hence a TEA system must satisfy two distinct sets of requirements for proper thermal management. This has been described graphically in Fig. 4-1. For an adsorption cycle perfectly tuned to the TE device as well as a particular cooling load, the following options could address a change in heat load:

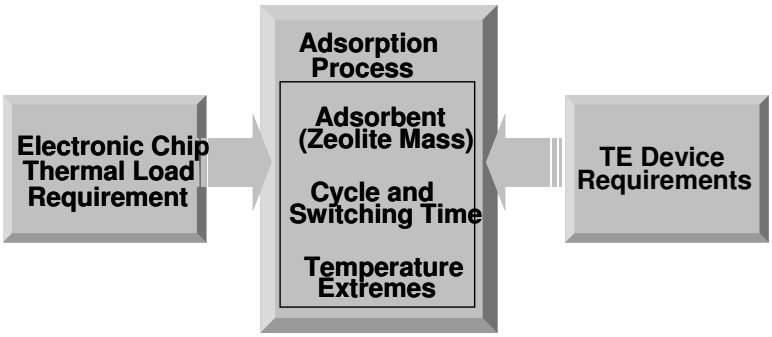

Fig. 4-1 Illustration showing the terms dictated on the adsorption process by TE device and Electronic chip thermal load requirements. The adsorption process has three parameters namely adsorbent mass, cycle & switching time and temperature extremes during the cycle that may be adjusted to satisfy both electronic chip and TE device requirements.

To address an *increase* in heat load, the following could be done:

1. Increase the mass of the zeolite in the adsorption beds.
2. Increase the extent of heating of the adsorption beds, i.e. increase the difference between T_F and T_I.
3. Increase the frequency of vapor adsorption from evaporator, or in effect decrease the cycle time of the system.

Similarly, in order to address a decrease in heat load, following could be done.

1. Decrease the mass of the zeolite in the adsorption beds.
2. Decrease the extent of thermal variation during adsorption process.
3. Decrease the frequency, i.e. increase the cycle time.

In the following section, we discuss, ways for the TEA system to adjust to varying heat dissipation from the electronic chip, while still satisfying the thermal operating conditions of a TE device.

4.1.1 Varying the mass of zeolite in adsorption beds

For any practical adsorption system, designing beds that could vary the mass of zeolite, presents complexity in bed design. While beds with internal partitions have been

designed for research purposes ([60], [67]), miniaturizing them and making them work in harsh environment may defeat the objective of having less moving parts.

4.1.2 Varying the extent of temperature variation

An increase or decrease in temperature variation during adsorption and desorption process accordingly changes the total water adsorbed in an adsorption cycle (Fig. 4-2). This feature can be used to adsorb more or less water vapor according to the thermal load requirement. While this is easily done for adsorption systems that use a variable temperature heat source for regeneration and for low temperature applications where hot and cold face temperature of TE device could be varied, in the case of high temperature application, a similar approach poses challenges that make it less attractive. Challenges relate to the low temperature difference across which a TE device is capable of pumping heat, with good COP, at high temperatures (ref: Fig. 3-2).

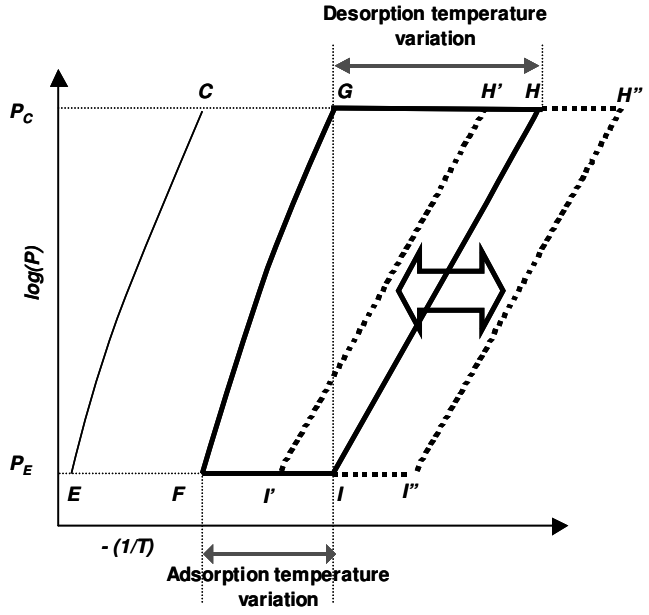

Fig. 4-2 A shift in process H-I in either direction can lead to a change in total temperature variation in adsorption and desorption processes, thus leading to similar changes in total water uptake. It must be noted that zeolite water content at constant pressure, is a function of temperature only.

A shift of process $H-I$ towards right hand side for a greater water uptake during a cycle will increase the temperature at $H(T_H)$, as is apparent from Fig. 4-2, in the adsorption cycle, thus making it less favorable for TE device based heat regeneration. On the other hand, a shift of process $H-I$ towards left for a reduced water uptake will change the amount of heat to be regenerated by the TE device. It can be seen that for the initial cycle $I-F-G-H$, the process $H-I$ is at a temperature higher than process $F-G$, thus rendering the heat transfer from process $H-I$ to $F-G$ effortless for the TE device. For the cycle $I'-F-G-H'$ however, some part of the heat transferred from $H'-I'$ to $F-G$ would be against an unfavorable temperature gradient (see Fig. 4-3). [*Heat transfer from* $H'-K$ *to* $F-J$ *is from a region of higher to lower temperature, whereas heat transfer from* $K-I'$ *to* $J-G$ *is from a region of lower to higher temperature. The points* J *and* K *are obtained such that the energy requirement of process* $J-G-H'$ *equals that of process* $K-I'-F$ *, and that both* J *and* K *have the same temperature* ($T_J = T_K$).] This extra addition in load on TE device is, however, compensated by the reduction in heat pumping requirements associated with adsorption and desorption processes. The adsorption process reduces from $I-F$ to $I'-F$ and desorption process from $G-H$ to $G-H'$. A study of the net effect of reduction and increase in heat load due to shift of $H-I$ towards the left should make it clear if this could be a desirable option to manage a reduced heat load.

For analysis we consider a hypothetical TEA system with condenser temperature 'T_C' = 200 ^{0}C and evaporator temperature 'T_E' = 150 ^{0}C. Temperature at $G(T_G)$ is considered about 10 ^{0}C higher than temperature at condenser (T_C). Equilibrium water content of zeolite at point $G = (w_G)$ and $I = (w_I)$ are calculated by using the Zeolite-Water adsorption equations 3.1 – 3.3. Drawing constant water uptake lines downwards and

upwards from G and I respectively, and marking their intersection with lines of constant pressure P ($= P_E$ and P_C) gives us points F and H respectively. It must be noted that zeolite water content at points $F =$ (w_F) and $H =$ (w_H) are equal to w_G and w_I respectively. A zeolite mass of 200g is considered in each bed. Using equation 4.1, this amount of zeolite gives us a total water intake of 3g during each cycle (assuming a cycle time of 600s – close to the cycle time assumed by *Ng et al* [45]) and using equations 4.2-4.6, a manageable heat dissipation rate of 9W is obtained, which is typical for applications like ignition module, anti-skid braking system [38] and oil well data acquisition [48]. For this system the energy required or given off during each of the cycle processes was obtained using the energy relations given by *Cacciola et al* ([75], [76]), equations 3.4-3.7. The temperature at various cycle points and the energy per unit time needed/ given off by various processes were calculated and has been shown in Fig. 4-4.

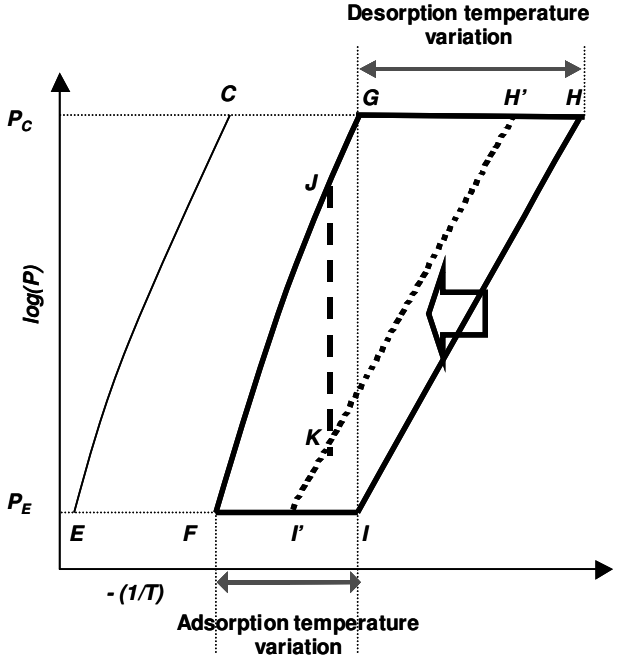

Fig. 4-3 Leftward shift of H-I to the new position H'-I' brings parts of the process H'-I' at a lower temperature than some parts of the process F-G. J-G is at a higher temperature than K-I'.

A MATLAB code was developed to calculate the total heat load that would have to be pumped against an adverse temperature difference by the TE device for a certain temperature at $I(T_I)$. Corresponding values of manageable cooling load were also calculated by the code. Results have been plotted in Fig. 4-5.

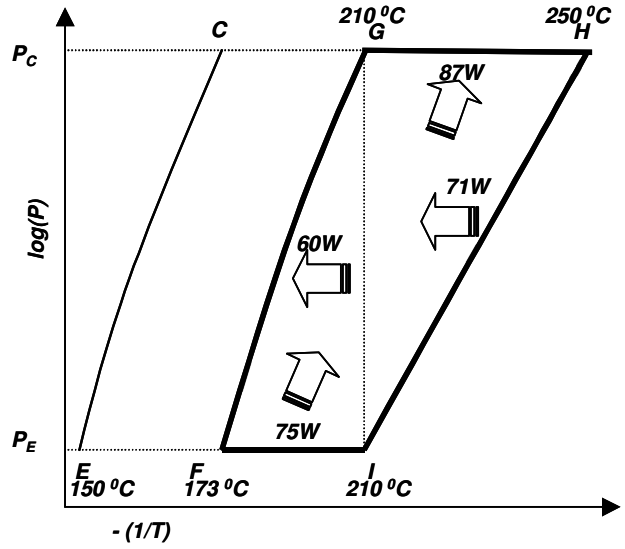

Fig. 4-4 Diagram showing the energy per unit time required/ given off by various processes. 75W would have to be pumped from adsorbing bed (process I-F) and 87W delivered to the desorbing bed (process G-H). Similarly 71W should be pumped during the isosteric cooling process (H-I) and 60W delivered to isosteric heating phase (process F-G).

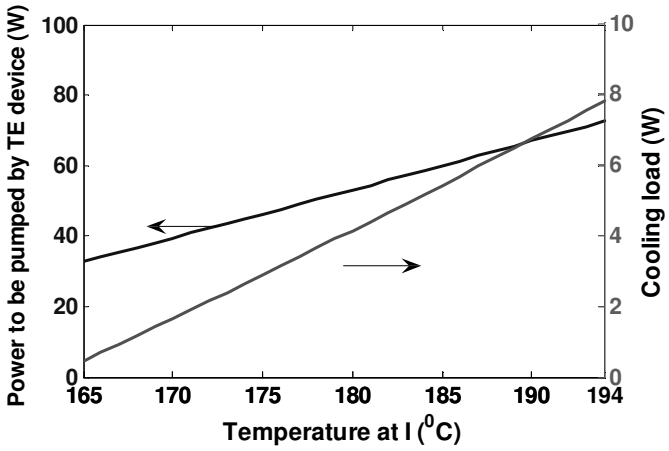

Fig. 4-5 Variation of power to be pumped against an adverse temperature gradient and manageable cooling load with varying temperature at I.

From Fig. 4-5, it can be observed that both the manageable cooling load and the power that the TE device would have to pump against an unfavorable temperature gradient decreases as the process $H-I$ is moved towards left. Hence leftwards shift of process $H-I$ could be a possible answer to a decreased cooling load.

4.1.3 Varying the cycle time

Varying the cycle time or the frequency of vapor collection from evaporator unit can be another way to manage varying heat load. This would mean carrying out the same cycle, but with a reduced or increased cycle time. Thus for a shorter cycle time same amount of vapor will be adsorbed in a shorter time, enabling the system to manage an increased heat load. A longer cycle time will do just the opposite. Since the adsorption-desorption processes remain unchanged i.e. the temperatures at various cycle points (F, G, H and I) remain unchanged, the energy to be pumped to or from any of the processes ($I-F$; $F-G$; $G-H$; $H-I$) will also remain unchanged. Thus a shorter cycle time would imply the same amount of heat of adsorption/ desorption being pumped in a shorter time interval, thus leading to an increase in the 'power' handled by the TE device. Since TE device efficiencies are typically much less than unity, an increased heat-pumping rate would lead to an increase in power input to the TE device. This must be kept under check, because increased power input will further lead to increase in hot and cold side temperatures of TE device and further deteriorate its efficiency (ref: Fig. 3-2).

However, before our analysis we must have a look at the energy requirements of the cycle in detail. We revisit Fig. 4-4. The stated energy requirement is 'cycle-time-averaged.' Hence if the cycle time were 1 second, the processes $H-I$ and $I-F$ would need to reject

71 J and 75 J respectively, and likewise the processes $F-G$ and $G-H$ would require 60 J and 87 J. However, since the total cycle time would have to be apportioned between heat regeneration (heat exchange between adsorption and desorption processes) and heat recovery (heat exchange between constant volume heating and cooling processes) phases, these energy transfers would not get the entire 1-second duration. We have further assumed that the time for heat regeneration and recovery is apportioned in the ratio 3:2. This ratio is a more conservative estimate than what has been used by other researchers (Fig. 4-6). Fig. 4-7 graphically explains the notion of apportioning heat regeneration and recovery times.

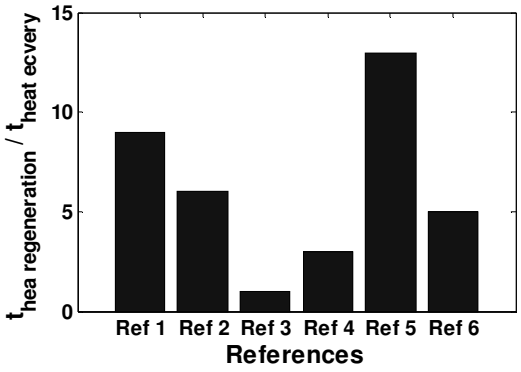

Fig. 4-6 Ratio of heat regeneration and recovery times considered by various researchers. Ref 1 : [42], Ref 2: [45], Ref 3: [52], Ref 4: [77], Ref 5: [90], Ref 6: [62].

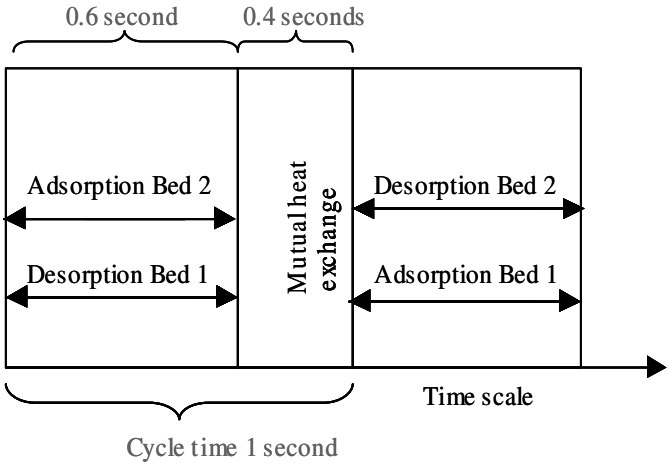

Fig. 4-7 Appropriation of cycle time between adsorption-desorption and mutual heat exchange (isosteric heating and cooling) processes.

With the apportioned time taken into account, the power terms for different processes ($I-F$; $F-G$; $G-H$; $H-I$) would be 125 W, 150 W, 145 W and 177 W respectively. These figures may go up (more load on TE device) with a decrease in cycle time, or may come down (less heat pump load on TE device) with an increase in cycle time. An increase in heat pump requirement will require more electrical power input for the TE device and hence more inefficiencies in the process. In order to prevent this, a solution is proposed wherein multiple TE devices will be used and the number of devices 'active' will vary as per the heat pump requirement. Here the decision regarding the number of active TE devices becomes critical to the efficient performance of the adsorption cooling system. This decision can be made under different criteria. Below we have considered three such criteria and described their application.

1. Each active TE device operates at it maximum COP.
2. Each TE device operates at conditions that allow maximum heat to be pumped from the cold side to the hot side.
3. The electrical power input to TE device has an upper limit.

Following assumptions were made to simplify the analysis.

1. The heat transfer between constant volume heating and cooling phases is ignored, since it takes place from a region of higher temperature to a region of lower temperature.
2. The hot side temperature of the TE device is considered as the average of temperatures at the ends of process $G-H$, i.e $(T_G + T_H)/2$. The cold side temperature of the TE device is considered as the average of temperatures at the end of processes $I-F$, i.e $(T_I + T_F)/2$.

3. Thermal resistance between the adsorption bed and the TE device interface is ignored.

Under these assumptions, Fig. 4-8 shows the performance of the TE device in terms of its COP, and heat pump rate. Commercially available TE device HT8-7-30 from Laird Technologies [71] was considered for this analysis.

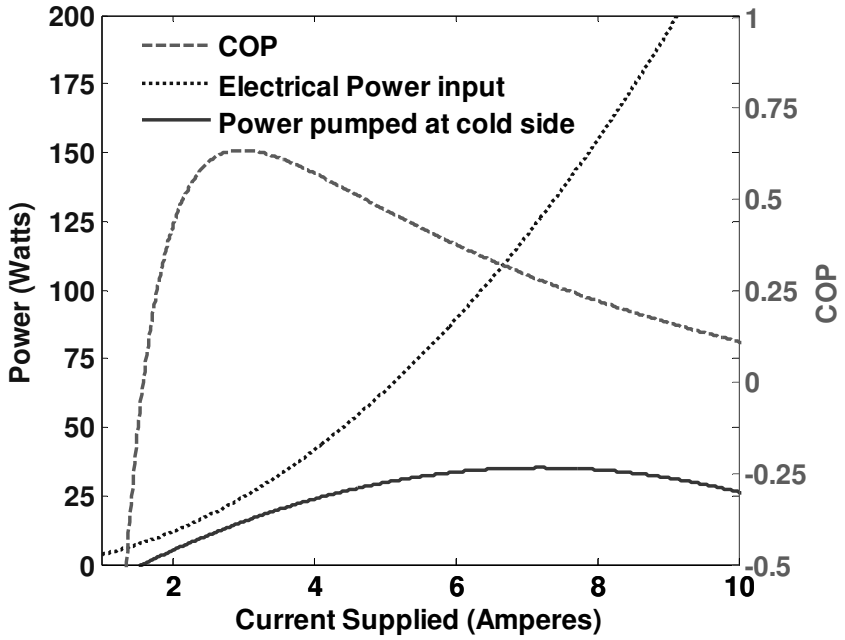

Fig. 4-8 Performance of the TE device in terms of COP, power input and power pumped, plotted against various current supply.

From Fig. 4-8 it is apparent that the maximum COP of the TE device is not consistent with the conditions under which maximum power is pumped at the cold side. Maximum COP corresponds to a current supply of 2.5 A, whereas maximum power pumped at cold side corresponds to a current supply of 6.7 A. Under these conditions the power pumped at the cold side is 15 W and 35 W respectively. Imposing a condition that maximum input power available for a TE device could only be 50 W, we observe that the power pumped from the cold side would be nearly 30 W. At this stage we know the power pumped at cold side under all the three conditions. Next, considering the same system

parameters, as they would be for a cycle time of 1 s, we consider the cycle time varying from 0.5 s to 2 s, which corresponds to the cooling load varying from 18 W to 4.5 W (cycle time of 1 s corresponds to 9 W of cooling load). As discussed before, for every cycle time, the power to be pumped out of process $I-F$ and the power to be pumped into process $G-H$ would be different (increasing with decreasing cycle time and vice-versa). We consider the power pumping capacity of a TE device under the three conditions (as discussed before) and use it to determine the total TE devices required to fulfill the total power to be pumped out of process $I-F$. Fig. 4-9 shows a plot of the number of TE devices required for various cycle times, with each cycle time corresponding to a unique cooling load (cooling load varies linearly from 18 to 4.5W as cycle time varies from 0.5 to 2 seconds).

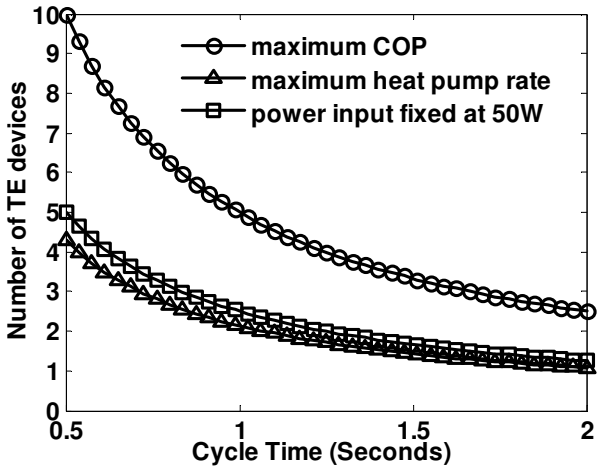

Fig. 4-9 Number of TE devices required for various cases. The plot is continuous, however only integer values will be valid for the number of TE devices.

The plot obtained shows that the criteria based on maximum COP gives the most number of TE devices to be operated for a given cooling load. The TE devices estimated on the basis of maximum power pumped from cold side is the least. The number of TE devices estimated depending on a constant electrical power (50W) input to each device lies in

between the values obtained by the other two criteria. The corresponding COPs for the cases plotted in Fig. 4-8 are 0.65 (maximum COP), 0.5 (power supply of 50W to individual TE devices) and 0.3 (maximum heat pump rate from cold side). These COP values remain constant across the values of cycle time. The maximum number of TE devices needed to address the highest cooling load (corresponding to lowest cycle time) may have to be included in the design of the adsorption bed, since more TE devices would require more surface area to thermally connect with the adsorption beds. *Ng et al* [45] have used 9 TE devices (each 40mm x 40mm) arranged on adsorbent beds with a circular face (aimed at cooling conventional desktop electronics), whereas *Sinha et al* [82] have used 5 TE devices (30mm x 33 mm) arranged in a linear fashion, which could be more suitable for inclusion in long cylindrical spaces, as in housing of oil well electronics.

At this stage it could be argued that a strategy to keep a fixed number of TE devices active (where the fixed number is decided by the worst case scenario corresponding to maximum possible cooling load) irrespective of variation in cooling load may always suffice. While such an approach will always have minimum possible heat pumping load on each TE device (since all TE devices will share the load equally), it may not be an efficient arrangement. Fig. 4-10 (a representation of Fig. 4-8), shows that for case 1 (maximum TE COP) a decrease in the heat pump load for individual TE devices will shift point 1' towards left, thus pushing point 1 downhill along the COP curve. For case 2 (fixed input electrical power to each TE device) however, a leftwards shift of point 2' will drive point 2 uphill towards a region of improved COP, till the condition of maximum COP is achieved, beyond which the COP will decrease. A similar behavior will be observed for case 3 (maximum heat pump rate from cold face). Hence it is clear that in order to have maximum possible COP,

with varying cycle time (and hence varying cooling load) few TE devices will need to be shut down.

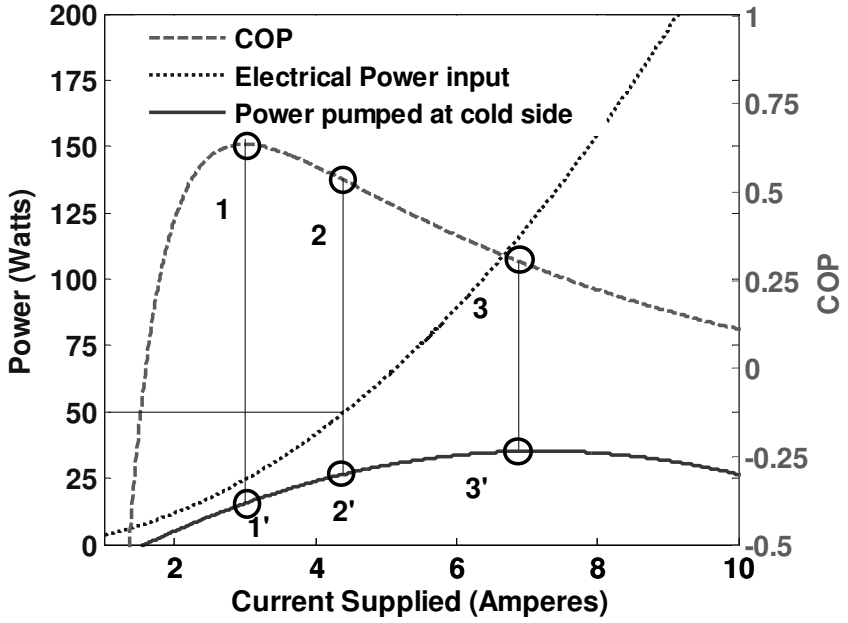

Fig. 4-10 A representation of figure 14 explaining why few TE devices will need to be shut down with decreasing cooling load.

It should be noted that while calculations have been carried out on the basis of power to be pumped from process $I-F$, the power delivered to process $G-H$ would be in excess of the requirement. Beds may have cooling arrangement to reject the heat not utilized during the desorption process. This could be without any active heat pumping mechanism, because the temperature during desorption phase is always greater than the surrounding (condenser) temperature. The added heat transfer area for this heat rejection should not affect system miniaturization as the temperature difference across which heat needs to be rejected could be as high as 50 ^{0}C.

4.2 Conclusions

Since TE devices have their own unique thermal needs, the adsorption cycle, not only has to cater to the cooling load, but also to the thermal requirements of the TE devices. A TEA system perfectly tuned to the thermal requirements of the TE device may only address a specific cooling load and have little flexibility in managing varying cooling loads. This will make the system impractical as heat dissipated by electronics remains dynamic during operation. In the work presented, methods have been proposed that make it possible to tackle varying heat load, while still maintaining good performance from TE devices.

The proposed method dictates an increase in the number of active TE devices, along with a reduction in cycle time to counter increased cooling load. For a reduction in cooling load, the cycle time will be increased with fewer active TE devices. Another approach to manage a reduction in cooling load is a 'leftwards shift' of the isosteric cooling process. A more complex maneuver could be a combination of 'leftward shift' and changes in cycle time, as well as the number of active TE devices.

For the proper functioning of the methods proposed in this chapter, a control mechanism would have to be implemented that could decide upon the number of TE devices to be kept active and the appropriate cycle time. An electronic system, it could easily fit within the miniaturized cooling system, or within the electronic module that the system is supposed to cool. It should add only a small additional thermal load to the already existing harsh environment electronics.

CHAPTER 5: System simulation and experiments with the conventional cycle

This chapter describes the experiments that were carried out to demonstrate the working of TEA chiller in thermally harsh environment. The prototype of a thermoelectric adsorption heat pump was fabricated and experiments were carried out for a targeted condenser and evaporator temperature of 165 ^0C and 140 ^0C respectively. A coefficient of performance (COP) of 0.2 was obtained and the heat load managed by the system during experiment was estimated to be about 4W. A mathematical model of the heat pump was also prepared and the experimental results were compared with the model simulations. The experiments were carried out with the conventional adsorption cycle running in adsorbent beds.

5.1 Experimental set-up

An experimental set-up was fabricated and assembled. Fig. 5-1 shows the schematic of the set-up. A brief description of the parts of the set up is given below.

5.1.1 Adsorbent beds and thermoelectric assembly

The adsorption bed was made out of stainless steel shell and copper plate. The steel shell had a semi-circular cross-section measuring 6.3 cm in diameter and 20 cm in length. Steel end caps were provided on either end with provisions for vapor outlet/ inlet, resistive heater, thermal probe and cooling fluid pipes. Perforated fins were brazed on to the inward face of the copper plate for efficient heat transfer into the zeolite mass. Fins were perforated so that the vapor transport inside bed should not be hindered. Fig. 5-2-left shows a cut out view of the CAD model of the adsorbent bed. Copper plate was brazed to the steel casing for a pressure tight enclosure. Fig. 5-2-right shows the CAD model of a single adsorbent bed

with copper plate attached. Fig. 5-3 shows the photographs of the actual bed assembly. Zeolite-13X beads with an average diameter of 2.21mm (SYLOBEAD-514 from Grace Davison ([83], [84])) was used to fill up the space inside the bed. APPENDIX A shows the distribution of mass and diameter of individual zeolite beads. Five TE devices (HT8-7-30 from Laird Technologies [71]) were placed on the copper face and sandwiched between two beds. Thermal interface pads (Gap Pad 5000S35 from Bergquist Company [85]) were used to provide thermal connection between the copper and the TE device surfaces.

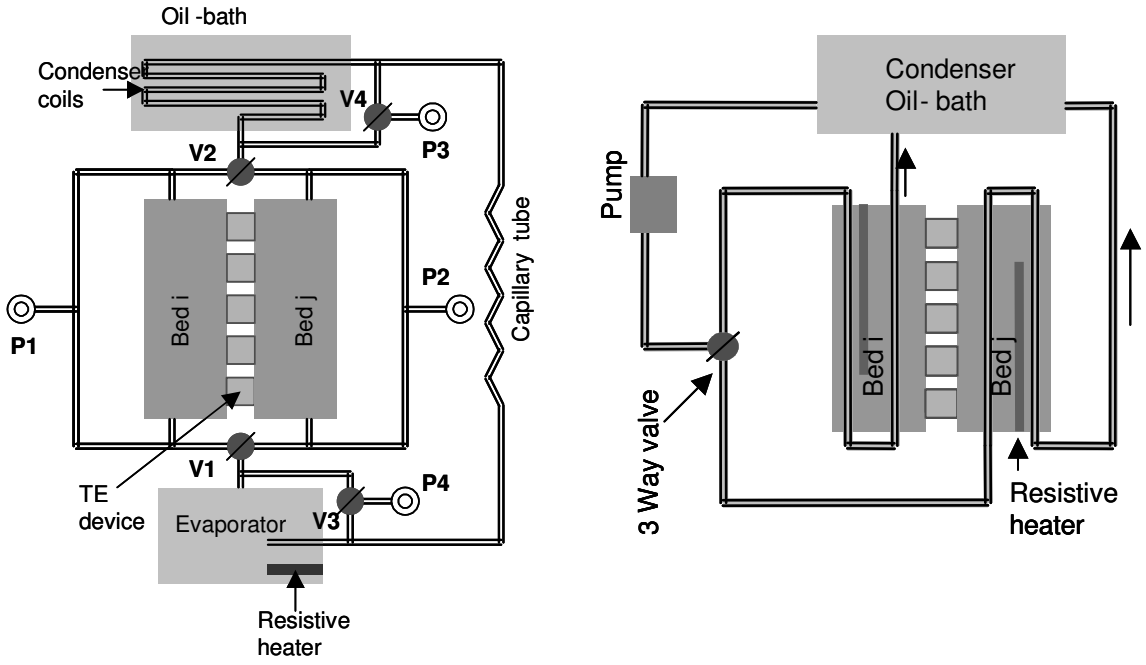

Fig. 5-1 (Left) Schematic diagram of the experimental set-up showing condenser, evaporator, adsorption beds and the refrigerant flow loop. (Right) Schematic diagram of the cooling fluid flow loop through the adsorption beds. P1...3 are the pressure transducers. Valves V1 and V2 help connect beds with either condenser or evaporator. Valves V3 and V4 help measure evaporator and condenser inlet and outlet pressure by using just two pressure transducers (P3 and P4). The resistive heaters shown in the beds were used to preheat the beds and maintain their temperature to 'thermally harsh' levels during the experiment.

5.1.2 Evaporator and Condenser

Evaporator is a partially water filled cylindrical stainless steel chamber with end caps designed to have provisions for refrigerant (water) inlet-outlet, capillary tube and vapor

outlet to adsorption beds and a resistive heater. The resistive heater simulates power dissipation by an electronic chip module. Condenser is realized by coiled steel tubing (1m in length, with an inner and outer diameter of 4.8and 6.4 mm respectively) immersed in an oil bath (glycol based heat transfer fluid with the commercial name Duratherm G [86]). The refrigerant circuit between the condenser and evaporator was completed by a steel-tubing (diameter $1/16^{th}$ of an inch), which acted as an expansion valve. Fig. 5-4 shows the photographs of the evaporator and condenser assembly.

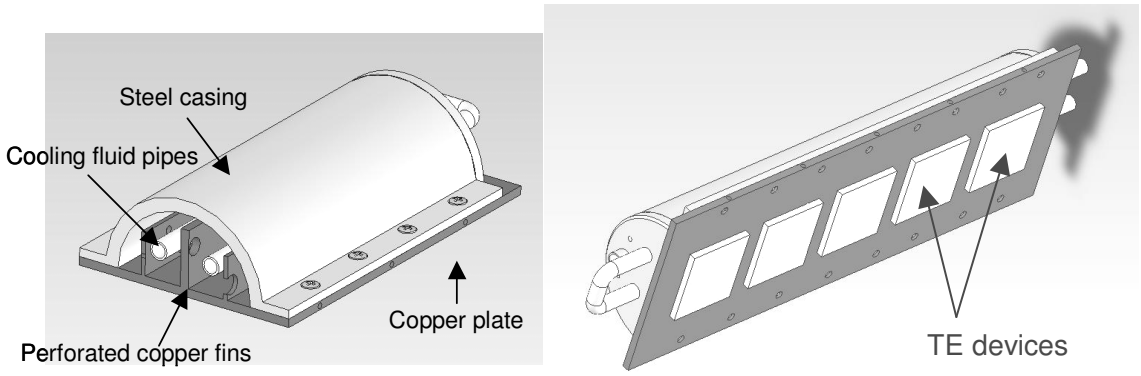

Fig. 5-2 (Left) A cut-out section of the adsorption bed. The cooling fluid lines and perforated fins attached to copper plate could be seen here. (Right) Back view of the bed, which includes the copper plates and TE devices attached with the help of a thermal interface material.

5.1.3 Harsh Environment

The condenser assembly was placed inside an oven. The oven was equipped with a temperature control unit that enabled precise control of heat rejection temperature. For the rest of the set up (comprising of adsorbent beds, evaporator and tubing work) that was placed outside the oven for easy handling during experiment, the simulation of harsh temperature was achieved by pre-heating and keeping the heat trapped by heavy insulation.

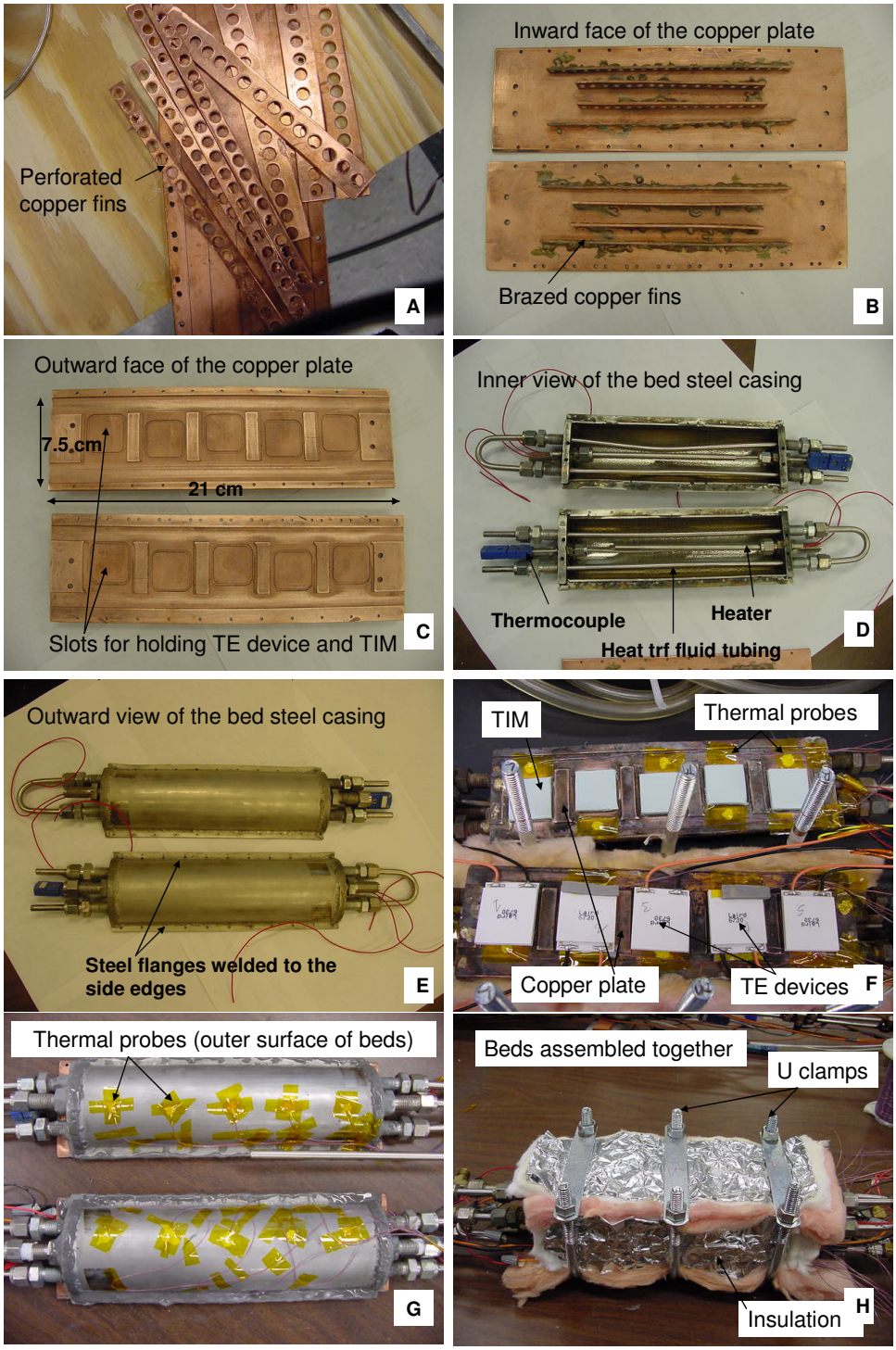

Fig. 5-3 Adsorbent bed assembly. (A) Perforated copper fins, (B) Copper fins brazed to copper plate, (C) Other side of copper plate showing slots for TE device, (D) Bed casing showing the tubes, thermal probe and heater, (E) Outer view of bed casing, (F) Bed copper plate with TIM (Thermal Interface Material) and TE devices, (G) Outer face of bed casing, showing the thermal probes, (H) Assembled beds heavily insulated.

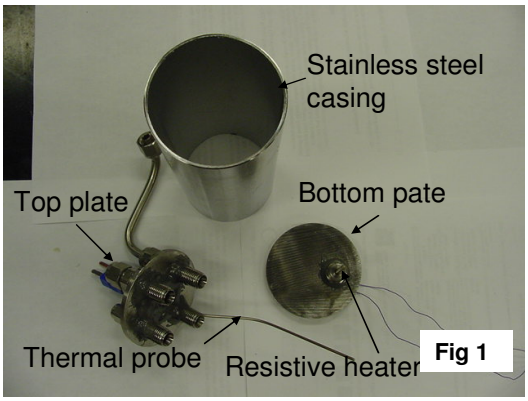

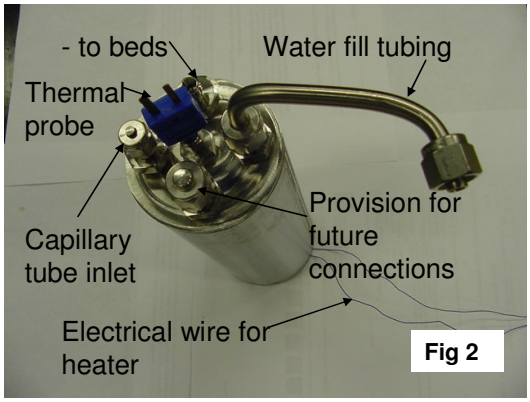

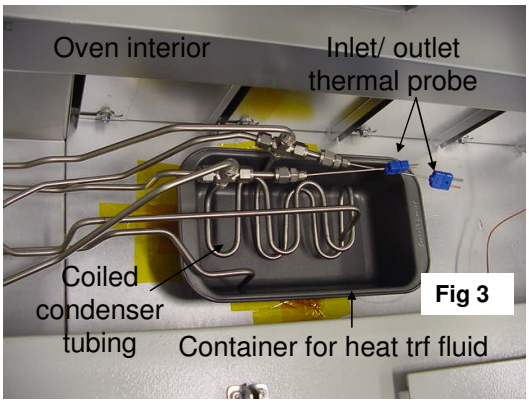

Fig. 5-4 Fig 1 shows the steel casing and the top and bottom cap plates for the evaporator assembly. Fig 2 shows the assembled evaporator. Fig 3 shows the condenser coils assembled in a pan. The pan was filled with heat transfer fluid and placed inside the oven to simulate thermally harsh heat rejection temperature.

5.1.4 Overall experimental set up

The overall experimental set up comprised of the adsorbent bed-thermoelectric assembly along with evaporator, condenser, connecting tubing, power supply, data acquisition system and vacuum and water fill station. Fig. 5-5 shows the photograph of the experimental set up.

5.2 Mathematical modeling of the system

Energy and mass balance equations were used along with Langmuir linear driving force model for adsorption to model the various system processes. For energy balance, a lumped capacitance model was used to model the active and inactive components of the

beds, evaporator and the condenser. Similar methods of modeling adsorption cooling systems have been described in the literature ([42], [52], [56], [59], [66], [75], [76], [87]-[95]) with good agreement with experimental results. Equations presented below give a mathematical description of the various processes.

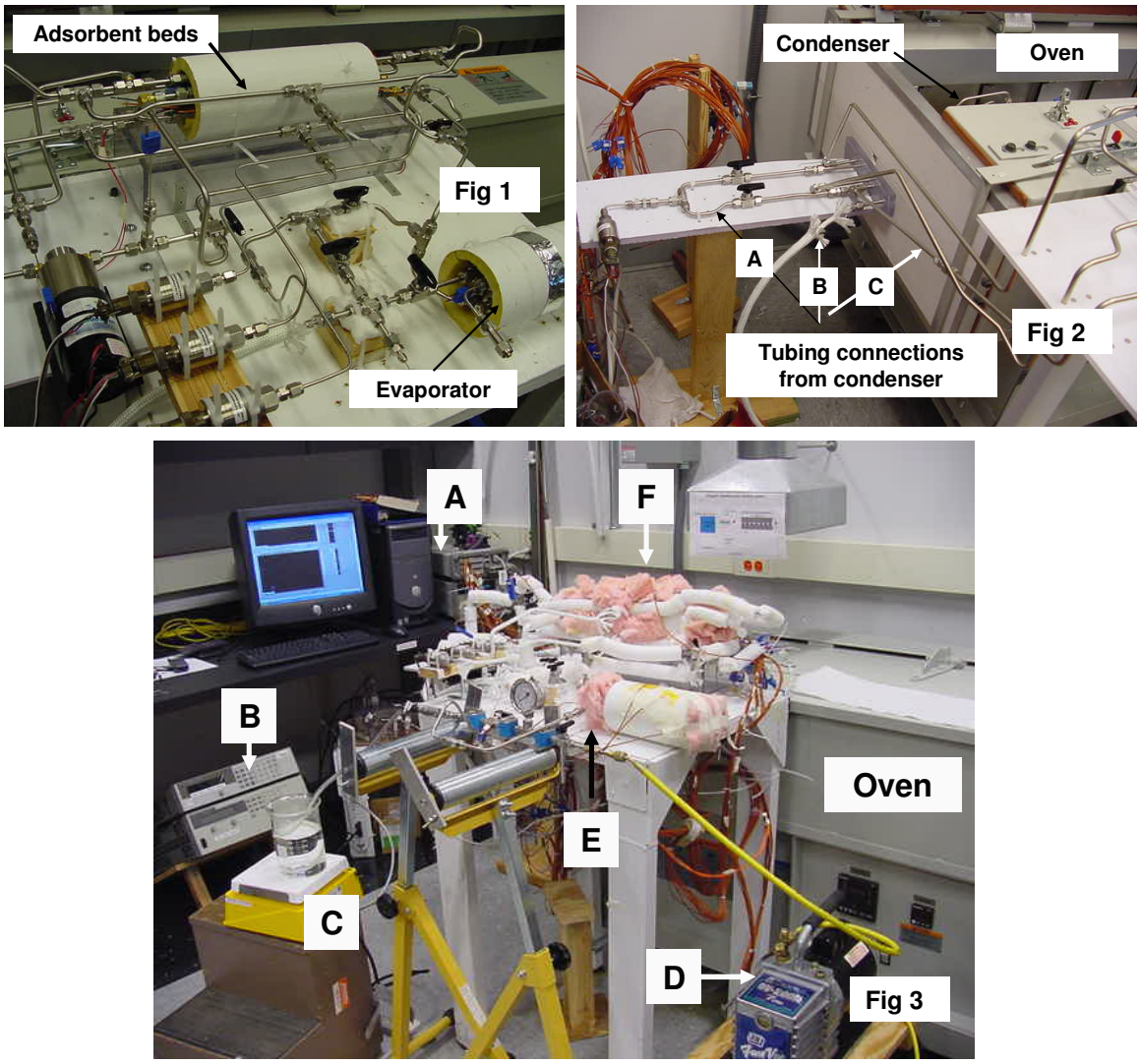

Fig. 5-5 Fig 1 shows the bed and evaporator assembly along with tubing connections. Fig 2 shows the tubing connections that connect bed and evaporator assembly to the condenser unit that is placed inside the oven. Fig 3 shows the overall set up. A: data acquisition unit, B: power supply unit, C: Water degassing station, D: Vacuum pump, E: evaporator assembly, F: adsorbent beds assembly.

5.2.1 Linear driving force model

The rate of change of water uptake during adsorption and desorption was determined by a Linear Driving Force (LDF) model.

$$\dot{w} = k(w^* - w) \qquad \textbf{eq. 5.1}$$

$$k = k_1 \exp((-k_2)/T) \qquad \textbf{eq. 5.2}$$

Here w refers to the water uptake at the bed temperature and pressure and k is the temperature dependant rate constant for the linear driving force model. k_1 and k_2 are constants obtained from literature ([89], [96]). w^* is the equilibrium water uptake at the bed temperature and pressure determined by equations 3.1-3.3. The authenticity of these equations was determined by comparison with experimental results available in literature. Authenticity of the commercially available zeolite sample was determined by X-ray diffraction analysis. (APPENDIX B and APPENDIX C describe these authenticity tests. APPENDIX D describes the reliability of zeolite samples in the wake of constant hydrothermal cycling.) Although LDF model is a simplistic model for adsorption kinetics, its has been used by various researchers to model non-equilibrium adsorption processes ([52], [56], [89], [96]) and its validity on a macro scale has been shown by *Sircar et al* [97].

5.2.2 Energy balance equation for evaporator

The energy balance equation for the evaporator can be written as:

$$\lambda_e \dot{T}_e = \frac{V_e^2}{\Omega_e} - U_{e\_ambient}(T_e - T_a) + \psi_e \qquad \textbf{eq. 5.3}$$

Here ψ_e represents the rate of change of energy due to mass transfer across the evaporator boundary.

$$\psi_e = \dot{m}_{capillary\_out}(h_f(T_c) - h_f(T_e))$$
$$+ \dot{m}_{evap\_in}\left(h_g(P_b, T_b) - h_f(T_e)\right)$$
$$- \dot{m}_{evap\_out}\left(h_g(T_e) - h_f(T_e)\right) \quad \textbf{eq. 5.4}$$

Here subscript 'b' represents bed '*i*' and '*j*' when multiplied with mass terms related to the two beds respectively.

5.2.3 Energy balance equation for condenser

$$\lambda_c \dot{T}_c = -U_{c\_oilbath}(T_c - T_a) + \psi_c \quad \textbf{eq. 5.5}$$

Here ψ_c represents the rate of change of energy associated with condenser due to mass transfer across the condenser boundary.

$$\psi_c = \dot{m}_{cond\_in}(h_g(P_b, T_b) - h_f(T_c))$$
$$- \dot{m}_{cond\_out}\left(h_g(T_c) - h_f(T_c)\right) \quad \textbf{eq. 5.6}$$

Here subscript 'b' represents bed '*i*' and '*j*' when multiplied with mass terms related to the two beds respectively.

5.2.4 Energy balance equation for the adsorbent beds 'i' and' j'

$$\lambda_b \dot{T}_b = \frac{V_b^2}{\Omega_b} - U_{b\_ambient}(T_b - T_a)$$
$$+ \left(\frac{T_{b\_tec} - T_b}{R_{th\,b\_tec}}\right) + \psi_b ; b = i, j \quad \textbf{eq. 5.7}$$

Here ψ_b represents the rate of change of energy due to mass transfer across the boundary of the bed.

$$\psi_b = -1 \times M_z w_b(\dot{h}_g(P_{b,} T_b) - \Delta\dot{H}_{ads})$$
$$+ (\Delta_{eb})(F_{eb}) M_z \dot{w}_{b1}\left(\Delta H_{ads} - \left(h_g(P_b, T_b) - h_g(T_e)\right)\right)$$

$$+(1-\Delta_{eb})(F_{eb})M_z\dot{w}_{b2}(\Delta H_{ads})$$
$$+(\Delta_{bc})(F_{bc})M_z\dot{w}_{b3}(\Delta H_{ads})$$
$$+(1-\Delta_{bc})(F_{bc})M_z\dot{w}_{b4}(\Delta H_{ads}-(h_g(P_b,T_b)-h_g(T_c))) \quad \textbf{eq. 5.8}$$

Here $\Delta_{xy}=1$ if $P_x > P_y$. Also $F_{xy}=1$ if the valve between the components 'x' and 'y' is open. If the valve is in close state, $F_{xy}=0$.

5.2.5 Mass balance equation for the evaporator, condenser and adsorbent beds

The various mass flow terms for the evaporator, condenser and the beds have been described in the following equations.

$$\dot{m}_{evap\_in}=(-1)\dot{w}_{i2}M_{z\_i}+(-1)\dot{w}_{j2}M_{z\_j} \quad \textbf{eq. 5.9}$$

$$\dot{m}_{evap\_out}=\dot{w}_{i1}M_{z\_i}+\dot{w}_{j1}M_{z\_j} \quad \textbf{eq. 5.10}$$

$$\dot{m}_{cond\_in}=(-1)\dot{w}_{i3}M_{z\_i}+(-1)\dot{w}_{j3}M_{z\_j} \quad \textbf{eq. 5.11}$$

$$\dot{m}_{cond\_out}=\dot{w}_{i4}M_{z\_i}+\dot{w}_{j4}M_{z\_j} \quad \textbf{eq. 5.1}$$

The various '*w*' terms in the above equations have been described below.

$$\dot{w}_{bi}=\Delta_{be}F_{be}k_b(w^*_{be}-w_b);b=i,j \quad \textbf{eq. 5.13}$$

$$\dot{w}_{b2}=(1-\Delta_{be})F_{be}k_b(w^*_{be}-w_b);b=i,j \quad \textbf{eq. 5.14}$$

$$\dot{w}_{b3}=\Delta_{bc}F_{bc}k_b(w^*_{bc}-w_b);b=i,j \quad \textbf{eq. 5.15}$$

$$\dot{w}_{b4}=(1-\Delta_{bc})F_{bc}k_b(w^*_{bc}-w_b);b=i,j \quad \textbf{eq. 5.16}$$

$$\dot{w}_b=\dot{w}_{b1}+\dot{w}_{b2}+\dot{w}_{b3}+\dot{w}_{b4};b=i,j \quad \textbf{eq. 5.17}$$

In the above set of equations the subscripts '*bx*', where *b= i,j* and *x = 1,2,3,4* refer to various directions for refrigerant flow between adsorbent bed, evaporator and condenser. '*b1*' and '*b2*'refer to flow 'out of' and 'into' the evaporator respectively, whereas '*b3*' and '*b4*'

refer to flow 'into' and 'out of' the condenser. The various thermal mass terms can be expressed as:

$$\lambda_b = M_{z\_b} Cp_z + M_b Cp_b; b = i, j \qquad \textbf{eq. 5.18}$$

$$\lambda_b = M_{ref\_b} Cp_{f\_b} + M_b Cp_b; b = c, e \qquad \textbf{eq. 5.19}$$

5.2.6 ThermoElectric (TE) device

The TE device is modeled along with the contact resistances associated with the interface between TE surface and the bed surface. The equations for modeling the TE device are modified forms of equations 2.2-2.5. Fig. 5-6 shows a schematic of the TE device sandwiched in between two adsorbent beds. The diagram depicts the contact resistances as well as the assumed direction of heat flow for mathematical formulation.

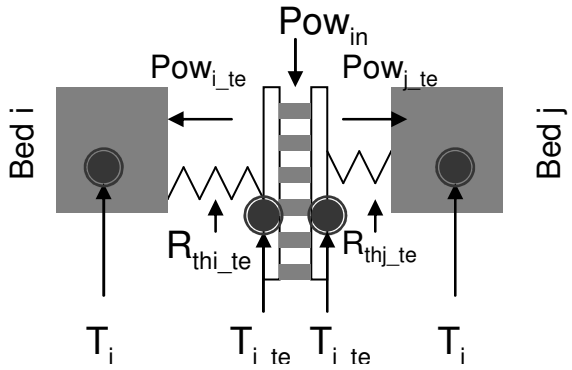

Fig. 5-6 Pictorial view that describes the heat flow path and the thermal resistances considered during the modeling of TE device interface with the adsorbent beds.

$$Pow_{i\_te} = \frac{\left(T_{i\_te} - T_i\right)}{R_{th\,i\_te}} \qquad \textbf{eq. 5.20}$$

$$Pow_{j\_te} = \frac{\left(T_{j\_te} - T_j\right)}{R_{th\,j\_te}} \qquad \textbf{eq. 5.21}$$

$$Pow_{in} - Pow_{i\_te} = Pow_{j\_te} \qquad \textbf{eq. 5.22}$$

$$\lambda_{b\_te}\dot{T}_{b\_te} = num(2N)\left(-\alpha\frac{I}{num}F_{te} - k_{te}G\right)T_{b\_te}$$

$$+ num(2N)k_{te}GT_{b\_te} + \left(\frac{T_b - T_{b\_te}}{R_{th,b\_te}}\right)$$

$$+ \frac{num(2N)\rho}{2G}\left(\frac{I}{num}\right)^2 \qquad \textbf{eq. 5.23}$$

In the above equation, the subscript may correspond to either bed i.e. $b = i, j$. Also the flag variable F_{te} = 1 when the direction of current is such that bed 'i' is heated and bed 'j' is cooled by the TE device. For the opposite condition, F_{te} = -1. These equations were solved using a MATLAB code in conjunction with the REFPROP database [80].

5.2.7 Certain specific system parameters

Table 5-1 Some key parameters of the adsorbent beds

M_b (b = i,j)	1.2176 kg
C_{pb} (b = i,j)	454.93 J-kg^{-1}-K^{-1}
Inert thermal mass = M_b x C_{pb}	553.92 J-K^{-1}
M_{z_b} (b = i,j)	0.135 kg (i), 0.145 kg (j)
C_{pZ}	1000 J-kg^{-1}-K^{-1}
Active thermal mass = M_{z_b} x C_{pZ}	135 J-K^{-1} (i); 145 J-K^{-1} (j)
Inert mass ratio = $(M_{z\_b} \text{ x } C_{pZ})/(M_{z\_b} \text{ x } C_{pZ})$	0.33
Ω_b (b = i,j)	96 Ω
$U_{b\_ambient}$ (b = i,j)	0.1 W-K^{-1}

Table 5-2 Key parameters of the evaporator and condenser

M_e	0.73 kg
C_{pe}	500 J-kg^{-1}-K^{-1}
M_c	0.42 kg
C_{pc}	500 J-kg^{-1}-K^{-1}
Ω_e	411 Ω
$U_{e\_ambient}$	0.063 W-K^{-1}
$U_{c\_oilbath}$	3.5 W-K^{-1}

Table 5-3: Some key parameters of the TE device

λi_te (thermal mass of TE device face adjacent to bed 'i'. Ceramic plate made up of Al_2O_3)	2.76 J-K^{-1}
λ_{j_te} (thermal mass of TE device face adjacent to bed 'j'. Ceramic plate made up of Al_2O_3)	3.13 J-K^{-1}
N	71
G	$0.171x10^{-2}$
Ω_{thi_te}	0.76 K-W^{-1}
Ω_{thj_te}	0.76 K-W-1
$\varrho = 4.35x10^{-8}x\ Tavg-2.754x10^{-6}$; $T_{avg} = (T_{i\_te} + T_{j\_te})/2$	
$k_{te} = 2.91x10^{-5}xTavg^2-0.019xTavg+4.81$;	
$\alpha = -2.025x10^{-9}xTavg^2+1.42x10^{-6}x\ Tavg-4.49x10^{-5}$;	

5.2.8 Comparison of the mathematical model with data in literature.

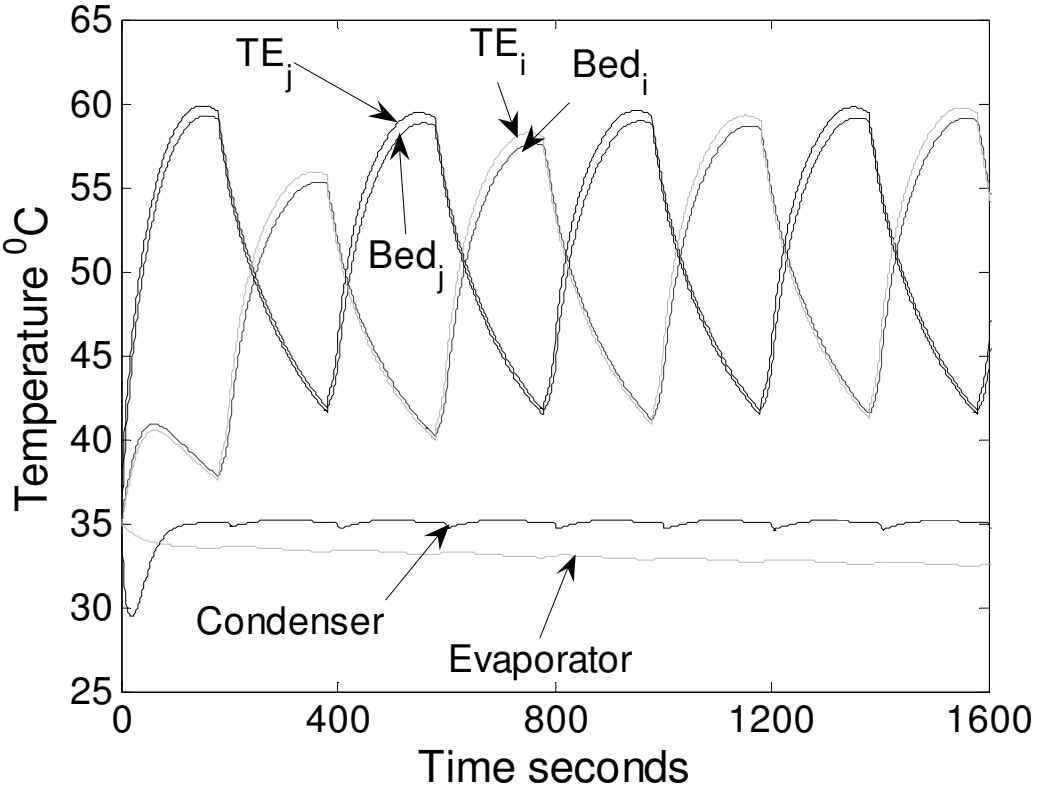

Fig. 5-7 Silica gel-Water TEA system behavior as obtained by the mathematical model developed in this chapter.

The mathematical model was compared with figure 5 in the literature by *Gorodn et al* [42]. Relevant values for silica gel –water system were taken from the work by *Gordon et al* and plugged into the mathematical model. Fig. 5-7 show the comparison.

From the figure presented above, it can be observed that the mathematical model does correctly predict the thermal behavior, however the temperatures of individual components of the TEA system, such as adsorbent beds, evaporator and condenser etc differ by as much as 20 ^{0}C when compared to the results obtained by *Gordon et al*. This difference could be attributed to the differences between the model developed in this chapter and the model used by Gordon et al. The model used by Gordon et al does not explicitly deal with thermal mass values of the hot and cold face of TE device. Paper by Gordon et al also does not explicitly mention the value of thermal resistance at the interface between TE devices and the adsorbent beds. Also heat transfer coefficient values for bed insulation were not provided.

5.3 Experimental procedure

Before the start of the experiment a vacuum pump was used to vacuum the system. At the same time resistive heaters inside the adsorbent beds were powered on to heat the beds to a temperature varying from 160 ^{0}C to 200 ^{0}C. This ensured desorption of water vapors from zeolite beds and their removal by the vacuum pump. Once the system was vacuumed, boiling water was introduced into the evaporator unit. Boiling of water before introduction insured removal of dissolved air. A 'water fill station' (same as the one used by *Jakaboski* [46] was used to drive water into the vacuumed evaporator. Flow of water was driven by atmospheric pressure. A system of valves ensured containment of water inside the

evaporator and prevented it from spilling to other sections of the system such as beds and condenser.

Once a certain amount of water was introduced (400 ml), the resistive heaters inside the evaporator were switched on. At the same time the oven heater was also initiated to raise the temperature of condenser-heat transfer fluid bath to the temperature of the 'thermally harsh environment.'

To start the experiment, the system was activated by sequential operation of valves and power supply to the TE device according to a pre determined switching and cycle time. In the beginning the valve connecting the evaporator to the capillary tube is kept in the 'off' position till the condenser is pressurized above the evaporator pressure. This is done to prevent any back flow of water from evaporator to condenser. This assumes significance because initially a vacuum exists in the condenser, whereas the evaporator pressure corresponds to saturation pressure of water at a temperature above 100 ^{0}C.

Agilent 6652A (0-20V, 0-25A) DC power supply unit was used to supply power to the TE devices. Power to the resistive heater (that simulated electronics chip heat dissipation) was supplied by Agilent 6634B (0-100V, 0-1A) DC power supply unit. Power for the pressure transducers were supplied by Agilent E3631A DC power supply unit. A variac transformer directly connected to the AC supply was used to power the resistive heaters inside the adsorbent beds. The oven that has an inbuilt temperature controller was directly powered by AC mains supply. Agilent unit 34970A was used to capture temperature, pressure and power supply data. This unit was controlled by a LabView program that activated the data acquisition unit every 10 seconds. Data was directly stored on a

computer's hard disk. Table 5-4 shows the sequence of the operation of valves and power supply during the experiment.

Table 5-4: Operating conditions

	Adsorption Bed 'i' Desorption Bed 'j'	Isosteric-heating Bed 'i', Isosteric-cooling Bed 'j'	Desorption Bed 'i' Adsorption Bed 'j'	Isosteric-cooling Bed 'i', Isosteric-heating Bed 'j'
Valve: V1	Evaporator--> Bed 'i'	Closed	Bed 'i'--> Condenser	Closed
Valve: V2	Bed 'j'--> Condenser	Closed	Evaporator --> Bed 'j'	Closed
TE Device Voltage, Amps	6V, 9.5 A	3V, 4.5A	6V, 9.5 A	3V, 4.5A
Time	8 minutes	4 minutes	8 minutes	4 minutes

5.4 Results and discussions

Fig. 5-8 shows the variation of the pressure in evaporator condenser and the bed with time. It must be noted that expansion valve is not opened until a few cycles after the condenser pressure goes above the evaporator pressure. Fig. 5-9 shows the pressure behavior as the expansion valve connects the condenser and evaporator. Thereafter evaporator temperature rises till it exhibits steady behavior. The stable thermal behavior of the system has been shown in Fig. 5-10.

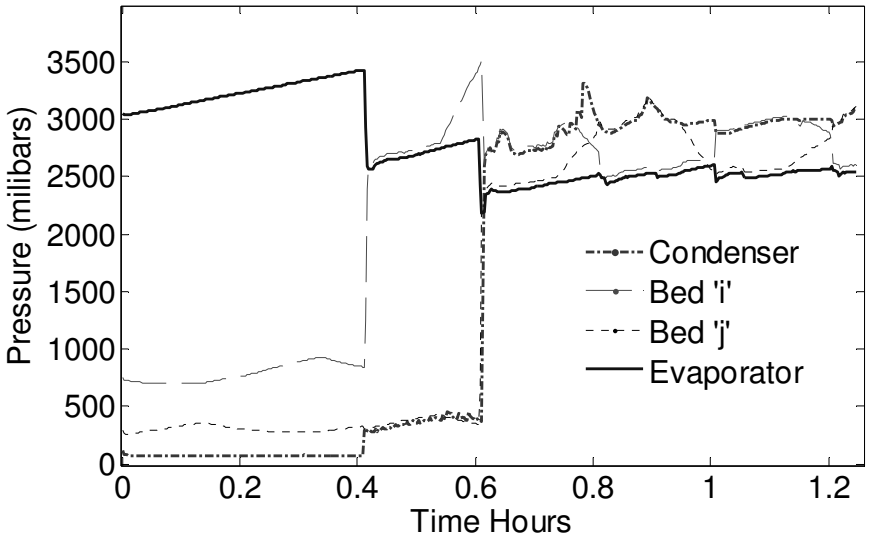

Fig. 5-8 Pressure variation during the initial few adsorption-desorption cycles. Condenser pressure rises from near vacuum to surpass evaporator pressure. Adsorption-desorption cycles start at 0.4 hours.

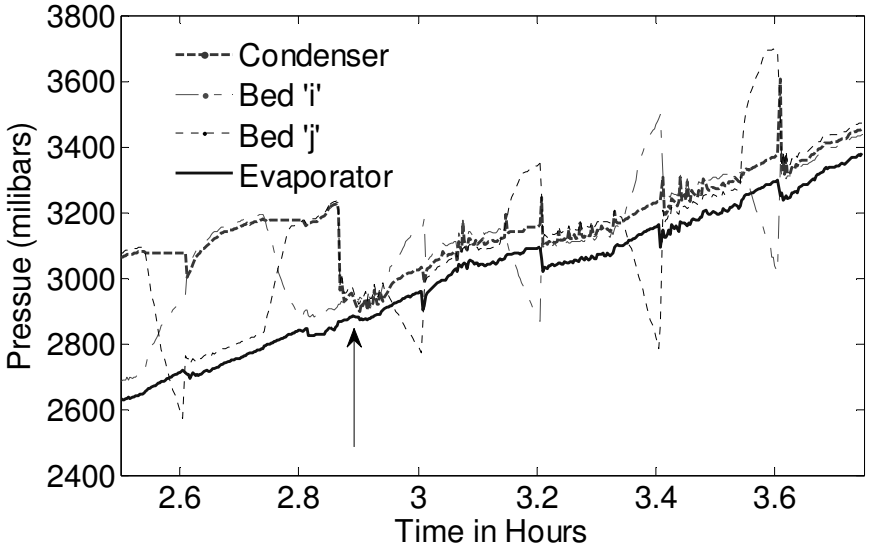

Fig. 5-9 Arrow indicating the point where an expansion valve connects the condenser and evaporator.

Throughout the experiment the resistive heater inside the bed was kept 'on' to compensate for the heat losses through insulation. Similarly, for the evaporator, a component of the power supplied was lost through the insulation. The heat loss through insulation of adsorbent beds and evaporator has been shown in [appendix HXX] This was accounted for while calculating the real thermal load managed by the system. However, the

heat leakage through the external surface of tubes connecting different system components together was assumed negligible for the purpose of this study. Also assumed negligible were any pressure losses from the adsorbent beds. The voltage and current supplied to the TE device has been plotted in figure 5-9. The sum of electrical power provided to the adsorbent bed-TE device arrangement, less the heat leakage through bed insulation, has been plotted in figure 5-10. Here the plot of electrical power input to evaporator, less the heat leakage through its insulation, has also been plotted.

Figure 5-10 gives us vital information about the COP of the system as a heat pump. Estimating the area under the plot for net power to bed+TE device will determine the total energy provided for the time window of the plot. Similarly the area under the plot for net power provided to evaporator will determine the heat pumped from evaporator. A ratio of the two will indicate the overall system COP, which was calculated to be approximately 0.2.

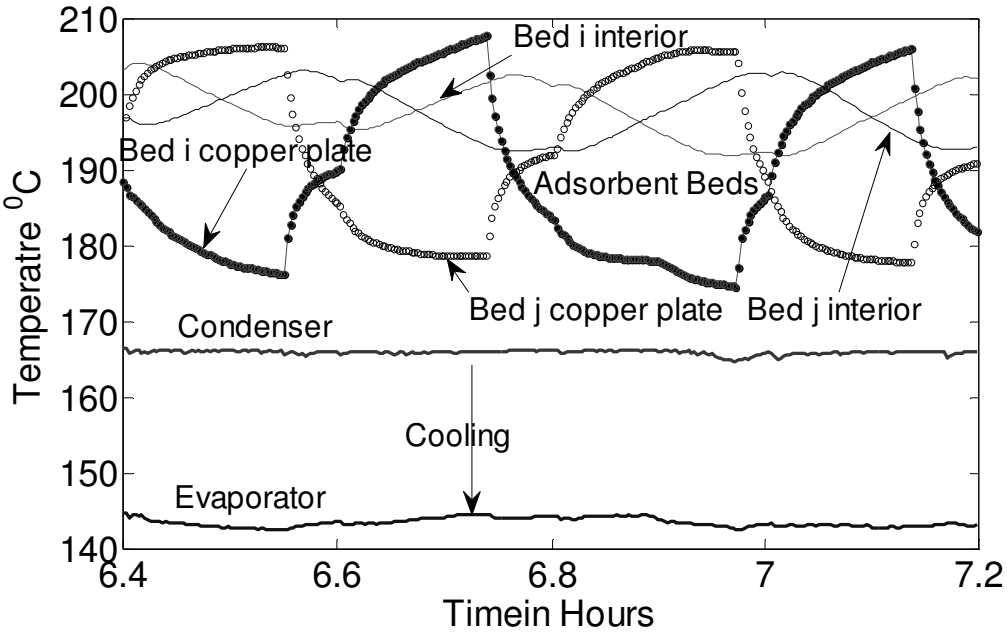

Fig. 5-10 Temperature plot after the thermal behavior of the system became stable.

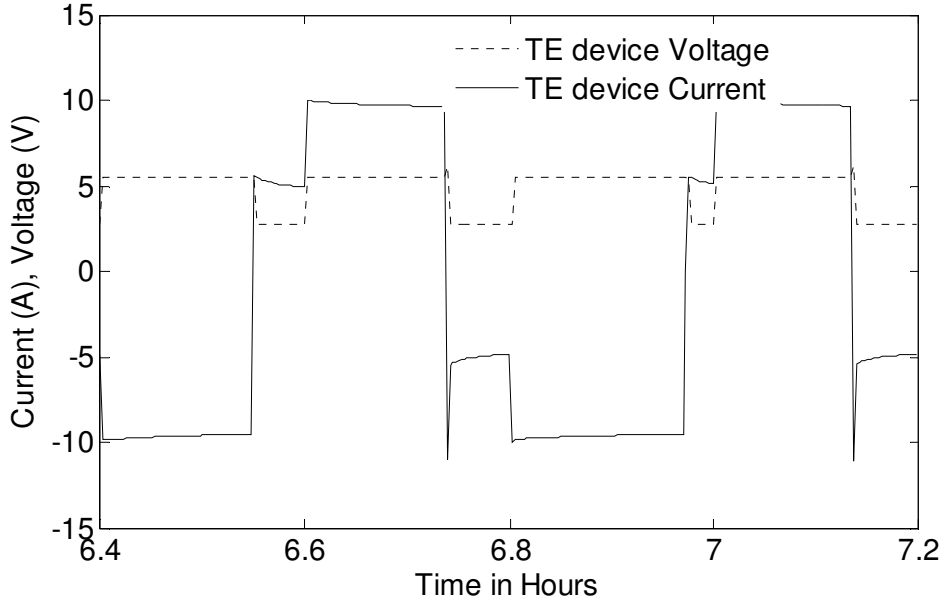

Fig. 5-11 Plot showing the voltage and current supply to TE device. It must be noted that absolute value of voltage supplied has been plotted. The change in voltage polarity is reflected by the change in the direction of current flow (here the change in the sign of the current from positive to negative and vice-versa).

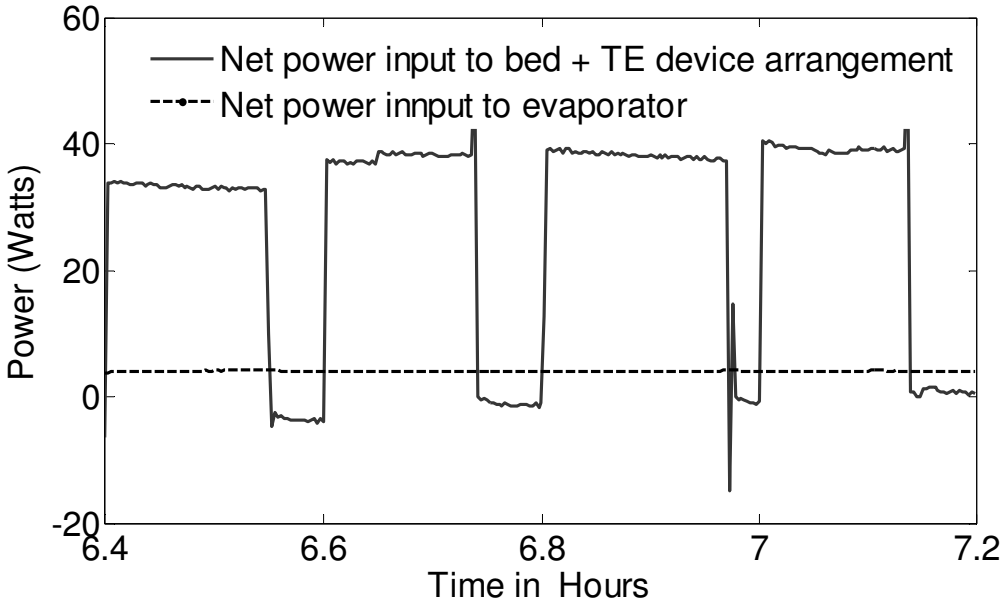

Fig. 5-12 Net power input to beds+TE device arrangement has been compared with net power input to the evaporator.

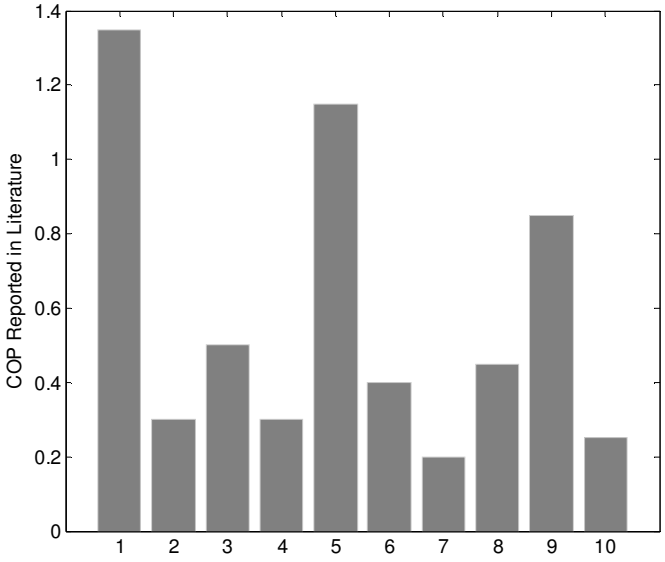

Fig. 5-13 Value of COP as reported by various researchers. 1: Liu et al [50]; 2: Anyanwu et al [51]; 3: Wang et al [68]; 4: Dawoud et al [54]; 5: Hajji et al [56]; 6: Zhang et al [59]; 7: Sward et al [60]; 8: Restuccia et al [61]; 9: VanBenthem et al [62]; 10: Lu et al [65].

The value of COP obtained during experiment compares well with those reported in literature. Figure 5-11 shows the various COPs for the zeolite-water adsorption systems. It must be noted that the reported COPs do not necessarily represent an adsorption system with TE driven heat regeneration. Another differentiating factor is that none of the systems were used for harsh environment cooling. However, for near room temperature cooling, experiments involving an adsorption heat pump with thermoelectric regeneration were carried out by Ng et al [45]. The system contained silica gel-water as the adsorbent – adsorbate pair and the COP was in the vicinity of 0.7.

Figure 5-12 presents a plot of bed, evaporator and condenser temperatures for the mathematical simulation and the experiment. The simulated temperature compares well with experimental for the beds and the condenser, however it is widely different for the evaporator. The experimental values for evaporator temperature differ by about 10% from

the corresponding values obtained from simulations. Simulations show much less cooling than what is observed during experiments. This could be a possible result of neglecting parasitic heat losses through tubing insulations and refrigerant vapor leakage throughout the set-up.

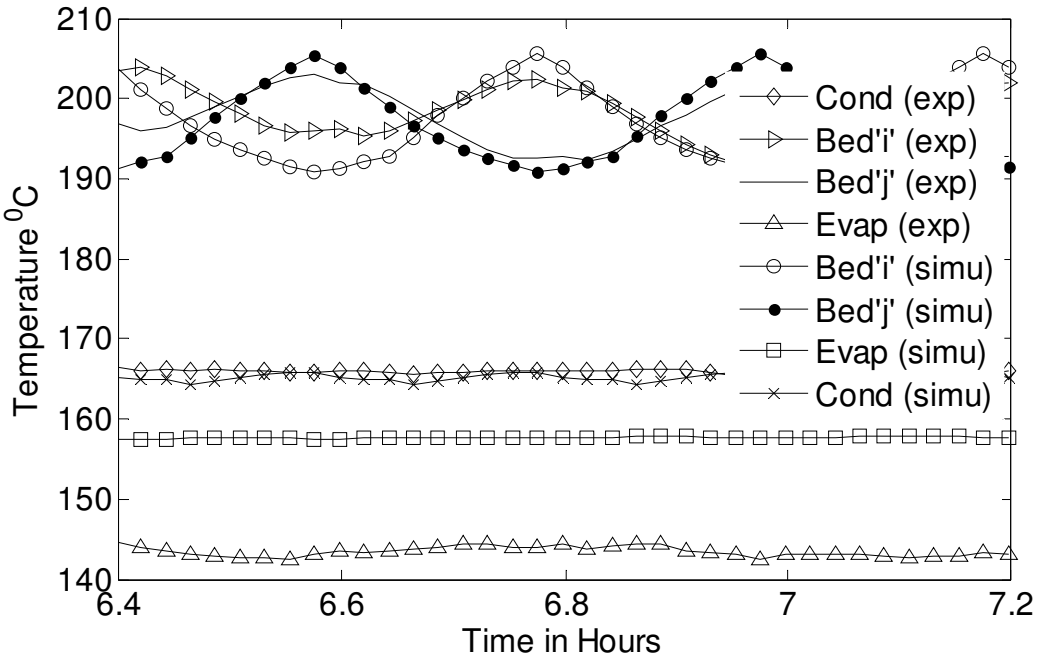

Fig. 5-14 Comparison of simulated and experimental temperature at the beds, the condenser and the evaporator.

5.5 Error estimation in the experimental readings

Errors for various measurements have been reported in Table 5-5. These values were used along with equations 5..24 to obtain the errors in various parameters such as Power and water uptake of zeolites. According to the equation [108], for a parameter $Param = f(x_1, x_2, x_3, ...x_n)$ that is a function of several variables x_1, x_2, x_3... x_n, with the associated errors in variable measurement being x_{1err}, x_{2err}, x_{3err}... x_{nerr}, the error in the calculation of parameter is given by:

$$Param_{error} = \left[\left(\frac{\partial Param}{\partial x_1} x_{1err} \right)^2 + \left(\frac{\partial Param}{\partial x_2} x_{2err} \right)^2 + \left(\frac{\partial Param}{\partial x_3} x_{3err} \right)^2 + ... \left(\frac{\partial Param}{\partial x_n} x_{nerr} \right)^2 \right]^{(1/2)}$$

eq. 5.25

Table 5-5 Errors for various measurements.

Parameter	*Error*
Temperature readings	+/- (1+ 0.75%) ^{o}C
Voltage measurement AC (Bed resistive heaters)	+/-(0.06% of reading + 0.04% of 100V)
Current measurement AC (Bed resistive heaters)	+/-(0.1% of reading + 0.04% of 1A)
Voltage measurement DC (TE device power supply)	+/-(0.07% of reading+15mV)
Current measurement DC (TE device power supply)	+/-(0.35% of reading + 44mA)
Voltage measurement DC (Evaporator resistive heater)	+/-(0.03% of reading + 12mV)
Current measurement DC (Evaporator resistive heater)	+/-(0.1% of reading + 2.5e-6A)
Pressure measurements	+/- (7.3635) milibars
Insulation heat loss analysis (beds)	+/- 0.4358 W
Insulation heat loss analysis (evaporator)	+/- 0.3993 W

Using equation 5.24, the error terms with power supply to evaporator, bed and TE device were calculated as +/-0.025 W, +/- 0.05 W and +/- 0.3W respectively. Hence in Fig. 5-12 the plot for net power supply to the bed + TE device assembly has an error of +/- (0.05+0.3+0.4358 insulation heat loss error) = +/-0.74W. Similarly the plot for net power supplied to evaporator has an uncertainty of +/-(0.025+0.39 insulation heat loss error) = +/-0.415 W.

The estimation of error in the readings should also incorporate the parasitic vapor losses taking place through the adsorbent beds. In order to incorporate these losses, pressure decay plot of the beds were considered. These plots were obtained by capturing the temperature and pressure decay data for the beds after the experiments were over. Fig. 5-15 represents a typical decay plot that was obtained for several experiments. The pressure

showed a rapid decline once the beds were allowed to cool naturally. The pressure was observed to fall below the ambient atmospheric pressure and then further rise back to the atmospheric pressure as the beds reached thermal equilibrium. This can be attributed to the fact that zeolite adsorbed water as it cooled down, thus creating a negative pressure in the bed. For the stage till the pressure was above atmospheric, a decline in total water content in the bed was also observed. This was due to the exit of vapor through cracks (openings) in the bed structure.

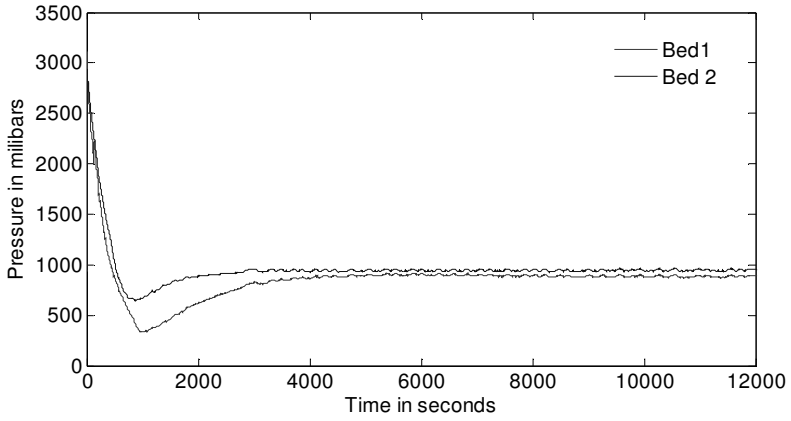

Fig. 5-15 Typical pressure decay plot that was observed

Since the difference between bed and ambient pressure *'ΔP'*, and the decline in vapor content with time (mass flow rate out of beds) was known, equation 5.25 was used to obtain the velocity of the vapor moving out. This exit velocity when combined with vapor density and mass flow rate (equation 5.26) provided an estimate of the cross-sectional area of the bed through which pressure was leaking out.

$$\Delta P = \rho(Velocity)^2 / 2 \qquad \textbf{eq. 5.24}$$

$$CrossSectionalArea = (mass\_flow\_rate)/[(Velocity)\rho] \qquad \textbf{eq. 5.25}$$

The estimated cross-sectional area was used to determine the vapor losses taking place during the experiments. A product of the vapor loss and latent heat of vaporization

provided an estimate of parasitic cooling through vapor leakage. This was observed to vary from 1.2 to 1.8 W.

5.6 Conclusion

The work presented in this chapter, shows the application of a prototype TE device driven adsorption system for harsh environment electronics cooling. The size of the adsorbent bed is compact enough for the system to fit inside a space of the order of a conventional desktop computer. The system was operated for a targeted evaporator temperature in the vicinity of 140 ^{0}C and a condenser temperature in the vicinity of 170 ^{0}C. The system has comparatively low COP of 0.2, however the mathematical estimation reveals that considerable scope for improvement exists in terms of heat transfer enhancement inside bed and proper insulation of system components.

CHAPTER 6: System simulation and experiments with modified cycle

In this chapter performance of a two-stage thermoelectric adsorption heat pump has been presented. Two-step adsorption aims to reduce the thermal variations at the hot and cold faces of the thermoelectric device, thus enhancing its performance. Here, adsorption takes place at two different pressures and this requires two evaporators at two different temperatures. This is unlike most 'conventional' adsorption systems where adsorption takes place at a single evaporator pressure. An experimental setup (for two-step adsorption) was fabricated and tested for a heat rejection temperature of 180 ^{0}C and cooling load varying from 4 to 6W. Experiments were also carried out for a single step (conventional) adsorption cycle for similar conditions to compare the performance of two-step 'modified' adsorption cycle vis-à-vis single step 'conventional' adsorption cycle..

6.1 Brief recap: need for modified cycle

The import of modified cycle in the context of harsh environment application of TEA cooling system has been described in detail in chapter 3. Here a brief recap of the benefits of the modified cycle is provided for the convenience of the readers. Fig. 6-1 shows a conventional cycle with point of highest cycle temperature 'T_H' and thermal swing marked on the Clausius diagram. Fig. 6-2 shows a modified cycle superimposed on a conventional cycle. Reduction of the highest cycle temperature and thermal swing (that aid the application of TE device in between beds) can be graphically observed. The modified cycle has two condensers and two evaporators. For experimental purpose however a slight modification was done to accommodate a simple apparatus. Instead of two condensers, only one condenser was chosen while the number of evaporators was still maintained at two. Fig. 6-3 describes the accompanying Clausius diagram for such a case.

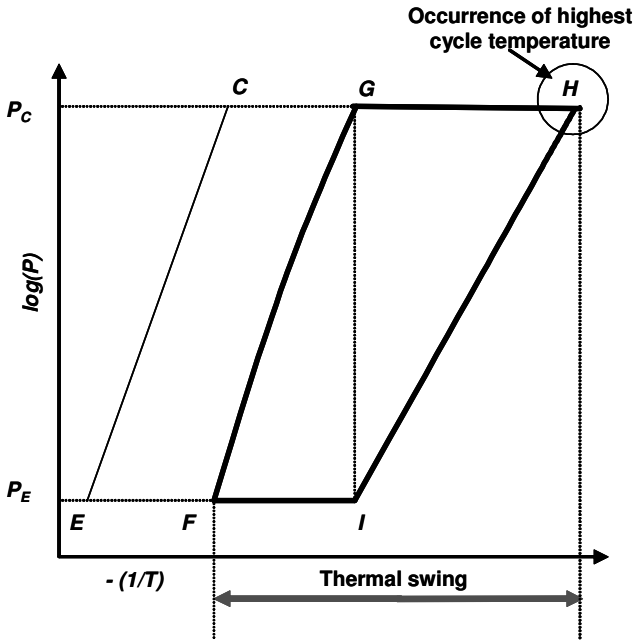

Fig. 6-1 Clausius diagram of an adsorption cycle showing thermal swing (maximum temperature variation during the entire cycle) and the highest temperature encountered (also the highest regeneration temperature at point H)

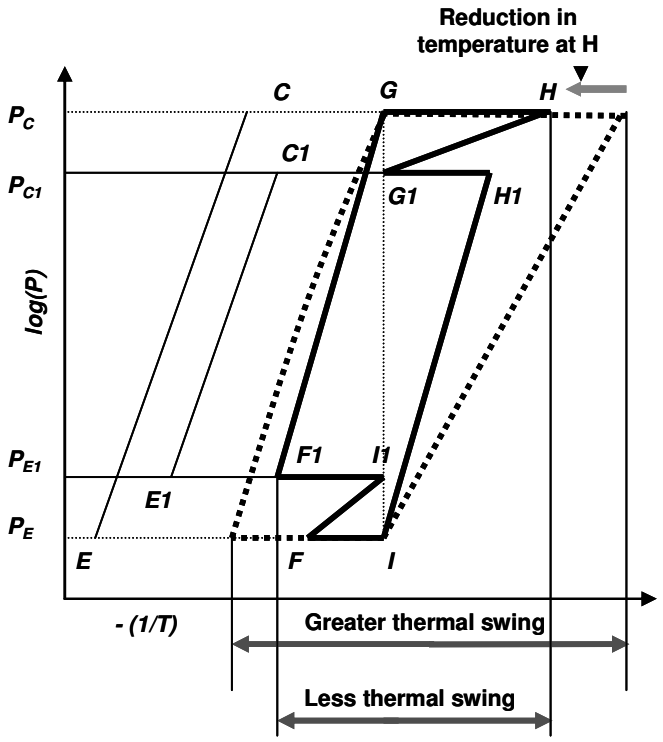

Fig. 6-2 Modified cycle as suggested by the authors, superimposed on a conventional cycle. The reduction in thermal swing and the retreat of highest regeneration temperature at H towards a lower temperature regime must be noted.

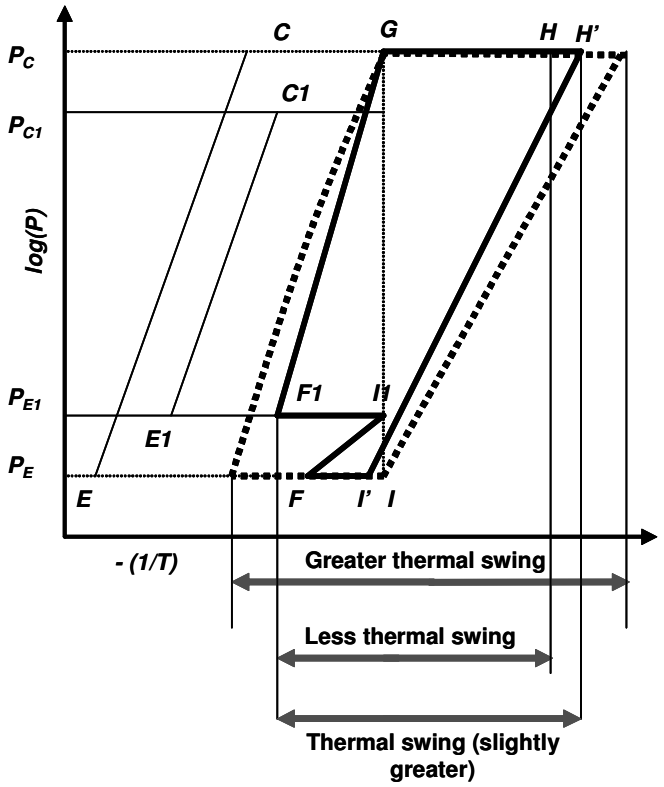

Fig. 6-3 Clausius diagram of a cycle (I'-F-F1-G-H'-I') with a single condenser and two evaporator arrangement. The arrangement leads to a small increase in thermal swing. In this arrangement, process H-G1 as shown in figure 4 is merged into process G-H by keeping the desorbing bed exposed to condenser pressure.

6.2 Experimental prototype

An experimental prototype was fabricated and assembled. The set was the same as described in the previous chapter, except for an extra evaporator unit. Fig. 6-4 shows the schematic of the set-up. A brief description of the parts of the set up is given below. A photograph of the set up has been shown in Fig. 6-5.

6.3 Experiment procedure

The experimental procedure used was the same as expressed in section 5.3. However since two evaporators were involved the sequence of operation of valves and power supply to the TE device was different from the one mentioned in the previous chapter.

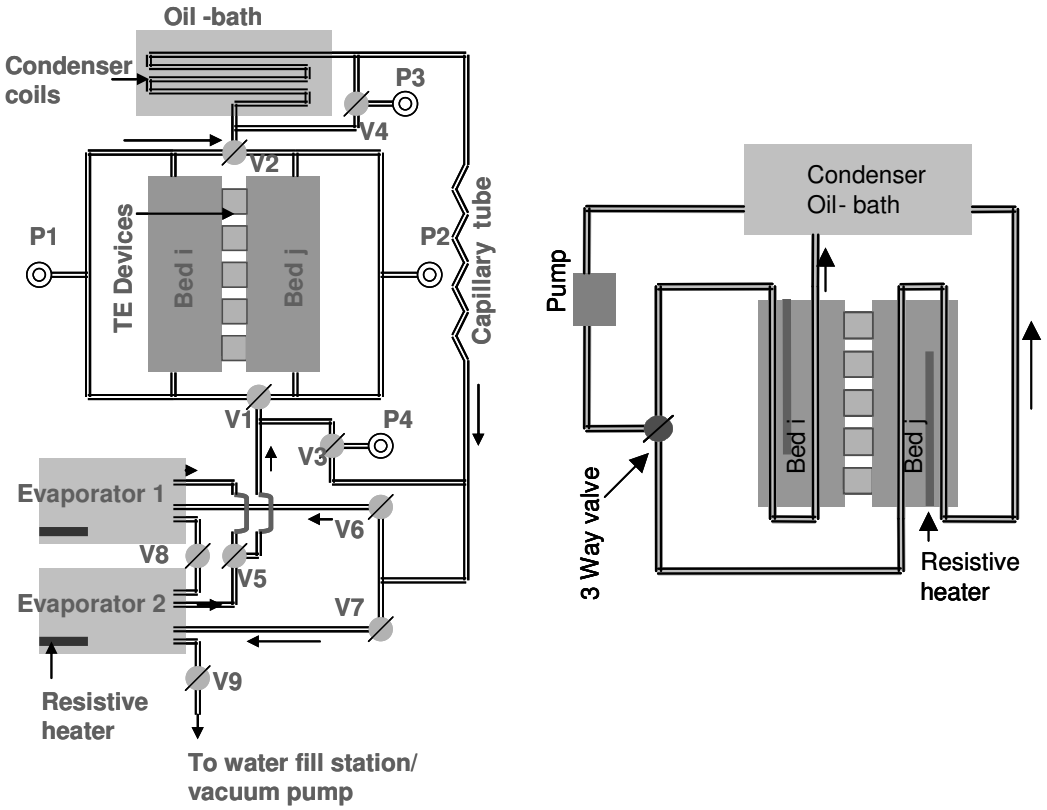

Fig. 6-4 (Left) Schematic diagram of the experimental set-up showing condenser, evaporator(s), adsorbent beds and the refrigerant flow loop. (Right) Schematic diagram of the cooling fluid loop through the adsorbent beds. P1...4 are the pressure transducers. Valves V1..V5 are three way valves. valves V6-V9 are two way valves. V1 and V2 help connect beds with either condenser or evaporator. Valves V3 and V4 help measure evaporator and condenser inlet and outlet pressure by using just two pressure transducers (P3 and P4). V5 helps connect any one of evaporator with the adsorbent beds. V6 and V7 connect evaporators with capillary tube. V8 allows for water to pass from evaporator 1 to 2 during filling operation. Also helps keep evaporators isolated during operation. V9 provides a link to water fill/ vacuum station.

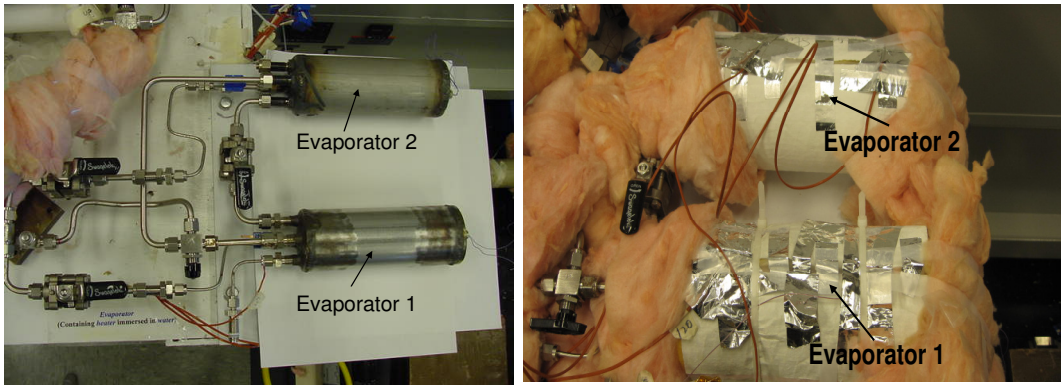

Fig. 6-5 Photographs of the two evaporator assembly. (Left) un insulated. (Right) Insulated.

Table 6-1 shows one complete block of operation. This block was repeated as the experiment continued. The understanding of the sequence of operation can be made simpler

if it is put in the context of both modified and conventional cycles. For the conventional (single step cycle) steps 1-4 would be repeated after step 4, whereas for the modified (two step cycle), steps 1-8 will be repeated after step 8. The sequence of operations has been designed such that the cycle time for both modified and conventional cycle is the same (= 12 minutes).

Table 6-1: Operating conditions for the two-step 'modified' adsorption cycle.

	Time (mins)	TE device voltage	TE device: Heat pump direction	Valve 1	Valve 2	Valve 5	Valve 6	Valve 7
Step 1	4	6V	bed i - bed j	evap - bed i	bed j - cond	to evap 1	evap 1	closed
Step 2	2	3V	bed j - bed i	closed	bed j - cond	to evap 1	evap 1	closed
Step 3	4	6V	bed i - bed j	evap - bed i	bed j - cond	to evap 2	closed	evap 2
Step 4	2	3V	bed j - bed i	closed	closed	to evap 2	closed	evap 2
Step 5	4	6V	bed j - bed i	evap - bed j	bed I - cond	to evap 1	evap 1	closed
Step 6	2	3V	bed i - bed j	closed	bed I - cond	to evap 1	evap 1	closed
Step 7	4	6V	bed j - bed i	evap - bed j	bed I - cond	to evap 2	closed	evap 2
Step 8	2	3V	bed i - bed j	closed	closed	to evap 2	closed	evap 2

The easy adaptability of the experimental set up for single –step 'conventional' adsorption cycle allowed experiments to be performed for both modified (two-step) and conventional (single step) adsorption cycles. It must be noted that while operating for the modified cycle, valves 8 and 9 always remained close. During operation of conventional cycle, one of the evaporator (evaporator 1) was isolated by making V5 connect to evaporator 2, closing V6 and keeping V7 open.

6.4 Results and Discussion

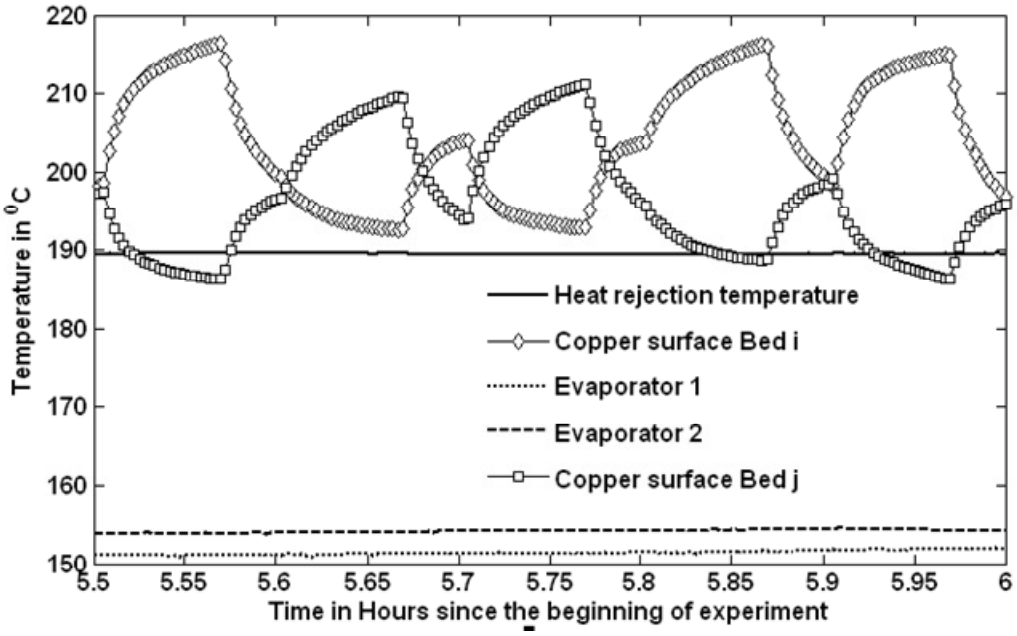

Fig. 6-6 Temperature at various components of the two-step adsorption cooling system at near steady state condition.

Fig. 6-6 shown above depicts the thermal behavior of the two step adsorption cycle at near steady state conditions. The experiment was truncated before a condition of perfect steady state could be achieved. At the time of the data capture, the rate of increase in temperature of evaporators was nearly 2 ^{0}C per hour. The peaks (and dips) in the temperature of a bed represent the process of pressurization (constant volume heating) and depressurization (constant volume cooling) respectively. Pressurization is followed by desorption (i.e. release of refrigerant vapors to condenser and depressurization is followed by adsorption (i.e. intake of refrigerant vapors from the evaporator). The two evaporator temperature plots in Fig. 6-6 are noteworthy as they show the two evaporators at slightly different temperature.

Fig. 6-7 compares the temperature behavior of a two-step (modified) adsorption cycle with a single-step (conventional) adsorption cycle for the same time duration. It can be observed that the bed temperatures in the single step adsorption cycle are higher than that of the 2-step adsorption cycle. The thermal swing (or the difference between extremes of temperature observed in a bed) is also lower for the 2-step adsorption cycle. The evaporator temperature in the single step adsorption cycle is slightly higher than the temperature of the two evaporators in the 2-step adsorption cycle.

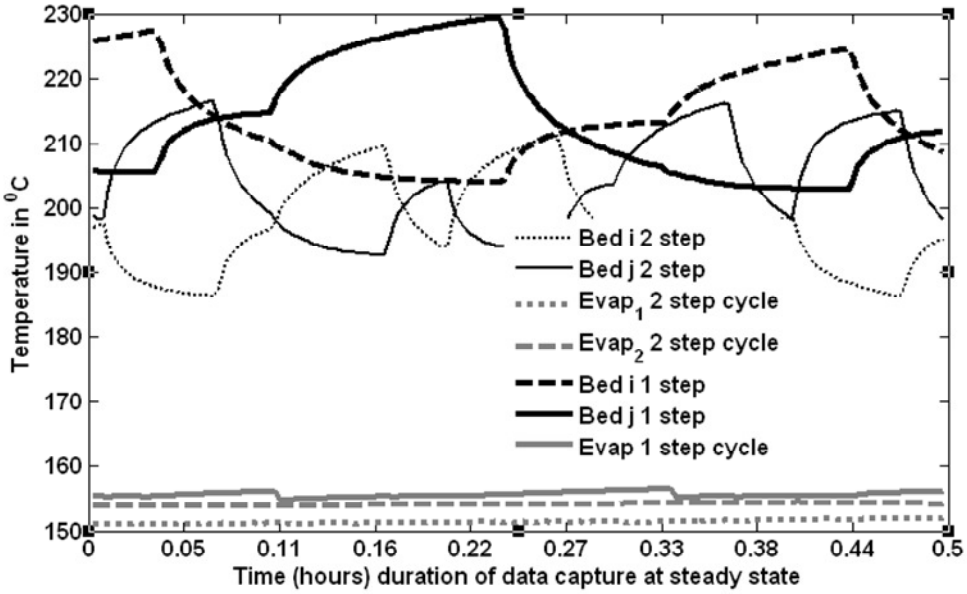

Fig. 6-7 Comparison of temperature at beds and evaporator(s) for a modified (2-step) and a conventional (1-step) cycle.

The main advantage of the 2-step cycle lies in the reduction in highest temperature and a drop in thermal swing for the adsorption beds. For both (2-step and single-step) experiments, the adsorption beds were heated to and maintained at 145 ^{0}C before the start of the experiment. Hence whatever heat was provided by the resistive heaters was completely lost to ambient through insulation at the initial steady state temperature. Any change in bed temperatures after the initiation of experiment was due to the alternate heating and cooling

performed by TE device. Hence, in order to conclusively prove the advantage of 2-step cycle over single-step, it must be shown that during the course of the experiment, both cycles were provided the same amount of average energy per unit time by TE device. Fig. 6-8 compares the electrical power input to TE device for both cycles. From the figure it can be observed that the area enclosed under both the power plots for a time interval of one cycle time (i.e 12 minutes: ref section 5) is the same.

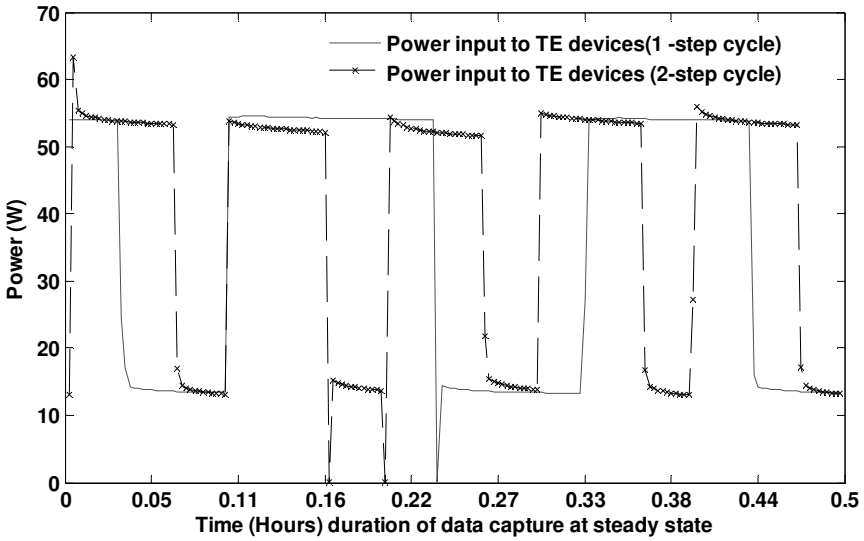

Fig. 6-8 Comparison of power input to TE devices for single as well as two step cycle experiments.

Fig. 6-9 compares the net energy input to the beds and TE devices with the heat dissipated at the evaporator(s). This has been shown for single-step as well as two-step adsorption cycles. 'Net' energy refers to total electrical energy input, less the energy lost as heat leakage through insulations. Under steady state the ratio of heat dissipated at evaporator(s) and the net energy input to beds and TE devices should be an indication of the overall system COP. The COP obtained for the single –step and two-step adsorption cycles are 0.28 and 0.35 respectively. Error analysis figures for this experiment are similar to the one described in section 5.5.

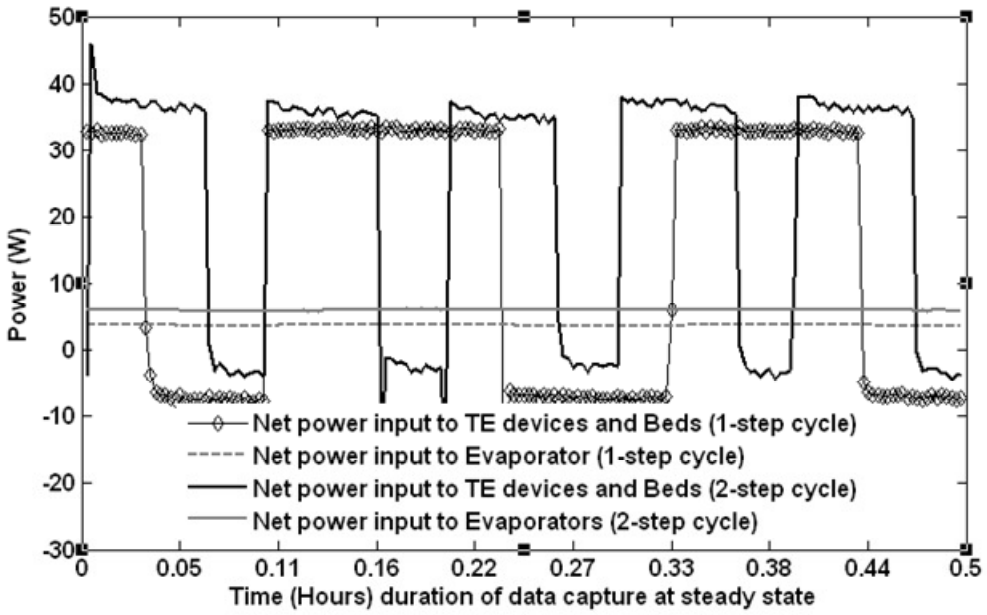

Fig. 6-9 Net power input to the various components of the systems. Plots have been made for both single-step and two-step adsorption cycle experiments.

6.5 Conclusions

The two-step adsorption cycle aims at reducing the temperature variations at the hot and cold faces of a TE device and at the same time reduces the overall temperature that the hot side may face during regeneration. This has the effect of improving the overall cycle efficiency. Experimental results show an improvement in COP over the single-step adsorption cycle and decrease in temperature variations across the TE device. However, a drawback that has not been well studied in this chapter is the effect of switching frequency on the performance of the TE device. The TE device-switching frequency doubles as we move from single-step to two-step adsorption cycles. This could have a negative effect on TE device performance.

CHAPTER 7: Comprehensive formulation for performance of TEA chiller and its comparison with adsorption and TE chillers

The seemingly low COP as observed during the experiments bring into question the validity of the expression $COP_{TEA} = COP_{ads}(1+COP_{TE})$ as suggested by Gordon et al [42]. While one primary reason could be the poor heat transfer inside the adsorbent bed, another could be the heal leakage through the bed insulations. The current theoretical work aims to incorporate the heat leakage and develop a comprehensive formulation for the COP of the overall TEA system. Also since TEA chiller comprises Adsorption and TE chillers, the use of TEA chillers must be justified on the basis of superior performance vis-à-vis TE and Adsorption chillers. The work presented in the current chapter describes a common framework that was developed to compare performances of the three dissimilar chillers. A heat rejection temperature range of 50 to 200 ^0C was considered for this investigation. Results show the effect of heat leakage through beds on the performance of TEA chillers, an optimum operating method to obtain COP system as $COP_{ads}(1+COP_{TE})$ and that a TE device is preferable for cooling up to a range of 20-30 ^0C below the ambient. Beyond this range a TEA chiller is a good option.

7.1 Comprehensive expression for the COP of TEA heat pump

Fig. 7-1 is a representation of Fig. 2-6-right with energy terms associated with various processes shown along the adsorption cycle. Referring to Fig. 7-1 Q_d and Q_{FG} represent the energy required by processes G-H and F-G respectively. Q_{HI} and Q_a represent the energy released by processes H-I and I-F respectively. Process H-I-I' is at a higher temperature than F-G-G', hence heat transfer from an adsorbent bed undergoing process H-I-I' to a bed undergoing process F-G-G' does not require any active heat pump mechanism. However heat released during the part of the adsorption process I'-F $(Q_a - \Delta_1)$ needs to be actively

pumped to the part of desorption process denoted by G'-H. Depending on the temperature difference between adsorbing and desorbing bed, the TE devices may or may not be able to pump all of the heat of adsorption to the desorbing bed. We include a parameter Δ_3 such that once the TE device has pumped $(Q_a - \Delta_1 - \Delta_3)$ to the desorbing bed, the rest of the heat, i.e. Δ_3, must be driven away from the adsorbing bed to the ambient. For this, the adsorption cycle is designed such that the temperature at point F(T_F) is greater than the ambient temperature.

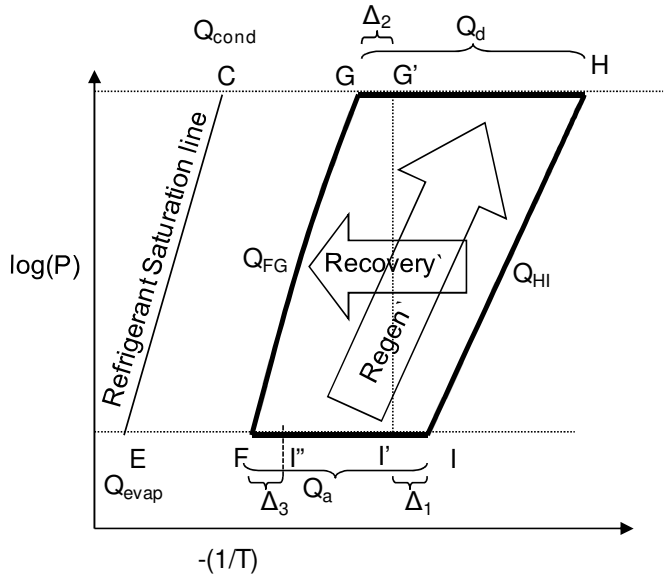

Fig. 7-1 Depiction of thermo physical processes on a Clausius-Clapeyron diagram. Adsorption (I-F), constant volume heating (F-G), desorption (G-H), constant volume cooling (H-I). The dotted line G'-I' represents a temperature T_{mid} such that heat released during H-I' equals heat required by F-G'. Also shown are heat recovery and regeneration.

Also, since the heat rejected at the hot face of a TE device is greater than the heat pumped at the cold face, the desorbing bed will get heat in excess of its requirement, which must be rejected to the ambient. Hence both beds must have appropriate cooling arrangements to drive out the heat that is not needed. This can affect the COP and it will be accounted for in our formulation.

COP of the adsorption chiller alone (i.e. without TE device, as described in section 2.2), is given by the ratio of heat pumped from the evaporator (Q_{evap}) to the total energy required during the cycle, i.e. energy required by the endothermic processes, less the energy recovered from the exothermic processes. COP of the TEA chiller is given by the ratio of heat pumped from evaporator (Q_{evap}) to the total electrical energy input into the TE device. The relationship between the COPs of adsorption chiller and the TE device that describes the overall COP of TEA chiller has been derived below.

Since the heat required by process to the left of T_{mid} (see caption Fig. 7-1) equals heat given off by process to the right of T_{mid}, we have:

$$Q_{FG} + \Delta_2 = Q_{HI} + \Delta_1 = Q_r \qquad \textbf{eq. 7.1}$$

Here Q_r is the total amount of heat that can be recovered. For an adsorption chiller, this is easily done by circulating heat transfer fluid from hot bed to the cool one, whereas in the case of TEA chiller, since beds are not in direct thermal contact due to the TE devices sandwiched in between them, some electrical power input is required to drive the heat. This power input is considered negligible for the analysis in this work. Using equation 7.1, the COP of the adsorption process can be expressed as:

$$COP_{ads} = \frac{Q_{evap}}{Q_{FG} + Q_d - Q_r} = \frac{Q_{evap}}{Q_{FG} + Q_d - Q_{HI} - \Delta_1} = \frac{Q_{evap}}{Q_{FG} + Q_d - Q_{FG} - \Delta_2} \qquad \textbf{eq. 7.2}$$

Similarly, the COP of the TE and TEA chillers can be expressed as:

$$COP_{TE} = \left(\frac{Q_a - \Delta_1 - \Delta_3}{Pow_{in}} \right) \qquad \textbf{eq. 7.3}$$

$$COP_{TEA} = \left(\frac{Q_{evap}}{Pow_{in}} \right) = COP_{ads} \left(\frac{Q_{FG} + Q_d - Q_{HI} - \Delta_1}{Q_a - \Delta_1 - \Delta_3} \right) COP_{TE} \qquad \textbf{eq. 7.4}$$

$$\Rightarrow COP_{TEA} = COP_{ads}\left(\frac{\Delta_1 - \Delta_2 + Q_d - \Delta_1}{Q_a - \Delta_1 - \Delta_3}\right)COP_{TE} = COP_{ads}\left(\frac{Q_d - \Delta_2}{Q_a - \Delta_1 - \Delta_3}\right)COP_{TE} \qquad \textbf{eq. 7.5}$$

If all of the heat dissipated by TE device at its hot end is used for desorption $\left(\Rightarrow Q_a - \Delta_1 - \Delta_3 + Pow_{in} = Q_d - \Delta_2\right)$, equation 7.5 can be expressed as:

$$\Rightarrow COP_{TEA} = COP_{ads}\left(\frac{Q_a - \Delta_1 - \Delta_3 + Pow_{in}}{Q_a - \Delta_1 - \Delta_3}\right)COP_{TE} = COP_{ads}\left(1 + COP_{TE}\right) \qquad \textbf{eq. 7.6}$$

This is also the expression obtained by *Gordon et al* [42] for the TEA chiller. This expression shows direct enhancement of COP_{ads} by a factor greater than unity i.e. $\left(1 + COP_{TE}\right)$. However, since the heat required by the desorption process is nearly equal to the heat released by the adsorption process, for this expression to be valid the TE device would have to be highly efficient. Most TE devices have COP less than unity and hence, the desorbing bed gets heat energy in excess of its requirements and the excess heat needs to be rejected to the ambient. Assuming that the heat requirement of the desorption process is some fraction $'\lambda'$ of the heat provided by the TE device, i.e. $\left(Q_d - \Delta_2\right) = \lambda\left(Q_a - \Delta_1 - \Delta_3 + Pow_{in}\right)$, equation 7.5 can be expressed as:

$$COP_{TEA} = COP_{ads}\left(\frac{\lambda\left(Q_a - \Delta_1 - \Delta_3 + Pow_{in}\right)}{Q_a - \Delta_1 - \Delta_3}\right)COP_{TE} = COP_{ads}\lambda\left(1 + COP_{TE}\right) \qquad \textbf{eq. 7.7}$$

Equation 7.7 gives a more realistic estimate of COP_{TEA}. Another fact to be noticed is that the final expression for COP does not contain Δ_3. This is significant, since it implies that the final COP is not affected by any heat rejection from adsorbing bed to the ambient.

7.1.1 Optimum method of operation for TEA chiller

Based on the observations in the above paragraph, it can be stated that assuring maximum value of 'λ' (i.e =1) will ensure the COP of the TEA chiller as $COP_{ads}(1+COP_{TE})$.

This will require good insulation for the desorbing bed so that all the heat that is delivered at the hot face of the TE device is utilized in desorption. Also since the heat delivered at the hot face of TE device is much greater than the heat pumped at the cold face, the process of desorption would get finished sooner than the process of adsorption. Thus once the desorption process is over, the adsorption bed would still need to be cooled for the remaining of the adsorption process. Since it has been shown that the final COP expression is independent of the term Δ_3, the heat of adsorption can be released to the ambient without having any effect on overall COP. While this is being done, the TE devices should be switched off. Hence an arrangement to reject heat of adsorption directly to ambient and to well insulate the beds during desorption will be required to realize this method of operation in practice.

7.2 TE, TEA or Adsorption chiller?

The TEA chiller, first proposed by *Gordon et al* [42] and investigated for near room temperature cooling of electronics by *Ng et al* [45], combines TE chiller and an Adsorption chiller. Both these systems can also independently serve as electronics coolers. Use of TE device for electronics cooling can be found in literature (*Chu et al* [98], *Simons et al* [99], *Lakhkar et al* [100], *Vandersande et al* [101], *Sahu et al* [102], *Moores et al* [103], *Nie et al* [104]). *Jakaboski* [46] has mentioned a few instances of using TE devices for cooling of harsh environment electronics. Likewise the use of an Adsorption chiller for electronics cooling has also been reported (*Suman et al* [105]).

Hence there is a need to investigate if a TE device, when applied alone, could outperform the TEA and the adsorption chiller by itself. This becomes important in the context of applications that only require moderate cooling below ambient, and in cases

where the ambient environment is thermally harsh (>125 ^{0}C). In the first context the TE COP may outweigh that of a TEA or an adsorption chiller. In the second, the performance of TE device deteriorates due to high temperatures, and gains in overall COP of TEA chiller due to heat regeneration become marginal. With recent advancements in TE technology (*Fleurial et al* [106] and *Venkatasubramanian et al* [107]), a quantitative performance comparison of TEA, AHP and TE devices is needed to justify the use of TEA heat pump over AHP or TE device.

7.2.1 Comparing mathematical formulations for COP

Equations 2.1, 2.6 and 7.7 provide expressions for the COP of TE, Adsorption and TEA chillers respectively. To justify the use of TEA chillers, following criteria must be met for identical evaporator and condenser temperature.

$$COP_{TEA} = COP_{ads\_TEA}\lambda(1 + COP'_{TE}) > \max(COP_{ads\_TEA}, COP_{ads\_alone}, COP_{TE}) \qquad \textbf{eq. 7.8}$$

In the above expression COP'_{TE} represents the COP of TE device while working as heat regenerator in between adsorbent beds, whereas COP_{TE} represents the same while directly pumping heat from the evaporator to the condenser. Likewise COP_{ads_alone} represents the COP of an adsorption chiller, standalone, without TE devices (as described in section 2.2), and COP_{ads_TEA} describes the COP of the adsorption chiller working in conjunction with TE devices in a TEA heat pump. Both COP_{ads_alone} and COP_{ads_TEA} are described by equation 2.6, but under different circumstances. Expanding equation 7.8 following conditions are obtained for the factor 'λ'.

$$\lambda > \left(\frac{1}{1 + COP_{TE}^{'}} \right) \qquad \textbf{eq. 7.9}$$

$$\lambda > \frac{1}{COP_{ads\_TEA}} \left(\frac{COP_{ads\_alone}}{1 + COP_{TE}^{'}} \right) \qquad \textbf{eq. 7.10}$$

$$\lambda > \frac{1}{COP_{ads\_TEA}} \left(\frac{COP_{TE}}{1 + COP_{TE}^{'}} \right) \qquad \textbf{eq. 7.11}$$

7.2.2 Determining similar conditions for comparison of dissimilar heat pumps

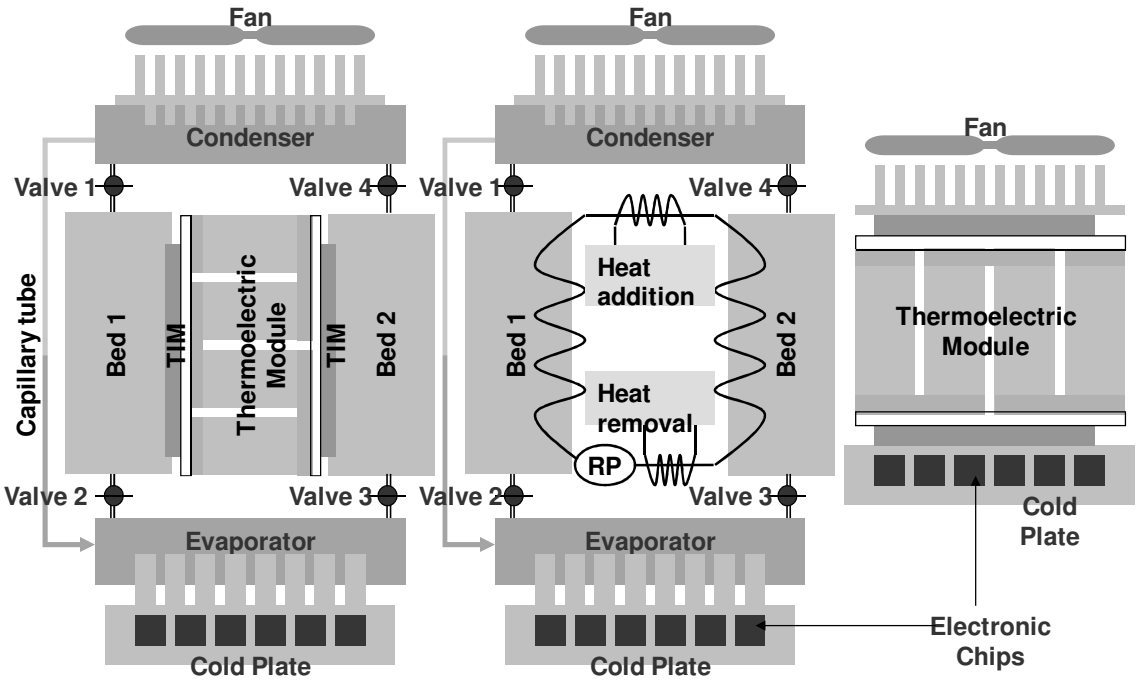

Fig. 7-2 Schematic for TEA (left), Adsorption (middle) and TE (right) chillers. For performance comparison purposes, the chillers are applied between identical heat source (evaporator) and heat sink (condenser) temperatures. Thermal resistance between electronic chips and cold plate (for all three chillers) and cold plate and evaporator (for TEA and adsorption chiller) is considered negligible. Equal input power is provided to all heat pumps. Diagram not to scale. TIM: Thermal Interface Material; RP: reversible (fluid) pump.

Equations 7.9-7.11 provide concise criteria to decide if TEA chillers should be preferred over TE or adsorption chillers, however various COP values must be obtained to

plug into those equations. A straightforward way to compare the heat pumps would be to assess their cooling capability for a given heat sink, heat source temperature and supply power (Fig. 7-2). However, since multiple parameters affect their performance, a standardization scheme is necessary before any comparison can be made. Most of these parameters have been listed in Table 7-1. Some of the parameters were assigned fixed values, while others were varied.

The various parameters were chosen keeping in mind the practicality of the heat pump application. Zeolite can retain water up to 22% of its weight at temperatures as high as 250 ^{0}C (at atmospheric pressure), hence zeolite-water pair was chosen to handle harsh environment applications. Recommendations for use of Zeolite-water pair at temperatures in the vicinity of 200 ^{0}C are found in literature (*Liu* [50], *Zhang*[59]). For a 40 ^{0}C temperature variation of the adsorbent bed, the change in water content for a bed containing 185g of zeolite will be sufficient to manage cooling loads of up to 10 W (this has also been shown in chapter 3), a typical cooling load for thermally harsh environment electronics ([47], [48]), and up to 30 W for near room temperature applications. Table 7-2 shows the manageable cooling load for various evaporator and adsorption process temperatures.

The thermal interface resistance between TE devices and the adsorbent bed was chosen on the basis of typical figures used in electronics packaging industry. Simons et al [99] mention the use of 0.18 mm layer of enhanced thermal grease with a thermal conductivity of 3.8 W/m-K for multi-chip module thermoelectric cooling applications at IBM. Using a similar thermal interface material for a 30 mm x 30 mm face of TE device will result in a thermal resistance of 0.052 K/W. The inert mass ratio of 0.5 has been justified in section 3.5

Table 7-1: The various parameters associated with TEA, Adsorption and TE heat pump.

Constant parameters applied to TEA, Adsorption and TE chillers	
Evaporator (Heat Source Temperature):	varied from (T_{cond} –50 ^{0}C) to (T_{cond} –5 ^{0}C) in steps of 1 ^{0}C
Condenser (Heat Sink Temperature):	varied from 50 ^{0}C to 200 ^{0}C in steps of 75 ^{0}C
Variable parameter dependant on chiller performance	
Heat pumped from source to sink:	noted from the simulation of mathematical models
TEA & Adsorption heat pump specific parameters	
Adsorbent-Adsorbate pair considered:	Zeolite13X-Water
M_z (Mass of Adsorbent):	185g in each adsorbent bed
Inert mass ratio for adsorbent beds (ratio of inactive to active thermal mass):	0.5
Temperature at points F, G, H and I of adsorption cycle:	decided as per a scheme described in a following section
Number of TE devices sandwiched in between beds:	5 of HT-8-7-30 from Laird Technologies [71].
Thermal resistance at the interface of TE device face and bed surface:	0.052 K W^{-1}
t_{cycle} (Cycle time of the sorption cycle):	Depends on the heat pump characteristics of the TE device. (The values can be known only after the execution of the mathematical model).
Switching time: (also known as the heat recovery time) considered 1/4th of the heat regeneration time.	$t_{cycle} = t_{heat\ regeneration} + t_{heat\ recovery}$; where $t_{heat\ recovery} = t_{heat\ regeneration}/4$
Electrical current drawn by TE device during heat regeneration:	Fixed at 3A for each TE device sandwiched between the beds.
Thermal interface resistance between TE device surface and adsorbent beds:	0.052 K W^{-1}
TE device parameters	
Heat source/ sink interface thermal resistance:	0.052 K W^{-1}
Number of TE devices deployed to pump the heat:	varied from 1 to 10
Thermoelectric material used:	Bismuth Telluride (Properties taken from literature, Gordon et al.[42])
Electrical current drawn by TE device:	depends on the power input to TEA chiller (decided in-situ during the execution of the mathematical model)

Table 7-2: Cooling load that can be managed by a single adsorbent bed containing 185g Zeolite 13X with 40 ^{0}C temperature variation during adsorption process. The temperature at the initiation of adsorption process (T_I) was assumed 60 ^{0}C higher than the evaporator temperature. Equations 3.1-3.3 were used to describe water adsorption properties of zeolite 13X (Cacciola et al [75],[76]).

tcycle = 600 s					
T_{evap} (^{0}C)	T_I (^{0}C)	T_F (^{0}C)	$\Delta w = w_F - w_I$	h_{fg} (10^6 J/kg)	$(M_z h^{fg} \Delta w)/t_{cycle}$ (W)
175	235	195	0.016	2.03	10
150	210	170	0.017	2.11	12
125	185	145	0.019	2.18	13
100	160	120	0.022	2.25	15
75	135	95	0.025	2.32	18
50	110	70	0.029	2.38	21
25	85	45	0.034	2.44	26

The number of TE devices in the TEA heat pump was fixed at 5, as in Sinha and Joshi [82]. This compares well with the 9 TE devices used by Ng et al [45]. The number of TE devices applied stand-alone between heat source and sink was varied from 1 to 10. This was done to include the possibility that several TE devices, possibly many more than those sandwiched in between beds, can be used to directly pump heat from evaporator to the condenser.

Another aspect that needed standardization was the placement of adsorption-desorption cycle on the temperature scale. The regeneration of the adsorbent usually takes place at a temperature much higher than that of the condenser. For an adsorption chiller the regeneration temperature (point H in the Clausius-Clapeyron diagram, Fig. 7-1) depends on the temperature at which heat is available, with typical values around 200 ^{0}C for a zeolite-water adsorption heat pump with a condenser/ evaporator temperature of 55 ^{0}C/ 5 ^{0}C (Cacciola et al [75]). In the case of TEA chiller the regeneration temperature will depend on the power supplied to the TE device. Also, it should be within the thermal operating limits of the TE device and higher regeneration temperature would mean lower performance from the TE device. Due to these considerations, the temperature at G' was chosen about 50 ^{0}C

higher than the condenser temperature for both Adsorption and TEA heat pumps (refer Fig. 7-3). G'-I' represents the T_{mid} temperature line (ref: caption Fig. 7-1).

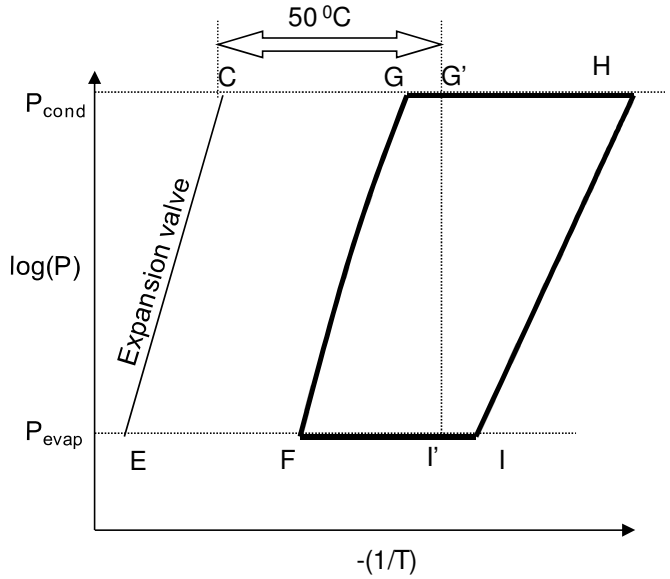

Fig. 7-3 Graphical description of the spacing between condenser and adsorption cycle on the temperature scale.

7.3 Method of performance calculation

This section describes the method that was adopted to obtain the performance of each of the chillers.

7.3.1 TEA chiller

Once the temperature at G' is fixed for the given condenser temperature, the amount of heat pumped by TE devices from adsorbing bed to desorbing bed is calculated for a given input electric current. Since adsorption and desorption involve an increase and decrease, respectively, in water content of zeolite in beds, the progress of these processes is measured in terms of water content parameter '*w*' (wt/wt ratio of adsorbed water and zeolite). Assuming an intermediate stage where water content in adsorbing bed had

progressed from $w_{I'}$ to $w_{1,a}$ (similarly from $w_{G'}$ to $w_{1,d}$ for the desorbing bed), a further infinitesimal amount of water increment during adsorption 'Δw_a' is considered (Fig. 7-4). This adsorption, from $w_{1,a}$ to $w_{2,a}$, $(w_{2,a} = w_{1,a} + \Delta w_a)$, should simultaneously correspond to desorption from $w_{1,d}$ to,$(w_{1,d} - \Delta w_d)$. The adsorbent bed temperatures for a given pressure and water content is calculated using the adsorption equilibrium equations 3.1-3.3.

With the temperatures at the beginning and end of the adsorption and desorption processes known, the amount of heat given off during an extent of adsorption process from w_x to w_y, $(w_y > w_x)$ is given by equation 3.4.

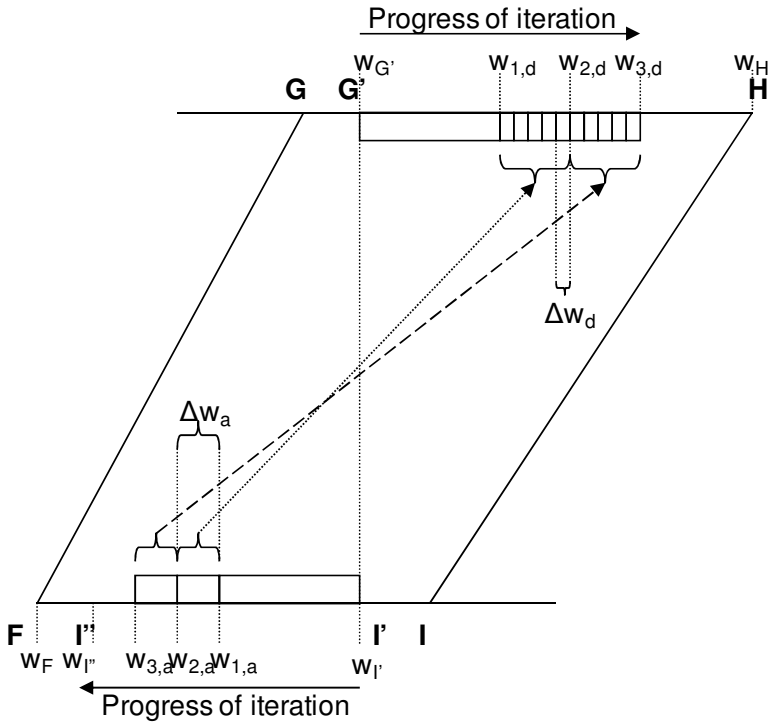

Fig. 7-4 Schematic of iterations to simulate heat pump by the TE device from adsorbing to desorbing bed. Broken arrows signify transfer of heat from adsorption to desorption processes.

Also since the current supply to the TE devices is known a-priori, the heat pump rate at the cold face (q_c) and the rate of heat delivery at the hot face (q_h) are calculated

using equations 2.2-2.5. During this calculation the temperature at the adsorbing and desorbing beds is considered as the average of temperatures at the beginning and end of the infinitesimal adsorption and desorption processes respectively. The time taken to pump ΔQ_{ads} (heat of adsorption released during adsorption from $w_{1,a}$ to $w_{2,a}$) is given by equation 7.12. Also since only a fraction 'λ' (ref: section 7.1) of the heat delivered at hot side (desorbing bed) is actually utilized for desorption, the net heat provided to the desorbing bed is obtained from equation 7.13. The value of 'λ' depends on the cooling arrangement, the heat leakage from the bed, and can be controlled. Hence its value is prescribed for a particular run of COP calculations. The heat actually required by desorption process is given by equation 3.6. It considers desorption progressing from w_y to $w_x, (w_y > w_x)$.

$$\Delta time = \Delta Q_{ads} / q_c \qquad \textbf{eq. 7.12}$$

$$\Delta Q_{delivered} = \Delta time \times \lambda \times q_h \qquad \textbf{eq. 7.13}$$

The heat delivered at the desorbing bed is greater than the heat needed for desorption (i.e. $\Delta Q_{delivered} > \Delta Q_{des}$). Hence successive iterations are run, and in each one, another infinitesimal 'Δw_d' is added to desorption process and the energy calculations, i.e equations 3.1-3.3, 2.2-2.5, 7.12-7.13 and 3.6 are repeated until the condition $\Delta Q_{delivered} = \Delta Q_{des}$ is achieved. At this stage the water content in the desorbing bed is $w_{2,d}$ as shown in Fig. 7-4.

Further, another infinitesimal adsorption step is considered. $w_{2,a}$ to $w_{3,a}, (w_{3,a} = w_{2,a} + \Delta w_a)$ (refer: Fig. 7-4). Desorption proceeds from $w_{2,d}$ onwards. The process mentioned above is repeated until the condition $\Delta Q_{delivered} = \Delta Q_{des}$ is achieved. At this stage the water content in the desorbing bed corresponds to $w_{3,d}$ as shown in Fig. 7-4.

Several iterations are run with progress in adsorption process (and corresponding progress in desorption process) and for each iterations the variables $\Delta time$, ΔQ_{ads}, $\Delta Q_{delivered}$ and ΔQ_{des} are calculated. Iterations are run until the heat pumped by the TE devices from adsorbing bed becomes negative (i.e. $q_c < 0$). This happens when the temperature difference between the cold and hot faces of the TE device is high enough for the TE device to pump any heat at its cold face. At this stage, the final extent of adsorption and desorption processes are noted as points I" and H on the Clausius diagram (Fig. 7-4). Since the heat delivered at desorbing bed is greater than the heat pumped from adsorbing bed, the extent of desorption is greater than the extent of adsorption, i.e. $(w_H - w_{G'}) > (w_{I'} - w_{I''})$. However in an adsorption heat pump the amount of water adsorbed should be same as the amount desorbed. Hence the mass fraction of water at the end of adsorption process (point F) is calculated as:

$$w_F = w_{I''} + ((w_H - w_{G'}) - (w_{I'} - w_{I''})) \qquad \textbf{eq. 7.14}$$

Assuming $(w_G - w_{G'}) = (w_{I'} - w_I)$, which is nearly the case, equation 7.14 satisfies the mass balance of water during the adsorption cycle, i.e. $[(w_G - w_H) = (w_F - w_I)]$. Using the value of w_F and pressure ($= P_{evap}$), temperature at point F can be calculated by equations 3.1-3.3. Now since, points F and H are known, points G and I can also be obtained respectively by equations 3.1-3.3. This is facilitated by the fact that processes F-G and H-I are characterized by constant water content in the beds and hence $w_G = w_F$ & $w_I = w_H$.

For the iteration to be successful, points G and I must lie to the left and right of T_{mid} line (i.e. line G'-I') respectively (refer Fig. 7-4 and Fig. 7-5a). This is because at the beginning of the iteration it is assumed that T_{mid} passes through adsorption and desorption

processes. This condition is violated for iterations that result in G and I being at the wrong side of T_{mid} as shown in Fig. 7-5b. For such cases further steps for COP calculation are dropped and the COP of TEA is assigned a value of zero. In order to obtain the COP value the iteration would have to be restarted with a modified condition that considers T_{mid} passing thru constant heating and cooling processes. Such cases have not been dealt with in the present work, because for zeolite-water pair, the T_{mid} line usually passes through adsorption (process I-F) and desorption processes (process G-H).

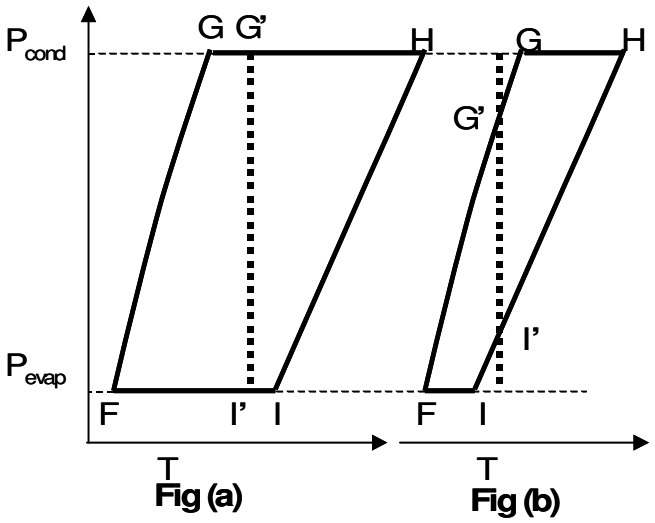

Fig. 7-5 Fig (a) left: T_{mid} line passes through adsorption and desorption processes. Fig (b) right: T_{mid} line passes through constant volume heating and cooling processes. Note, in fig (b) points G and I are on the opposite side of T_{mid} when compared with the fig (a).

For successful iterations, the heat released by the adsorption process from I" to F (denoted by Δ_3, refer section 7.1) is directly released to the ambient as the TE device is considered switched off for this extent of adsorption process. At this stage the heat load managed at the evaporator 'Q_{evap}' is obtained from equation 7.15 (equation 7.15 can be easily derived from equations 4.1 and 4.5). The heat required by constant volume heating

process F-G is given by equation 3.5 and heat required by constant volume cooling process H-I is given by equation 3.7.

$$Q_{evap} = M_Z (w_F - w_I) h_{fg,T_{evap}} (1-e); e = (h_{f,T_{cond}} - h_{f,T_{evap}}) / h_{fg,T_{evap}} \quad \textbf{eq. 7.15}$$

The adsorption-desorption process that has been discussed so far is followed by constant volume heating (process F-G, in the bed that just finished adsorption) and constant volume cooling (process H-I, in the bed that just finished desorption). During this stage energy from the cooling bed needs to be recovered to heat the bed undergoing constant volume heating. Since this heat transfer is from hotter to cooler bed, it does not need an active heat pumping mechanism. However, TE devices sandwiched in between the beds prevent any direct thermal contact in between beds. Heat can still be conducted across the TE device material, but this would take a longer time and result in vapor accumulation and temperature rise in evaporator. Hence, a small amount of electrical power is supplied to the TE device to hasten the process of heat recovery. For the purpose of this chapter, the amount of electrical power input during heat recovery phase is considered negligible for COP calculations. It is assumed that heat recovery should take nearly 25% of the time taken for heat regeneration. The amount of heat recovered 'Q_r' is given by equation 7.1 and can be calculated by using equations 3.4 and 3.5 or equations 3.6 and 3.7. At this stage appropriate values are plugged in equations 7.2-7.4 to obtain COP'_{TE}, COP_{ads_TEA} and COP_{TEA}.

7.3.2 Adsorption chiller

For calculating the COP of the adsorption chiller, following assumptions are made: (1) Power used for circulation of heat transfer fluid considered negligible for COP

calculations. (2) The bed parameters, and the cycle and switching time parameters are identical to the TEA chiller.

Since the power delivered is known (equal to the electrical power input to TEA chiller), the parameter to be found is Q_{evap}. Though Q_{evap} was calculated for the TEA chiller, its values for the adsorption chiller will be different because the adsorption-desorption cycle may not have the same end points (F and H), as calculated for the TEA chiller. Unlike the TEA chiller, where power is supplied to the TE device, here the entire input power is directly provided for the desorption process.

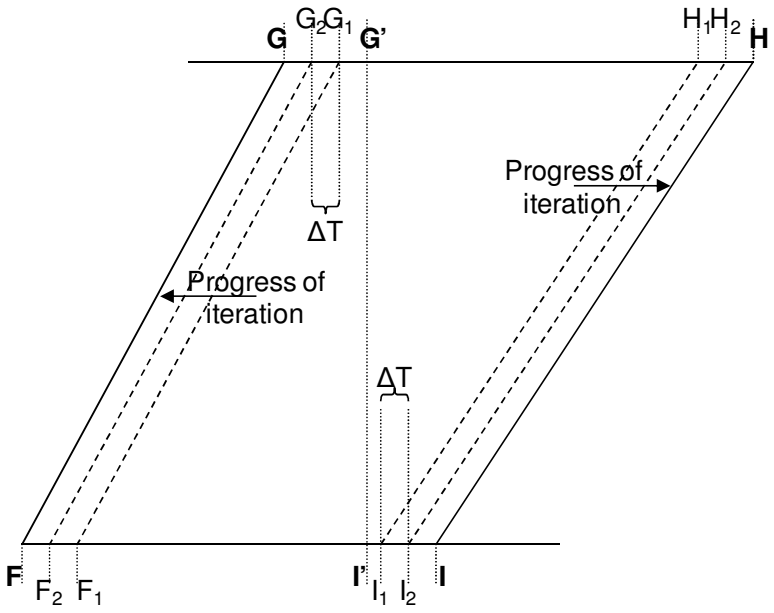

Fig. 7-6 Schematic of iterations to find out how far the adsorption and desorption processes in the AHP would go, if it were provided the same amount of energy as the TE devices in the TEA heat pump.

In order to find the values of F and H for adsorption chiller, iterations are carried out. A temperature to the left of G' and to the right of I' is chosen, and corresponding points F and H are calculated (Fig. 7-6) using equations 3.1-3.3. Next the total energy required by endothermic processes (F-G and G-H) is calculated, along with the amount of heat that could be recovered 'Q_r'. The amount of energy needed, less the energy recovered is

the 'net' energy required by the adsorption heat pump in one cycle. Iterations are repeated until this 'net' energy equals the energy input to TEA chiller in the above section (section 7.3.1). Since the 'net' energy monotonically increases with the progress of iteration, an iteration that starts with the value of 'net' energy being greater than that of total energy input to a TEA chiller during one cycle, does not yield a result. For such cases COP of adsorption chiller corresponding to the COP of the TEA chiller does not exist and hence the two chillers cannot be compared. The iteration is aborted in such a condition and the COP of adsorption chiller is assigned a value of 'zero'. For successful iterations (i.e. iterations that start with value of 'net' energy being less than total energy input to TEA chiller in one cycle time), the temperatures at F and H at the end of the iterations represent the extent of adsorption-desorption processes for the adsorption chiller. These parameters are used to calculate Q_{evap} in the same way as for the TEA chiller. COP_{ads_alone} is calculated by plugging appropriate values into equation 7.2.

7.3.3 TE chiller

The total power input into the TEA and TE chiller need to be identical to compare their performances. This requires a power matching operation because unlike the TEA and adsorption chillers that are supplied power with periodic variations, the power supply to TE chiller is continuous.

During the working of TEA heat pump, the voltage polarity across the TE device is flipped to account for the role reversal of the beds. This creates an uneven power profile. Fig. 7-7 gives a graphical explanation of the same. The power profile is averaged over one

cycle time to determine the power input for the stand-alone TE heat pump. Equations 2.2-2.5 are numerically solved to determine the TE device COP.

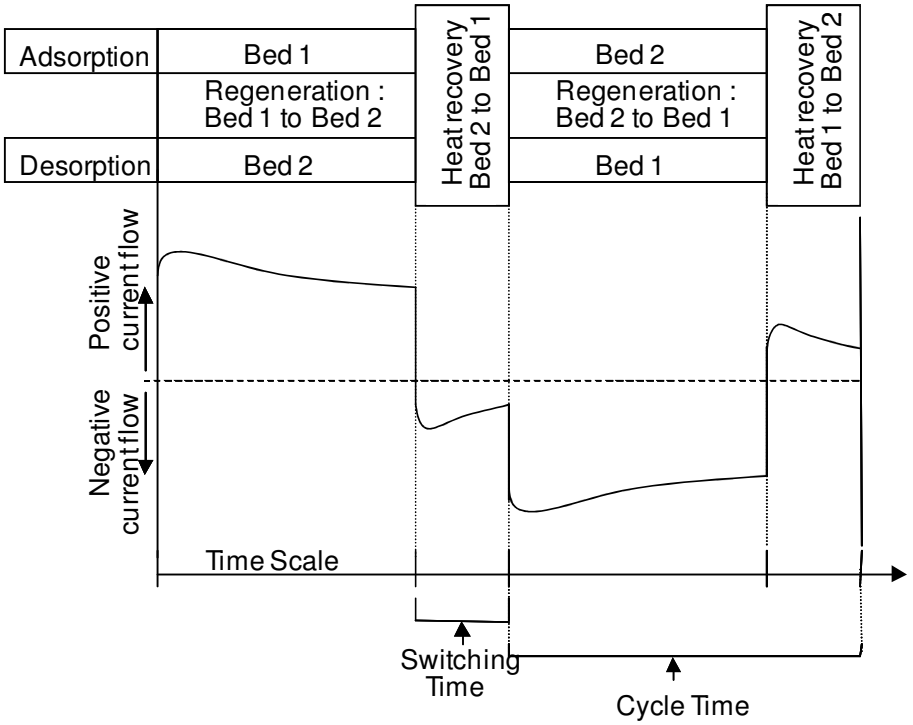

Fig. 7-7 Plot of current supply (also representative of power input to TE device) with time, for the TE device sandwiched in between sorption beds.

A graphical description of the method described is presented in APPENDIX F .

7.4 Results

First we take a look at the effect of heat loss from the desorbing bed on the performance eof the TEA chiller. Next, the adsorption, TEA and TE chillers have been compared in terms of COP for identical heat pumping and power input conditions.

7.4.1 Effect of heat loss from adsorbent beds on TEA chiller performance

First the results for a TEA chiller, when all excess heat provided by TE device at the desorbing bed is rejected to ambient, is presented. For such a case there is a one to one correspondence between adsorption and desorption processes (i.e. a water content increment of Δw in adsorbing bed corresponds to a water content decrement in the desorbing bed by the same amount.

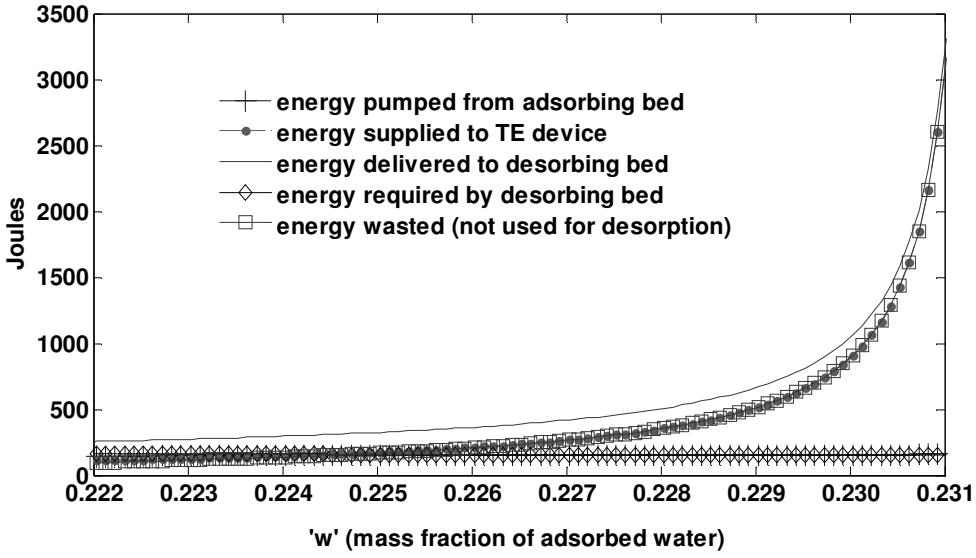

Fig. 7-8 A plot of various energy terms associated with the TEA chiller for the case when any excess heat at desorbing bed is rejected to ambient (and not utilized to further advance the desorption process).

In Fig. 7-8 the energy to be pumped out of adsorbing bed and to be delivered to the desorbing bed to effect an equal change of water content in both beds nearly overlap. These energy terms are less when compared to 'energy supplied', 'energy delivered' and 'energy wasted'. Plots depicting 'energy supplied' and 'energy wasted' nearly overlap. This implies that almost all of the electrical energy provided to the TE device is rejected to the ambient. The amount of heat rejected rapidly rises towards the end of the adsorption process (i.e. when the temperature difference between adsorbing and desorbing beds is the maximum,

and hence the TE device COP is the least). The fraction of heat delivered (to desorbing bed) that is actually used for desorption 'λ' gradually decreases from a value of 0.6 to ~0 (with an average value of 0.21) as seen in Fig. 7-9. From Fig. 7-9 one can also observe that the time taken for the adsorption and desorption of an equal amount of water vapor rapidly increases towards the end of the adsorption-desorption process. This is expected since the TE device pumps heat at a much slower rate at higher temperature difference between its hot and cold sides.

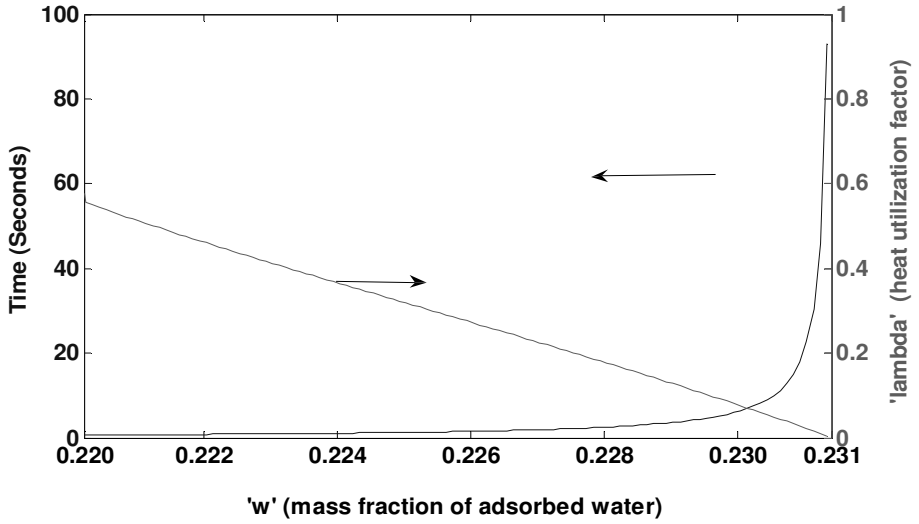

Fig. 7-9 Variation of 'λ' and time taken for successive adsorption-desorption steps.

Next we see the same plots for another case where all of the excess heat delivered to desorbing bed is not allowed to escape to ambient (Fig. 7-10 and Fig. 7-11), instead, it is used to further the desorption process. The heat rejection from the desorbing bed is controlled to maintain the fraction of utilized heat 'λ' at 0.75. In such a case the progress in adsorption by a certain increase in water content, can result in a much greater decrease in water content in the desorbing bed. Adsorption progresses to a much lesser extent (up to w

= 0.227) when compared to 0.23 in Fig. 7-8. λ varies from 0.8 to 0.77 during the iterations, (close to the targeted value of 0.75.

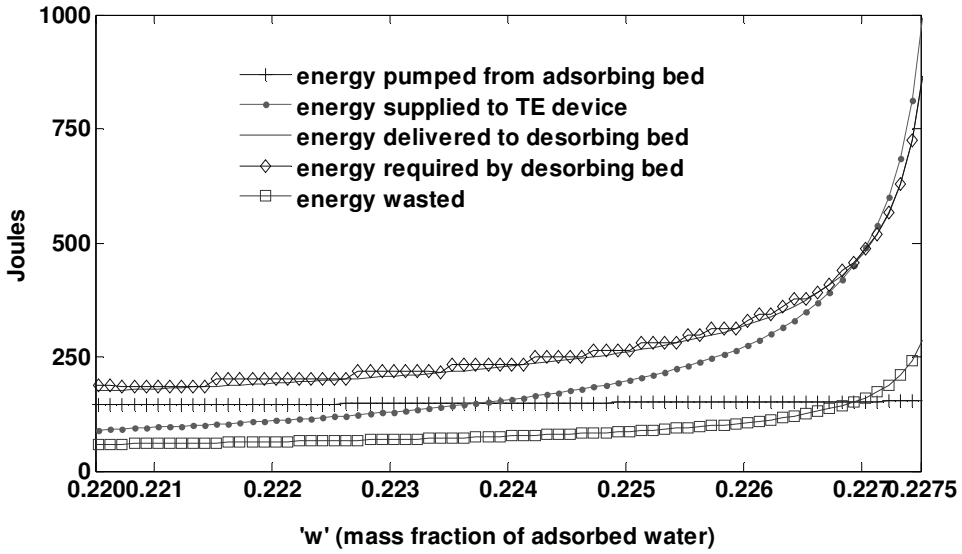

Fig. 7-10 A plot of various energy terms associated with the TEA chiller for the case when nearly 75% excess heat at desorbing bed is utilized to further advance the desorption process.

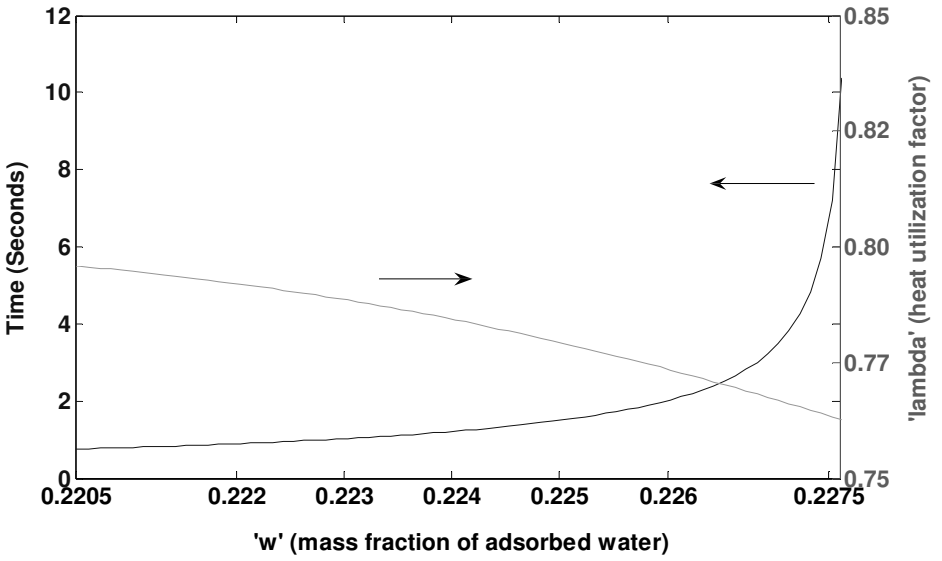

Fig. 7-11 Variation of 'λ' and time taken for successive adsorption-desorption steps with progress of adsorption in the adsorbing bed.

Critical values for the two cases depicted in Fig. 7-8, Fig. 7-9, Fig. 7-10 and Fig. 7-11 have been compared in Table 7-3. The case that captures most of the heat delivered to desorbing bed has a much higher COP, greater extent of adsorption and desorption (hence ability to manage greater cooling load 'Q_{evap}') and a shorter adsorption-desorption time 'Σ time'.

Table 7-3: Critical values for the cases of λ = 0.21 and λ = 0.75.

	T_F (^{0}C)	T_H (^{0}C)	$w_{I''}$	w_F	w_H	Σ time (seconds)	Q_{evap} (J)	$Pow_{in,TE}$ (J)	$Q_{desorption}$ (J)	$COP_{ads'}$	$COP_{te'}$	COP_{TEA}
λ = 0.21	224	278	0.2315	0.2315	0.2201	475	4000	66500	14300	0.28	0.25	0.06
λ = 0.75	214	287	0.2278	0.2356	0.2161	132	6940	17700	19800	0.34	0.63	0.4
For both cases $T_{condenser}$ = 200 ^{0}C, $T_{evaporator}$ = 175 ^{0}C, $T_{G'}$ and $T_{I'}$ = 250 ^{0}C. $w_{g'}$ = 0.2315 and $w_{I'}$ = 0.2201												

	T_{cycle} = Σ time + (Σ time)/4	Cooling load managed = Q_{evap}/t_{cycle}
λ = 0.21	593 seconds	6.74 W
λ = 0.75	165 seconds	42 W

7.4.2 Comparison of performance of adsorption, TE and TEA chillers

With the benefits of utilizing the heat delivered by TE device well established in section 7.4.1, performance of the chillers has been presented next for condenser temperatures of 200, 125 and 50 ^{0}C (Fig. 7-12, Fig. 7-13, Fig. 7-14) and 'λ' = 1.0. The evaporator temperature has been varied from T_{cond}-50 ^{0}C to T_{cond}-5 ^{0}C. In the plots presented COP_{TE}^{x} represents an arrangement that employs 'x' TE devices pumping heat in parallel in between evaporator and condenser. The electrical power input to the chillers during the iteration has also been plotted. The input power is a characteristic of the system and not specified during the iteration (only electrical current supplied to the TE device is specified), hence its graphical description assumes significance. Plot of power input along with COP can be used to estimate the cooling load managed by the chillers.

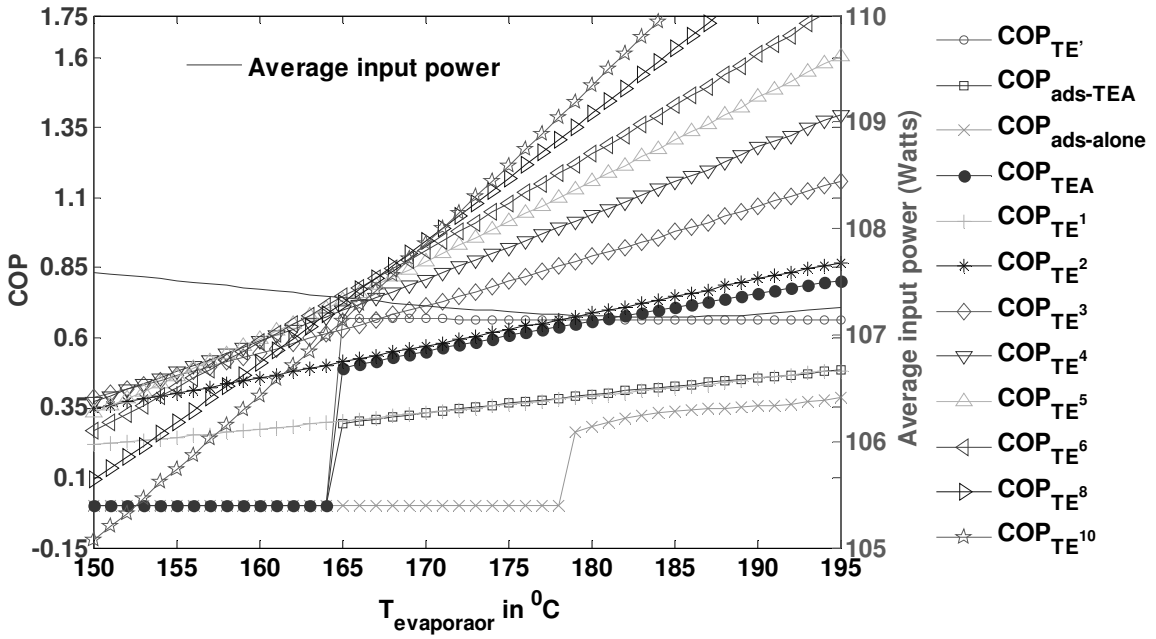

Fig. 7-12 COP plots of various chillers, along with input power, for a condenser temperature of 200 ^{0}C and heat utilization factor 'λ' ~ 1.0.

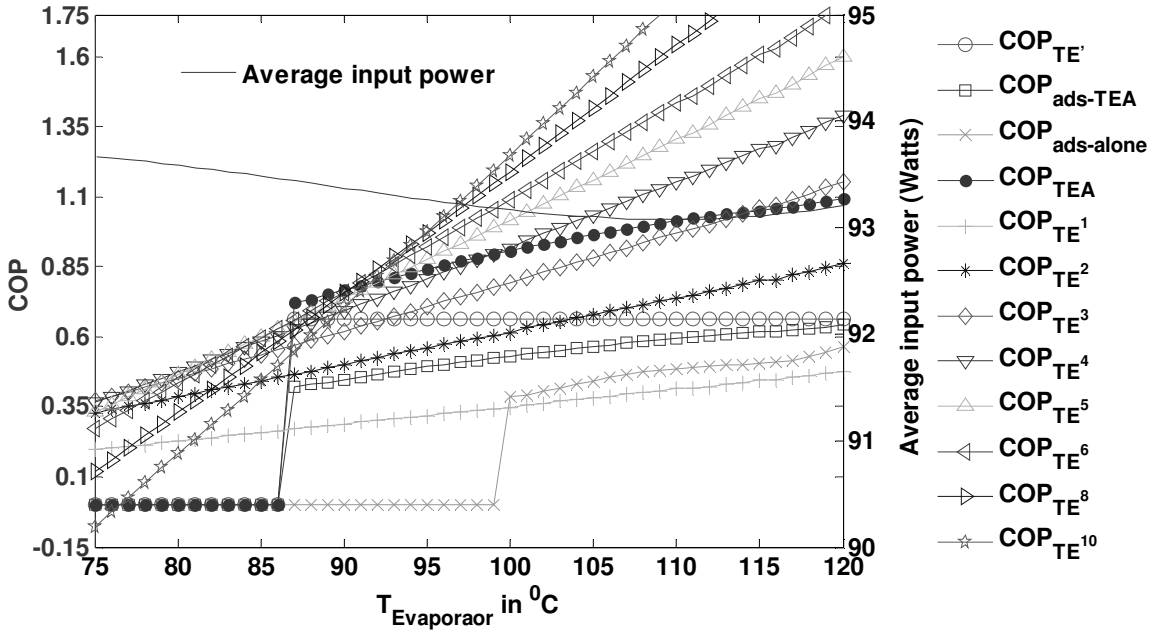

Fig. 7-13 COP plots of various chillers, along with input power, for a condenser temperature of 125 ^{0}C and heat utilization factor 'λ' ~ 1.0.

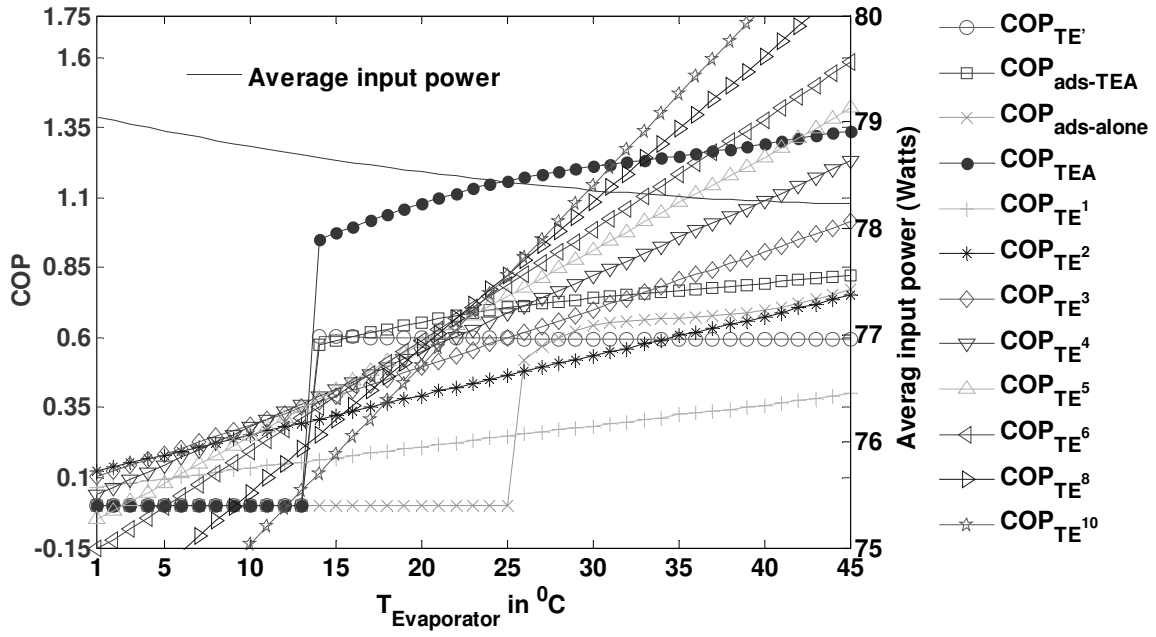

Fig. 7-14 COP plots of various chillers, along with input power, for a condenser temperature of 50 ^{0}C and heat utilization factor 'λ' ~ 1.0.

After having plotted the COPs of the chillers, next, the corresponding plot for 'λ' and various quantities on the right hand side of equations 7.9, 7.10 and 7.11 have been presented for a condenser temperature of 50 ^{0}C (Fig. 7-15). The right hand side terms in equations 7.9-7.11 provide a parameter that can be directly compared with λ to determine the suitability of TEA chiller over the other two. For instance, with reference to Fig. 7-15, for an evaporator temperature less than 30 ^{0}C, λ is greater than all other values, and hence a TEA chiller has superiority over the other two.

The TEA chiller is outperformed by a combination of TE devices pumping heat in parallel for most part of the evaporator temperature range (ref: Fig. 7-12, Fig. 7-13, and Fig. 7-14). Also up to a certain region on the evaporator temperature scale, higher COP is observed with increasing number of TE devices pumping heat in parallel. Beyond that region, application of increasing number of TE devices in parallel leads to a drop in COP. Since TEA chiller itself comprises numerous TE devices between beds, the dependence of

COP, for a constant power input, on the number of TE devices employed, must be investigated to derive maximum performance from TEA as well as TE heat pumps. This has been discussed next.

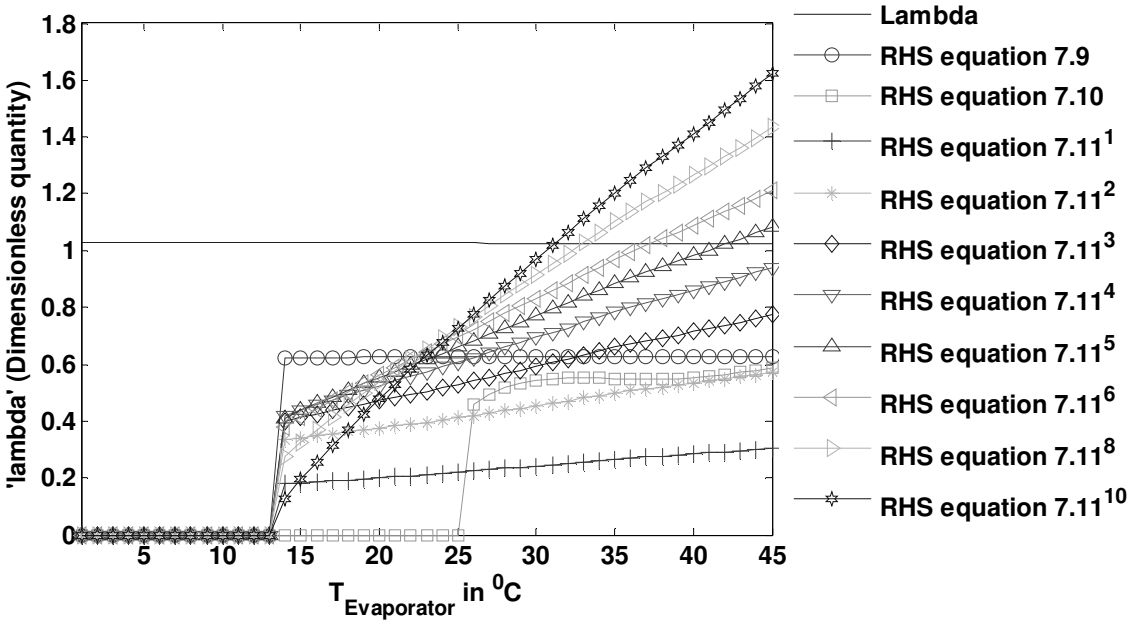

Fig. 7-15 Plot of 'λ' along with various right hand side terms involved in equations 7.9, 7.10 and 7.11 for T_{cond} = 50 ^{0}C.

Fig. 7-16-(top) shows the variation of COP with supply current. This is for a single TE device pumping heat between heat source and sink temperatures of 175 ^{0}C and 200 ^{0}C respectively. It can be observed that there is an optimum value of current for which the TE device COP is maximum. Fig. 7-16-(bottom) shows the variation of COP with number of TE devices applied for pumping heat in parallel. This is for a constant power supply of 100 W and same heat source and sink temperatures as used in obtaining the plot for Fig. 7-16-(top). Since the power supply, heat source and sink temperatures are constant, the number of TE devices employed will determine the voltage across and current drawn by each TE device. A close observation of the top and bottom plots in Fig. 7-16 reveals that the COP of

the cluster of TE devices is maximum when each TE device draws the same current that corresponds to maximum COP of a single TE device.

In light of the findings above, the performance of TEA, TE and adsorption chillers is re-evaluated. The iterations are run with the condition that TE devices in between the beds are supplied a current that corresponds to their maximum performance for a set of hot and cold side temperatures. Fig. 7-17 depicts the performance curves for a condenser temperature of 50 ^{0}C. It is observed that, within a lesser value of difference between evaporator and condenser temperatures, the COP of the TEA chiller surpasses the COP of any number of TE devices pumping heat in parallel. The improvement in COP is however counterbalanced by a reduction in the chiller's ability to manage cooling load. The average input power is close to 28 W. The same value for a constant current supply of 3A was 78 W (ref: Fig. 7-14).

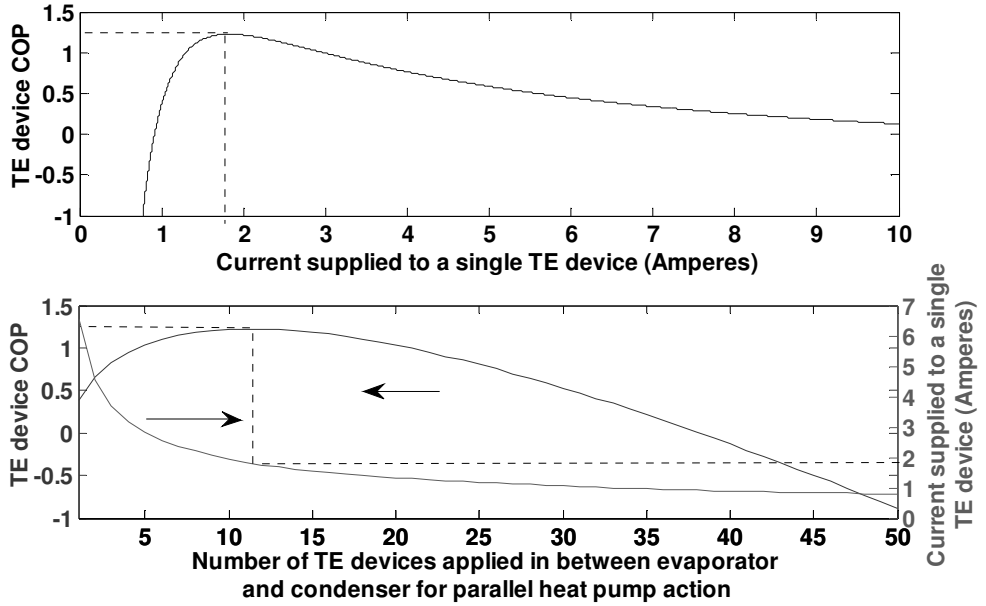

Fig. 7-16 (Top) COP variation of a single TE device pumping heat between heat source and sink temperatures of 175 ^{0}C and 200 ^{0}C respectively. (Bottom) COP of a group of TE devices pumping heat in parallel between same heat sinks and heat source for a constant power supply of 100 W. The current drawn by each TE device is plotted on the left ordinate.

In light of the findings above, the performance of TEA, TE and adsorption chillers is re-evaluated. The iterations are run with the condition that TE devices in between the beds are supplied a current that corresponds to their maximum performance for a set of hot and cold side temperatures. Fig. 7-17 depicts the performance curves for a condenser temperature of 50 ^{0}C. It is observed that, within a lesser value of difference between evaporator and condenser temperatures, the COP of the TEA chiller surpasses the COP of any number of TE devices pumping heat in parallel. The improvement in COP is however counterbalanced by a reduction in the chiller's ability to manage cooling load. The average input power is close to 28 W. The same value for a constant current supply of 3A was 78 W (ref: Fig. 7-14).

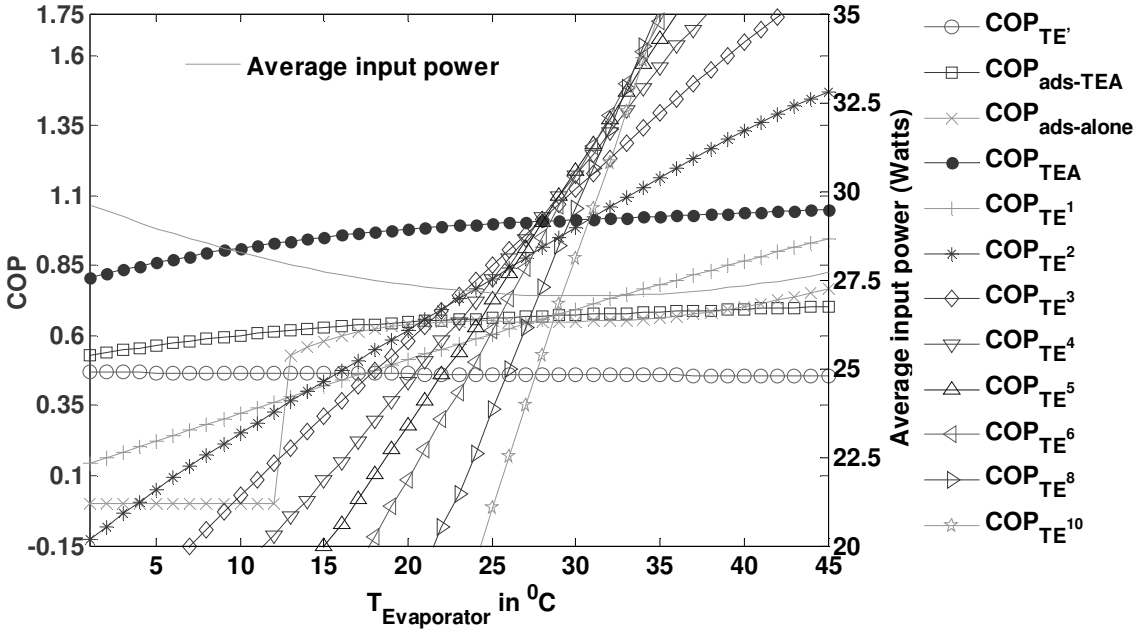

Fig. 7-17 COP plots of various heat pumps, along with input power, for a condenser temperature of 50 ^{0}C and heat utilization factor 'λ' ~ 1.0

While considering the results mentioned in this chapter, it must be noted that the inert mass ratio for the TEA and adsorption chiller was assumed 0.5, i.e. the inactive thermal

mass was considered half of the active thermal mass. The COP of the TEA and adsorption chillers can be greatly improved by further reduction in inert mass ratio. Another factor than can alter the results obtained is the placement of the adsorption cycle. For the current work T_{mid} was considered 50 ^{0}C higher than condenser temperature. During the iterations, T_{mid} may be placed closer or farther from the condenser on the temperature scale depending upon the availability of the TE devices that can withstand high operating temperature and/ or the temperature at which waste heat is available for regeneration.

7.5 Conclusions

TEA chiller provides a means of combining advantages of adsorption and TE chillers. Adsorption chillers offer scalability according to cooling load, and increased efficiency due to internal heat regeneration. TE devices offer a compact means of achieving heat regeneration. Thus inclusion of TE devices in between adsorbent beds of an adsorption chiller (that results in a TEA chiller) makes system miniaturization possible and opens a whole new area of application such as microelectronics thermal management. However the use of a TEA chiller would be beneficial only if its overall COP exceeds the individual COP of an adsorption, as well as a TE chiller under identical heat pumping conditions. The current work develops a self-consistent COP formulation of the three chillers, provides a reasonable standardization scheme and methodology to calculate and compare their performances.

It is found that the TEA chiller performance is strongly dependent on the heat rejection from adsorbent beds to the ambient. The formulation for the COP of TEA chiller, as found in literature, was modified by the introduction of a heat utilization factor 'λ' to incorporate the effect of heat loss from desorbing bed. It was shown that utilizing most of

the heat delivered to the desorbing bed to further the desorption process has a positive effect on the COP. Such a method of operation fulfills the thermal needs of the desorption process before the completion of the adsorption process. For the remainder of the adsorption process the TE device must be switched off and the adsorbing bed cooled by heat rejection to ambient. It has been shown that this heat loss (heat loss from adsorbing bed, once the thermal needs of desorption process has been satisfied) has no adverse effect on the COP of TEA chiller. This is an important result by the virtue of which it can be concluded that a realizable way to achieve maximum possible COP for TEA chiller has been described.

The present analysis shows that while TEA chiller's advantage over adsorption chiller always holds, its advantage over TE chiller is pronounced only at evaporator temperatures that are more than 25-30 ^{0}C below the condenser temperature. Also the performance of TEA chiller vis-à-vis adsorption chiller and TE chiller improve as the condenser temperature decreases from 200 ^{0}C to 50 ^{0}C. Synchronizing current supply that corresponds to maximum TE chiller performance can augment the performance of TEA chiller over TE chiller. This can be especially beneficial at higher condenser temperature (thermally harsh environment) to derive maximum performance from the TEA chiller. Such an operation will require a sensor and control mechanism to sense the temperature at hot and cold faces of TE chiller and accordingly provide optimum current.

The results presented in this work should be of help in deciding between TEA, adsorption and TE chillers for electronic cooling applications, from room temperature to thermally harsh ambient. It should also help thermal engineers dealing with TEA chillers in achieving maximum possible performance.

CHAPTER 8: Closure

In this chapter a brief description of the wok described in this dissertation has been presented. This is followed by a list of contributions. Further, the import of this work in development of sorption cooling technology has been discussed. This chapter ends with a recommendation for future studies.

8.1 Brief recap of the work presented in this dissertation

In this dissertation the necessity of an effective thermal management solution for thermally harsh environment electronics has been highlighted. The work points out reliability, compactness (miniaturization without loss of performance) and ability to cool for long durations without any human interference as main characteristics of the desired cooling system. In this backdrop the suitability of a regenerative thermoelectric adsorption cooling system for use in thermally harsh environment has been investigated. Studies made by *Gorodon et al* [42] and *Ng et al* [45], have already established the good performance of such a system for room temperature cooling of electronics. This made it attractive to look into performance of a similar system for high temperatures (150 – 200 ^{0}C).

Several challenges associated with high temperature application of the system have been identified and respective solutions proposed. Zeolite-13X water pair was proposed in place of silica gel water pair (silica gel water pair was used by *Gordon et al* and *Ng et al*). Further, the low thermal operating limit of TE devices was pointed out as a major hindrance in functioning of TEA systems at high temperature. The problem was not just with the highest adsorbent bed temperature during regeneration, but also with the high temperature swing during the adsorption cycle. A novel two step adsorption cycle ('modified') was

proposed to address this challenge. The advantages and drawbacks of the modified cycle vis-a-vis conventional cycle were studied and presented.

A TEA system tuned to thermal needs of the TE device was found to be less responsive to a dynamic thermal cooling load. Several options to address this challenge were evaluated and it was pointed out that a system with varying number of 'active' TE devices in between beds would be more suited to handle varying cooling loads from electronics. This was followed by description of an experimental and theoretical study of the performance of a prototype of the TEA cooling system. The TEA system was operated with both 'conventional' as well as 'modified' adsorption cycles. Experimentally obtained results were compared with simulated results and the 'modified' cycle was found to have a slight advantage over the conventional cycle in terms of lower bed temperatures and higher system performance.

Since the TEA system comprises TE and adsorption coolers and TE coolers can be compact electronic cooling devices in their own right, there was a need to justify the use of TEA coolers. A frame work was prepared to compare TEA, TE and adsorption cooling systems and their performances were compared for identical cooling situations. It was found that the TE A cooler could only be a good option if it were required to cool the electronics more than 30 ^{0}C below the ambient temperature.

8.2 Contributions of the current work

Following are the contributions of the work described in this dissertation.

1. Challenges with high temperature application of TEA cooling system has been identified and respective solutions proposed.

2. A modified cycle has been proposed that breaks the adsorption and desorption process into two steps, thereby reducing the highest temperature encountered during regeneration and the temperature swings in the adsorbent beds.

3. Several options have been evaluated to make the TEA system responsive to manage dynamic thermal cooling loads. It has been shown that by using varying number of 'active' TE devices in between beds, the system can efficiently handle varying heat loads.

4. Prototype of the TEA system was fabricated an experiments with the same were presented. Operation of the TEA system at thermally harsh temperatures has been demonstrated.

5. Mathematical model for the TEA system was developed and validated.

6. Comprehensive COP formulations for the TEA cooling system have been developed. This formulation takes into account the heat loss from adsorbent beds. It was shown that rejecting heat from adsorbing bed to the ambient and switching off the TE device (once the thermal needs of the desorbing bed has been met), has not adverse effect on the overall system COP.

7. In view of several factors, such as inert thermal mass, poor heat transfer inside beds, which hinder good performance of the TEA system, an optimum method of operation has been proposed to achieve maximum system COP. This is based on the contribution stated in the previous bullet (6).

8. A frame work for comparison of TE, TEA and adsorption cooling systems has been presented.

9. Performances of TE, TEA and adsorption cooling systems have been theoretically compared and it has been shown that TEA cooling system should be preferred for cooling of more than 30 ^{0}C below the ambient temperature. For cooling any closer to the ambient temperature TE device based options should be explored.

8.3 What this work may help in?

The import of the current work lies in opening up the field of high temperature cooling to sorption systems. This should encourage research on using sorption systems not just for thermally harsh region, but also for moderately harsh region with heat rejection temperatures of 80 ^{0}C to 150 ^{0}C. Current work also provides insight into experimental methods for TEA and TE chillers and provides inputs to decide on the suitability of TEA, TE and Adsorption cooling systems for a given cooling requirement. This should facilitate researchers in focusing on the right technology for the cooling problem.

Current work should also help increase the thermal envelope of operation for commercially available electronics. Since the operation of the TEA heat pump is independent of gravity, this technology is suitable for a several applications such as avionics and oil drilling applications.

8.4 Recommendations for future work

It has been a constant effort to make the current work as complete as possible, however due to many constraints (such as parallel progress in theoretical understanding of the system as well as development of mathematical model and fabrication of experimental set up) several aspects of the TEA system could not be experimentally investigated. This section lists works that should be carried out for a comprehensive study of the TEA system in harsh environment and to further extend the research in improving its performance and suitability for thermally harsh environment.

1. During this study it was observed that the experimental performance of the TE deice far outweighed the experimental performance of the TEA heat pump. The low

performance is attributed to the vapor leakage from beds and poor heat transfer inside the bed. During the fabrication of adsorbent beds, the copper plate had to be brazed to the steel casing and this led to development of copper oxide surface on the inner face of copper plate. This was difficult to remove and hindered heat transfer from copper plate to zeolite beads. Hence for future experiments on TEA system it is recommended to have an improved bed design that should be able to withstand high saturation pressure without any brazing requirements. The bed design should allow easy assembly and disassembly of bed, thus enabling the researcher to change adsorbents as needed. It is recommended to use O-rings to pressure seal the beds. Bed should be appropriately designed to facilitate placement of O-rings.

2. In the current work an electric resistive heater was used to simulate heat dissipation from electronic chips. Experiments could be more realistic if an electronic module is used with a cold plate assembly (with the cold plate assembly thermally coupled to evaporator with a fluid loop).

3. For future TEA experiments efforts should be made to automate the operation of the valves and make the experimental set up compact enough to fit inside the thermally harsh environment enclosure. In the present set up, only the condenser was placed inside oven, whereas the rest of the set up were heavily insulated and surrounded by room temperature air.

4. Although the current mathematical model is able to predict system behavior, it can be improved by incorporating a model for heat and mass transfer in porous media. This will help bring into picture the thermal transport processes inside the beds.

5. In the experiments described in chapters 5 and 6, the TEA system was operated with a predetermined power feed and cycle and switching time parameters. This allowed the system behavior to drift as per the response of the system to these constant input parameters. It is recommended to perform experiments in control mode, where the input parameters such as cycle & switching time, power supply etc should be varied depending on the temperature and pressure in beds, evaporator and condenser. This 'control' mode of operation will enable the system to better adhere to an engineered

adsorption cycle (such as a modified cycle with a predetermined highest regeneration temperature). This will help realize the benefits of the modified cycle more appropriately.

6. Although the studies in chapter 4 and 7 are based in well established adsorption and TE device physics, the findings must be experimentally validated. Especially the method of operation that predicts maximum possible performance of the TEA system must be experimentally validated.

7. Selection of appropriate adsorbent-adsorbate pairs is considered as a major area of research [54]. Several pairs have been suggested by various researchers ([87], [115], [116], [117]). These pairs should be analyzed for application in TEA system at thermally harsh environments. Such an analysis would have two distinct parts. While one should deal with suitable pairs for high temperature application of adsorption cooler, the other should deal with high temperature application of TEA cooling system.

APPENDIX A Mass and diameter distribution of individual zeolite beads

Zeolite 13X was obtained in the form of beads with an rated diameter of $1/16^{th}$ of an inch. However on physical inspection it was observed that zeolite beads varied considerably in terms of their mass as well as diameter. In order to find out an average diameter and mass for zeolite beads several zeolite samples were weighed and measured. The mass and diameter measurements were done with an accuracy of 0.001 g and 0.01 mm respectively. A sample size of 50 and 100 were chosen to estimate average mass and diameter respectively. Figures presented here show the distribution of mass and diameter for the zeolite samples. The average mass was calculated as 0.008 g, whereas the average diameter was calculated as 2.21 mm. These values were used to calculate the average density of the zeolite beads (individual zeolite beads were assumed spherical).

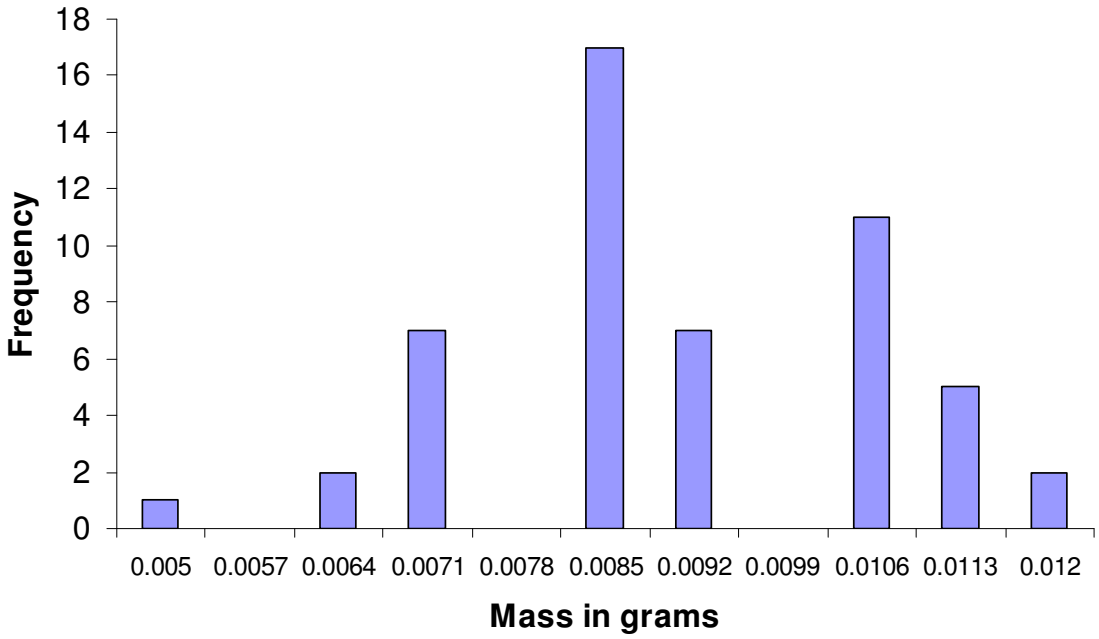

Fig. A-1 Mass distribution of zeolite beads (sample size 50)

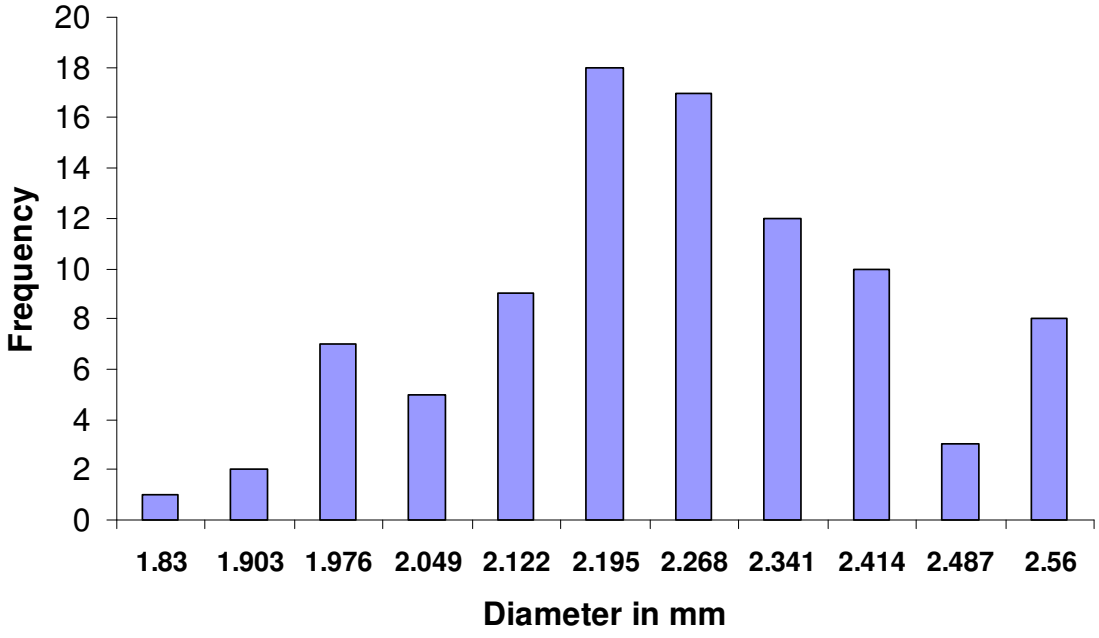

Fig. A-2 Diameter distribution of zeolite beads (sample size 100)

APPENDIX B Authenticity of zeolite samples

In this appendix the data regarding the authenticity of the zeolite samples have been presented. The authenticity of the zeolite 13-X sample obtained from Grace Davison [83] was ascertained by X-Ray diffraction analysis of a powdered form of the zeolite sample. The results were matched with known X-Ray diffraction patterns available in literature [109], [110].

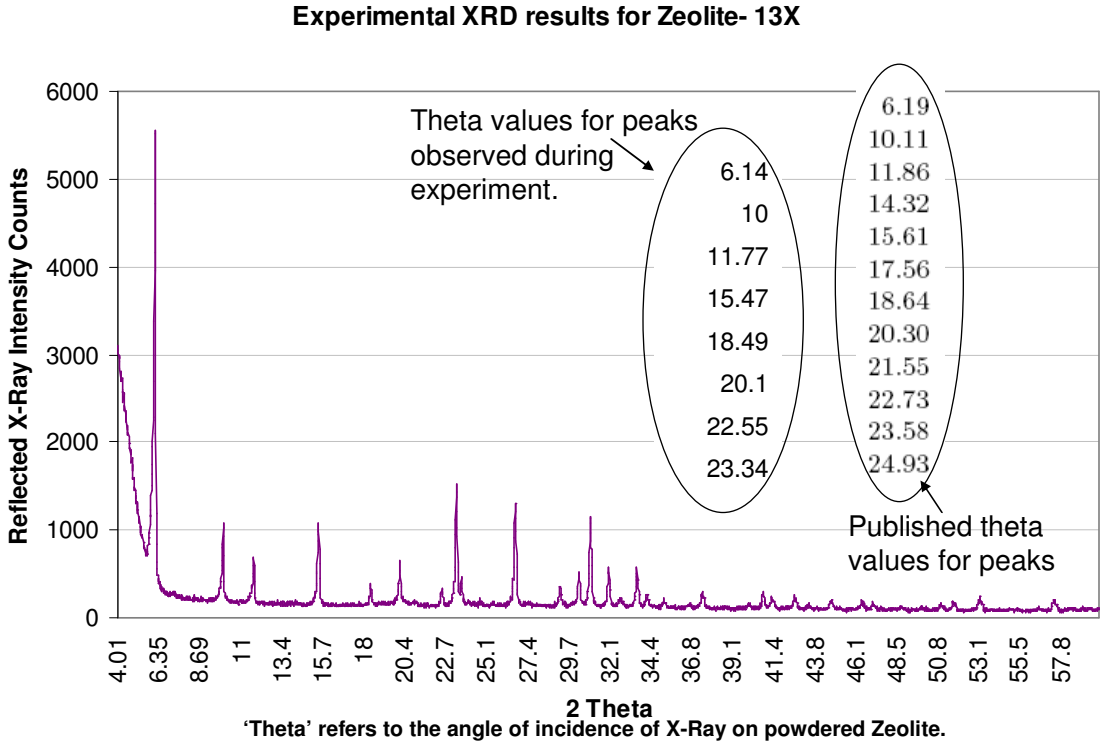

Fig. B-1 Plot sowing the peaks obtained during X-Ray diffraction analysis of the zeolite13X sample. The peaks matching with a known sample of zeolite 13X has been listed in ellipses.

APPENDIX C Validating the zeolite 13X-water adsorption isotherm equations

In this appendix, the authenticity of the equations used to determine the adsorption of water on zeolite 13X for a given temperature and pressure has been determined. The amount of water uptake in an adsorbent 'w' (= mass of water adsorbed/ mass of zeolite) is a function of the pressure and temperature inside the bed. For a given pellet of zeolite subject to pressure P and a uniform temperature T, the water uptake is given by w = f (P, T). This same function can also be used to obtain the value of any of the variables w, P and T, if the other two variables are known. In the present dissertation equations 3.1-3.3 describe the relationship between water content, pressure and temperature in an adsorbent bed.

These equations were used with appropriate values of constants from literature ([75][76]) to reproduce the various adsorption plots that were experimentally obtained by *Cortes et al* [111]. The plots obtained by the equations closely match the plots as presented in the work by Cortes et al.

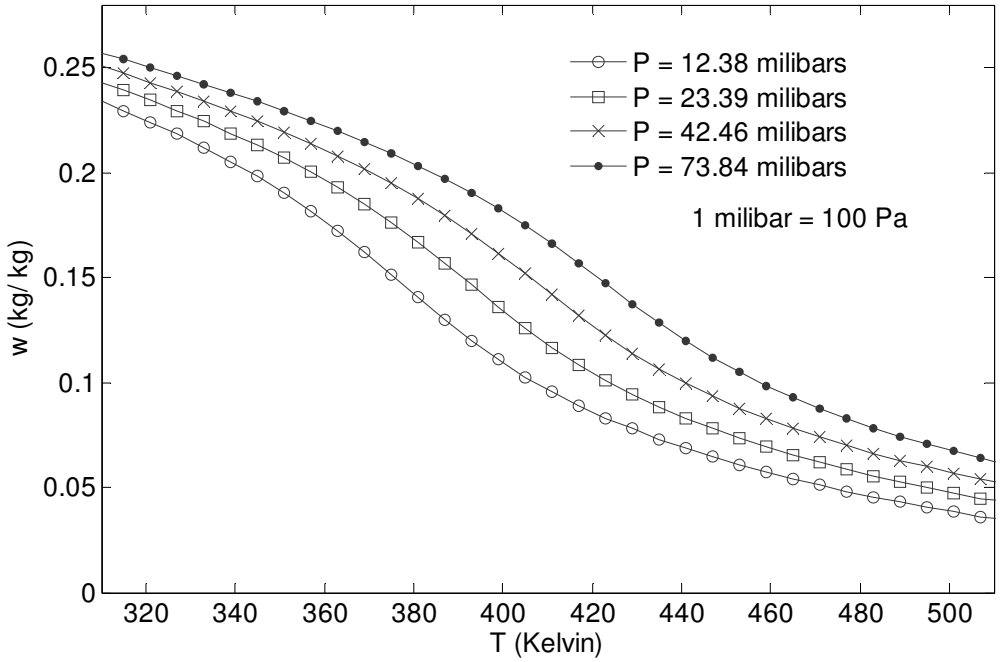

Fig. C-1 Isobars of water on zeolite 13X as obtained b using equations 3.1-3.3.

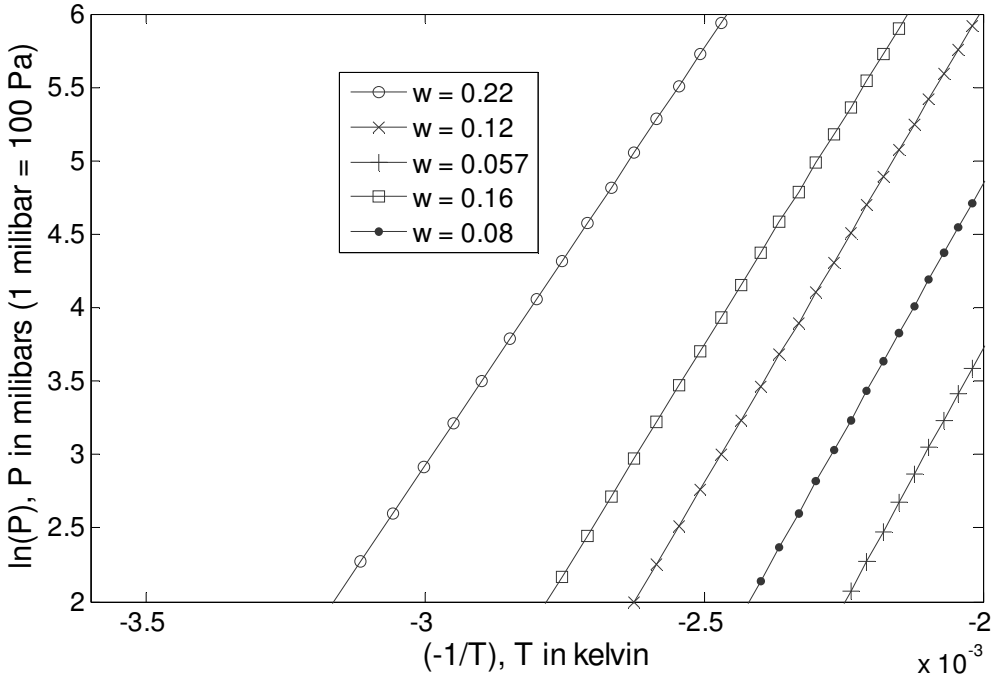

Fig. C-2 Isosteres of water on zeolite 13X as obtained by using equations 3.1-3.3.

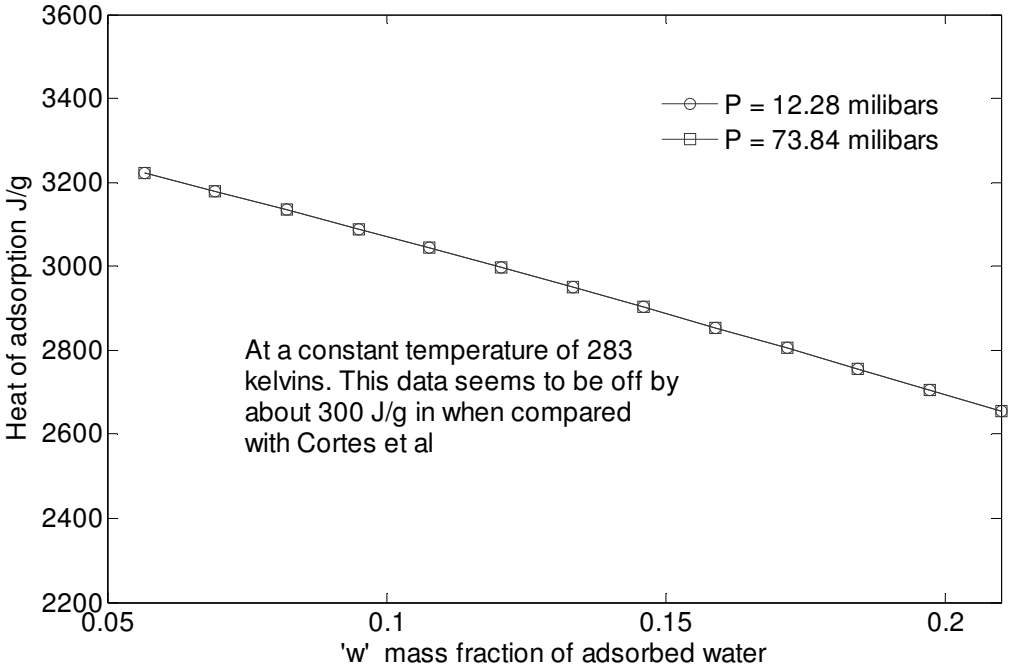

Fig. C-3 Isosteric heat o water zeolite 13X pair as obtained by equations 3.1-3.3

APPENDIX D Reliability of zeolite in the face of constant hydrothermal cycling.

Reliability of zeolite is important for the over all reliability of the TEA cooling system. Since the system must work without human interference or any maintenance issues, it must maintain a certain level of performance for a long time. In this regard the ability of zeolite as an adsorbent to retain its water adsorbing characteristics in the wake of constant hydro-thermal cycling is of vital importance.

In literature [112] it has been stated that Zeolite crystals are vulnerable in the view of high temperature and humidity. Their hydrothermal stability is a strong function of silicon/ aluminum ratio. The greater the amount of aluminum in a zeolite sample, more is the vulnerability of its crystal structure in the face of high temperature and humidity. For zeolite 13X the Si/Al ratio lies between 1-1.5. Type A zeolite (zeolite 4A has this ratio close to unity, whereas type Y zeolite have their Si/Al ratio varying from 1.5-3). Hydrothermal cycling tests on zeolite 4A and 13X were reported. The samples were subject to 725 two hour cycling during which the samples were repeatedly hydrated at room temperature and dehydrated at a temperature of 260 ^{0}C. Fig. D-1 plots the water content in the zeolite samples at similar temperature and pressure conditions, but after dehydration-hydration cycles. In comparison to 13X it appears that zeolite 4A is more resistant to hydrothermal ageing, however the data can not be considered consistent as one out of three zeolite 13X samples did not show much decay of water adsorption capability.

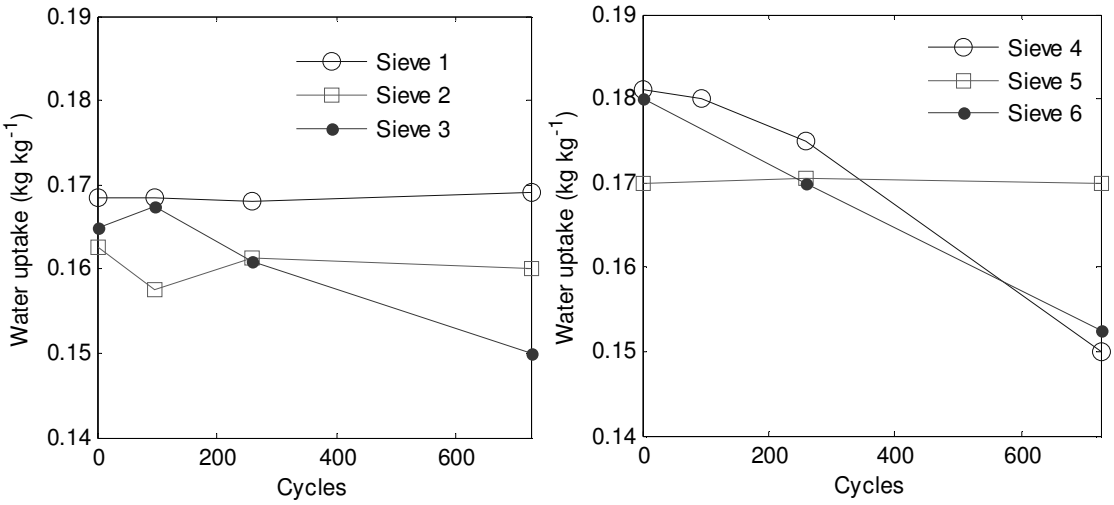

Fig. D-1 Effect of thermal cycling on water content of zeolite samples. Left figure is for zeolite 4A, right figure is for zeolite 13X. Plot based on data from literature [112].

In their work for measurement of thermal conductivity of zeolites, Griesinger et al [113] observed negligible change in thermo physical properties of zeolite after several cycles of hydration and dehydration.

Belding et al [114] have studied in detail the ageing of various desiccants with hydrothermal cycling and plotted the adsorption characteristic of several samples of zeolite 13X at different humidity of surrounding atmosphere and different ageing times. It was concluded that zeolite 13X offers better stability and less severe loss of water adsorption capacity when compared to other adsorbents such as silica gel.

During the experiments performed (as described in this dissertation), the degradation in performance was not noticeable due to the less number of thermal cycling involved, however , when observed under an scanning electron microscope, changes in the zeolite pellet matrix were observed. Fig. D-2 and Fig. D-3 present the photographs of a fresh and

used zeolite 13X sample. The used sample had undergone 16 hours of thermal cycling from 230 °C to 180 °C. Prominent differences were not observed in the two images.

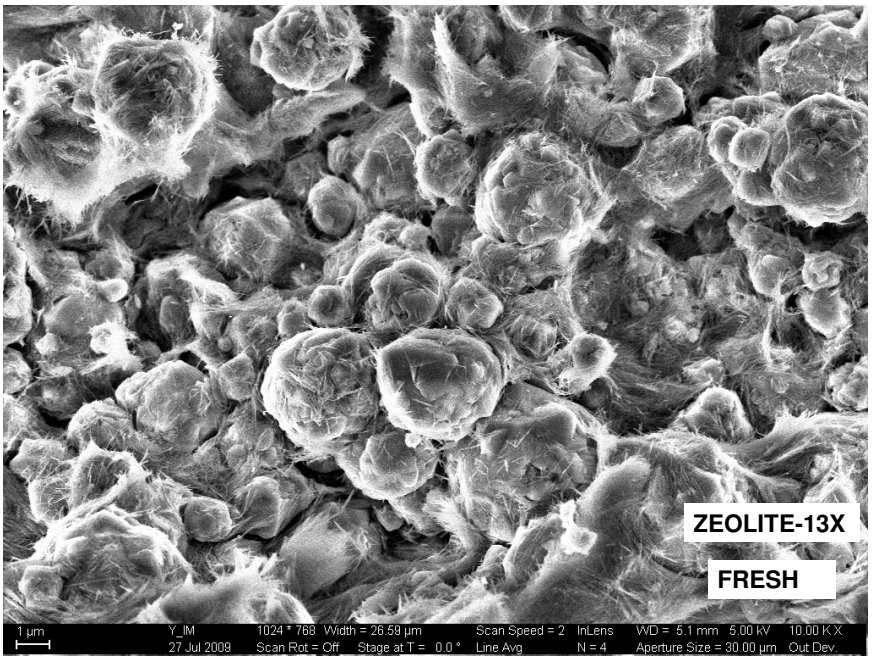

Fig. D-2: Scanning Electron Microscope image of a fresh zeolite-13X sample.

Fig. D-3: Scanning Electron Microscope image of a used zeolite sample.

APPENDIX E Heat loss through bed and evaporator insulation

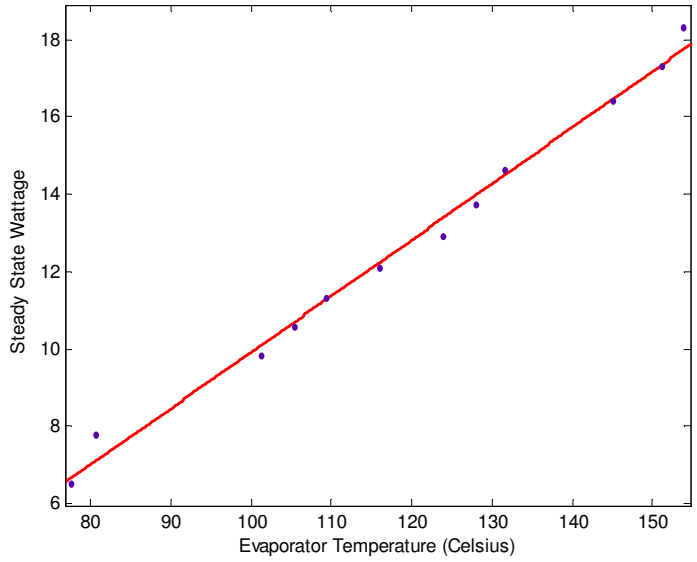

Fig. E-1 Plot showing steady state wattage required to maintain the evaporator at various steady state temperatures.

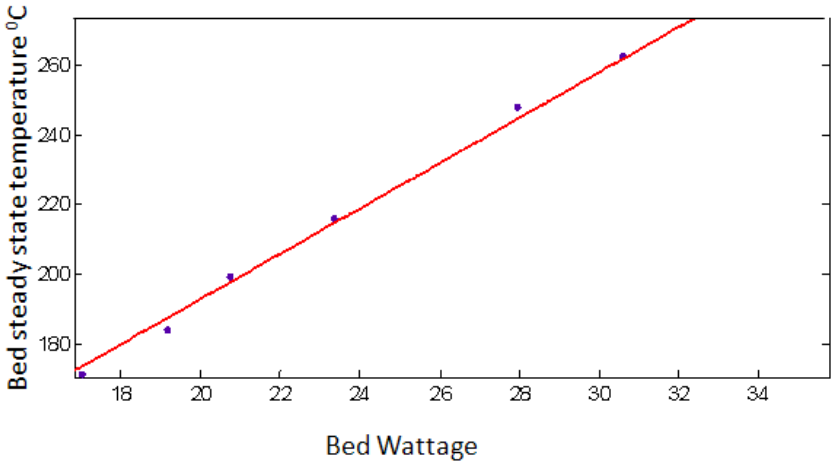

Fig. E-2 Plot showing the power supply in wattage required to maintain the beds at various steady state temperature.

APPENDIX F Algorithm for performance comparison of TE, TEA and Adsorption chillers

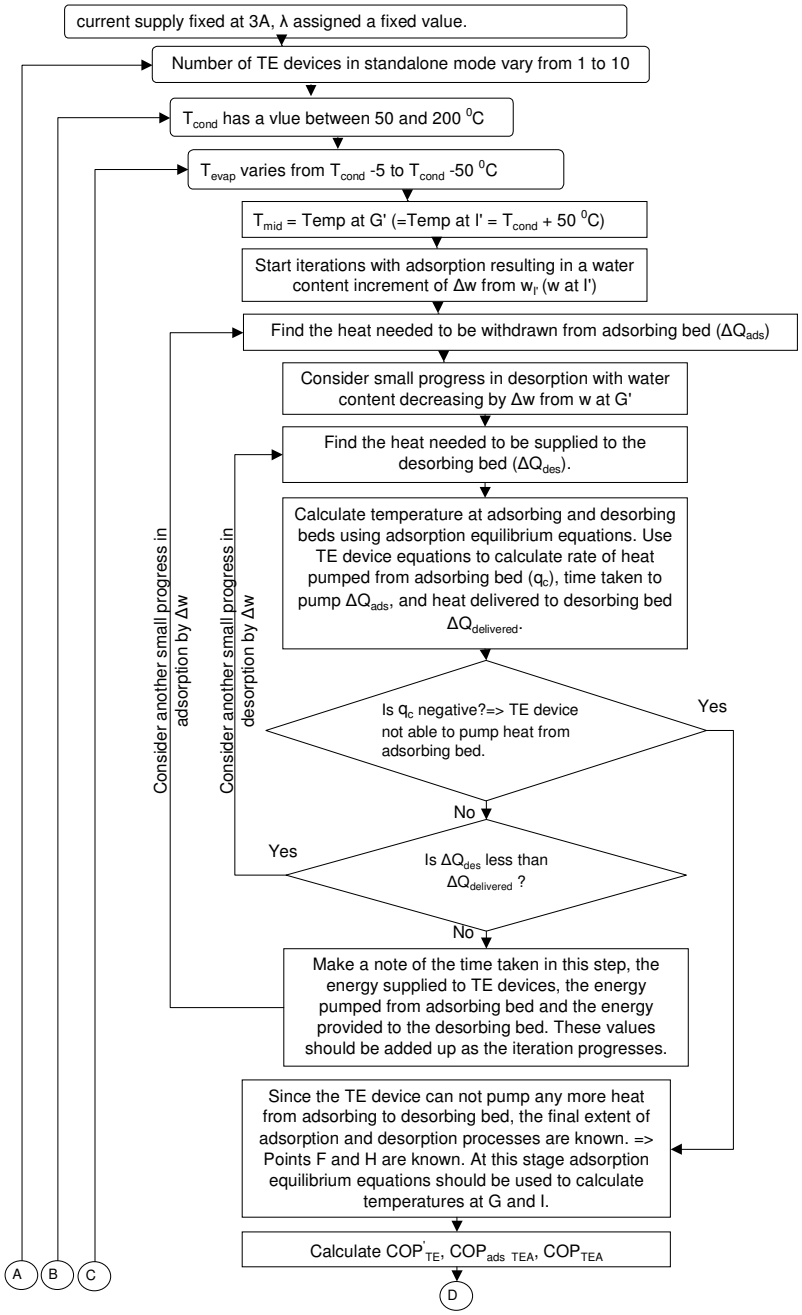

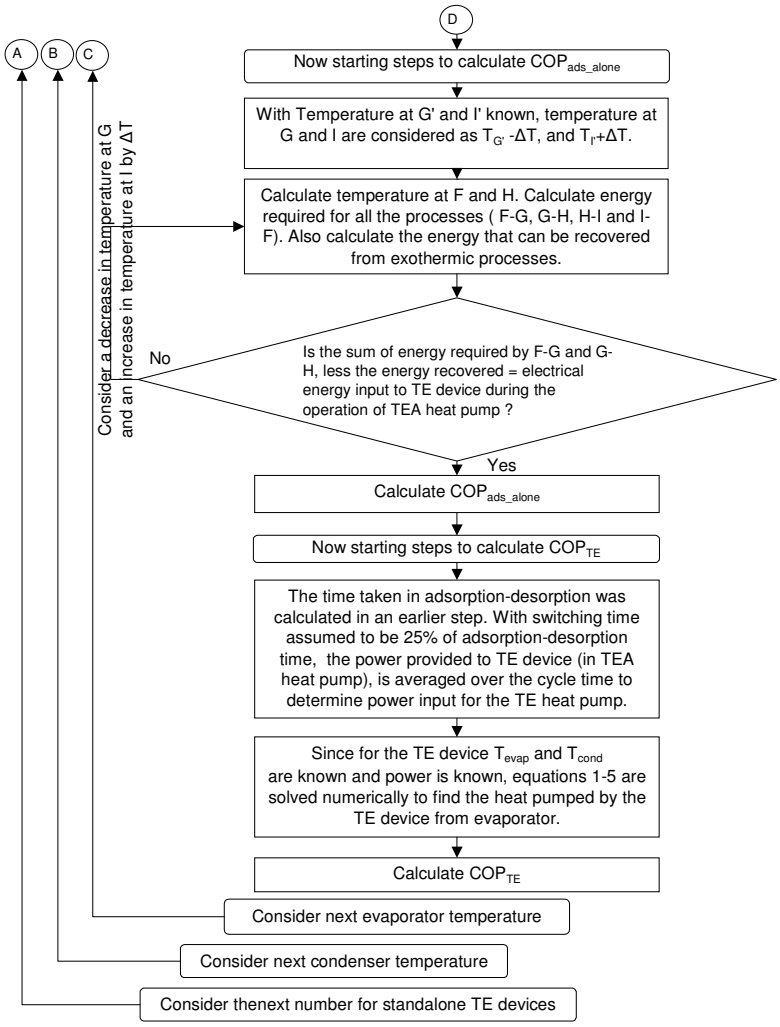

Fig. F-1 Flowchart describing method for mathematical computations.

References

[1] Braun, T., Becker, K. F., Sommer, J. P., Loher, T., Schottenloher, K., Kohl, R., Pufall, R., Bader, V., Koch, M., Aschenbrenner, R., Reichl, H., 2005, "High Temperature Potential of Flip Chip Assemblies for Automotive Applications", Proceedings of Electronic Components and Technology Conference, Vol 55, Issue 31, pp. 376-383.

[2] Werner, M. R., Fahrner, W. R., April 2001, "Review on Materials, Microsensors, Systems, and Devices for High-Temperature and Harsh-Environment Applications", IEEE Transactions on Industrial Electronics, Vol 48, No 2, pp, 249-257.

[3] Dreike, P.L., Fleetwood, D.M., King, D.B., Sprauer, D.C., Zipperian, T.E., 1994 "An Overview of High-Temperature Electronic Device Technologies and Potential Applications," IEEE Transactions on Components, Packaging, and Manufacturing Technology, Part A, Vol 17, Issue 4, pp 594- 609 ; Digital Object Identifier 10.1109/95.335047.

[4] Johnson, R. W., Evans, J. L., Jacobsen, P., Thompson, J. R., Christopher, M., 2004, "The Changing Automotive Environment: High-Temperature Electronics", IEEE Transactions on Electronics Packaging and Manufacturing., Vol 27, No 3, pp. 164-176.

[5] Deep Trek Workshop Proceedings 2001, National Energy Technology Laboratory. Available online at : http://www.netl.doe.gov/technologies/oil-gas/EP_Technologies/AdvancedDrilling/DeepTrek/index.html Last accessed 30th july 2010.

[6] James, P., Aug-Sept 2006, "Data Driven Drilling," Computing & Control Engineering Journal, Vol 17, Issue 4, pp 36-39.

[7] Boyes, J., June 1981, "The Eyes of the Oil Industry," Electronics and Power; Vol 27, Issue 6, pp 484-488; Digital Object Identifier 10.1049/ep.1981.0231

[8] Boyes, J., September 1981, "Erratum: The Eyes of the Oil Industry," Electronics and Power; Vol 27, Issue 9, pp 594, Digital Object Identifier 10.1049/ep.1981.0281

[9] Den Boer, J. J., July 1999, "The Use of High Temperature Electronics in Downhole Applications," The Third European Conference on High Temperature Electronics, HITEN 99, pp149-152, Digital Object Identifier; 10.1109/HITEN.1999.827480

[10] Traeger, R. K., Lysne, P. C., Feb 1988, "High Temperature Electronics Application in Well Logging," IEEE Transactions on Nuclear Science, Vol 35, Issue 1, Part 1-2, pp 852-854, Digital Object Identifier 10.1109/23.12845

[11] Anyuan, C., Ummaneni, R. B., Nilssen, R., Nysveen, A., Sept 2008, "Review of Electrical Machine in Downhole Applications and the Advantages," Power Electronics and Motion Control Conference, EPE-PEMC 13th, pp 799-803, Digital Object Identifier 10.1109/EPEPEMC.2008.4635365

[12] Cohen, J., Rogers, D. J., Malcore, E., Estep, J., 2002, "The Qwest for High Temperature MWD and LWD Tools," GasTIPS, GasTIPS is a publication of the Gas Technology Institute, US Department of Energy and Hart Energy Publishing.

[13] Tubel, P., Bergeron, C., Bell, S., 1992, "Mud Pulser Telemetry System for Down Hole Measurement-While-Drilling," Instrumentation and Measurement Technology Conference, IMTC '92, pp 219-223; Digital Object Identifier 10.1109/IMTC.1992.245147.

[14] Norman, J. H., 2001, "Non-Technical Guide to Petroleum Geology, Exploration, Drilling, and Production," Penn Well Corp. ISBN 0-87814-823-X

[15] McCluskey, F. P., Grzybowski, R., Podlesak, T., 1997, High Temperature Electronics, CRC Press, Chapter 1. ISBN 9780849396236

[16] Lall, P., Singh, N., Suhling, J.C., Strickland, M., Blanche, J, September 2005, "Thermo-Mechanical Reliability Tradeoffs for Deployment of Area Array Packages in Harsh Environments," Components and Packaging Technologies, IEEE Transactions on; Volume 28, Issue 3, pp 457-466; Digital Object Identifier 10.1109/TCAPT.2005.854162

[17] Braun, T., Becker, K.-F., Koch, M., Bader, V., Aschenbrenner, R., Reichl, H., January 2006, "High-Temperature Reliability of Flip Chip Assemblies," Microelectronics and Reliability, Volume 46, Issue 1, pp 144-154.

[18] Evans, J.L., Lall, P., Knight, R., Crain, E., Shete, T., Thompson, J.R., March 2008, "System Design Issues for Harsh Environment Electronics Employing Metal-Backed Laminate Substrates," Components and Packaging Technologies, IEEE Transactions on; Vol 31, Issue 1, pp 74 – 85, Digital Object Identifier 10.1109/TCAPT.2008.916792

[19] Chalker, P. R., April 1999, "Wide Bandgap Semiconductor Materials for High Temperature Electronics," Thin Solid Films, Volumes 343-344, pp 616-622.

[20] Bansal, S., Cho, J, Durocher, K., Kapusta, C., Knobloch, A., Shaddock, D., Schoeller, H., Xia, H., 2007, "Harsh-Environment Packaging for Down-hole Gas and Oil Exploration," A report prepared for: United States Department of

Energy; National Energy Technology Laboratory; by GE Global Research Center, Niskayuna NY 12118; November 18, 2007; Under DOE Award Number: DE-FC26-06NT42950; Last accessed at http://www.osti.gov/bridge/purl.cover.jsp?purl=/932889-XssxCt/ on 16th of October 2009.

[21] Grzybowski, R.R., 1998, "Advances in Electronic Packaging Technologies to Temperatures as High as 500°C," High-Temperature Electronic Materials, Devices and Sensors Conference, pp 207-215 ; Digital Object Identifier 10.1109/HTEMDS.1998.730699

[22] Mehregany, M., Zorman, C.A., Rajan, N., Chien Hung Wu., 1998, "Silicon Carbide MEMS for Harsh Environments," Proceedings of the IEEE; Volume 86, Issue 8, Aug. 1998 pp 1594-1609 ; Digital Object Identifier 10.1109/5.704265

[23] Normann, R. A., 2006, "First High-Temperature Electronics Product Survey 2005", Report by Sandia National Laboratories. Available from US department of Commerce National Technical Information Service. Online order can be placed at the following URL: http://www.ntis.gov/help/ordermethods.asp?loc=7-4-0#online

[24] Palmer, D. W., Heckman, R. C., 1978, "Extreme Temperature Range Microelectronics," IEEE Transactions on Components, Hybrids and Manufacturing Technology, CHMT-1(4), pp. 333-340.

[25] Stentoft, K., Petersen, M.L., January 2008, "Electronics in Harsh Environments-Product Verification and Validation," Reliability and maintainability symposium, RAMS, pp 456-462; Digital Object Identifier 10.1109/RAMS.2008.4925839

[26] Joshi, Y., Azar, Kaveh., Blackburn, D., Lasance, C. J. M., Mahajan, R., Rantala, J., 2003, "How Well can we Assess thermally Driven Reliability Issues in Electronic Systems Today? Summary of Panel Held at the Therminic 2002", Microelectronics Journal, 34, pp. 1195-1201.

[27] Krkac, O., Bilas, B., Ambrus, D., 2005, "Thermal Uprating of a Mixed Signal Microcontroller," Industrial Electronics, ISIE 2005. Proceedings of the IEEE International Symposium on; Volume 3, pp 1111-1116, Digital Object Identifier 10.1109/ISIE.2005.1529079

[28] Ohme, B., Feb 2007, "Deep Trek Re-configurable Processor for Data Acquisition (RPDA)," Report prepared for National Energy Technology Laboratory; U.S. Department of Energy; under DOE Award No.: DE-FC26-06NT42947; Available at http://www.netl.doe.gov/technologies/oilgas/publications/EPreports/NT42947_TSA.pdf Last accessed 16th October 2009

[29] Tarapata, G., Weremczuk1, J., Jachowicz1, R., Shan, X.C., Shi, C.W.P., 2009, "Construction of Wireless Sensor for Harsh Environment Operation," Proceedings of the Eurosensors XXIII conference; Procedia Chemistry 1 (2009) 465–468

[30] De Jong, P.C., Meijer, G.C.M., May 1999, "A Smart Accurate Pressure-Transducer for High-Temperature Applications [in Oil Wells]," Instrumentation and Measurement Technology Conference, IMTC/99. Proceedings of the 16th IEEE; Volume 1, pp 309-314, Digital Object Identifier 10.1109/IMTC.1999.776767

[31] Ambrus, D., Bilas, V., Vasic, D., May 2004, "A High-Temperature Low-Cost Rotational Speed Transducer for Oil-Well Telemetry," Instrumentation and Measurement Technology Conference, IMTC. Proceedings of the 21st IEEE; Volume 2, pp 1071-1074, Digital Object Identifier; 10.1109/IMTC.2004.1351248

[32] Ronald, A., Guidotti, F. W., Reinhardt, Judy Odinek., October 2004, "Overview of High-Temperature Batteries for Geothermal and Oil/Gas Borehole Power Sources," Journal of Power Sources, Volume 136, Issue 2, pp 257-262.

[33] Prazak, P R., May 1982, "A -55 to + 200°C 12-Bit Analog-to-Digital Converter," Industrial Electronics, IEEE Transactions on; Volume IE-29, Issue 2, pp 118-123, Digital Object Identifier 10.1109/TIE.1982.356647

[34] Longtin, J., Sampath, S., Tankiewicz, S., Gambino, R.J., Greenlaw, R.J., Feb 2004, "Sensors for Harsh Environments by Direct-Write Thermal Spray," Sensors Journal, IEEE; Volume 4, Issue 1, pp 118-121 ; Digital Object Identifier 10.1109/JSEN.2003.822218

[35] De Jong, P.C., Meijer, G.C.M., April 2000, "A High-Temperature Electronic System for Pressure-Transducers," Instrumentation and Measurement, IEEE Transactions on; Volume 49, Issue 2, pp 365-370 ; Digital Object Identifier 10.1109/19.843079

[36] Hussain, T., Micovic, M., Tsen, T., Delaney, M., Chow, D., Schmitz, A., Hashimoto, P., Wong, D., Moon, J. S., Hu, M., Duvall, J., McLaughlin, D., 2003, "GaN HFET Digital Circuit Technology for Harsh Environments," Electronics Letters, 39(24).

[37] Wondrak, W., Held, R., Niemann, E., Schmid, U., 2001, "SiC Devices for Advanced Power and High-Temperature Applications," IEEE Transactions on Industrial Electronics, 48(2), pp. 307-308.

[38] Ohadi, M., Qi, J., 2004, "Thermal Management of Harsh-Environment Electronics", 20th Annual IEEE Semiconductor Thermal Measurement and Management Symposium, pp. 231-240.

[39] ITRS (International Technology Roadmap for Semiconductors) Available online. http://www.itrs.net, (ITRS Edition reports and Ordering >2007 Update> Assembly and Packaging). Last accessed October 2008.

[40] Mahefkey, T., 1994, "Thermal Management of High Temperature Power Electronics Limitations and Technology", Proceedings of Second International High Temperature Electron Conference, Charlotte, NC, pp. IX-21-IX-2.

[41] Lamers et al, 1981, "Well Logging Evaporative Thermal Protection System," US Patent 4,248,298. Available online at www.uspto.gov

[42] Gordon, J. M., Ng, K. C., Chua, H. T., Chakraborty, A., 2002, "The Electro-Adsorption Chiller: A Miniaturized Cooling Cycle with Applications to Micro-Electronics," International Journal of Refrigeration, 25, pp. 1025-1033.

[43] Jeong, S., 2004, "How Difficult is it to Make a Micro Refrigerator?", Intl J of Refrigeration, 27, pp. 309-313.

[44] Khan, J., Zubair, S. M., 1999, "Design and performance evaluation of reciprocating refrigeration systems," International Journal of Refrigeration, Vol. 22, pp. 235-243

[45] Ng, K. C., Sai, M. A., Chakraborty, A., Saha, B. B., Koyama, S., 2006, "The Electro-Adsorption Chiller: Performance Rating of a Novel Miniaturized Cooling Cycle for Electronics Cooling," ASME Journal of Heat Transfer, Vol 128, pp. 889-896.

[46] Jakaboski, J. C., 2004, "Innovative Thermal Management of Electronics Used in Oil Well Logging", Master's thesis, Georgia Institute of Technology, Atlanta, http://etd.gatech.edu/theses/available/etd-05142004-111910/ Last accessed June 30, 2010.

[47] Bennett, G. A., 1992, "Compact Acoustic Refrigerator," US Patent 5,165,243. Available online at www.uspto.gov.

[48] Bennett, G. A., 1988, "Active Cooling for Downhole Instrumentation: Preliminary Analysis and System Selection," A report issued in public domain by Los Alamos National Laboratory. Available at http://www.osti.gov/bridge/purl.cover.jsp?purl=/5360643-5IxyoX/ Last accessed 15th October 2009.

[49] Ziegler, F., 2002, "State of the art in sorption heat pumping and cooling technologies," International journal of Refigeration, Vol. 25, pp. 450-459.

[50] Liu, Y., Leong, K. C., 2006, "Numerical Study of a Novel Cascading Adsorption

Cycle," International Journal of Refrigeration, 29, pp. 250-259.

[51] Anyanwu, E. E., Ogueke, N. V., 2005, "Thermodynamic Design Procedure for Solid Adsorption Solar Refrigerator," Renewable Energy, 30, pp. 81-96.

[52] Chahbani, M. H., Labidi, J., Paris, J., 2004, "Modeling of Adsorption Heat Pumps with Heat Regeneration," Applied Thermal Engineering, 24, pp. 431-447.

[53] Vasilev, L. L., Mishkinis, D. A., Antukh, A. A., Vasilev, Jr L. L., 2007, "Solar-Gas Solid Sorption Refrigerator," Kluwer Academic Publishers, Adsorption, 7, pp. 149-161.

[54] Dawoud, B., 2007, "A Hybrid Solar-Assisted Adsorption Cooling Unit for Vaccine Storage," Renewable Energy, 32, pp. 947-964.

[55] Yong, L., Sumathy, K., 2005, "Performance Analysis of a Continuous Multi-Bed Adsorption Rotary Cooling System," Applied Thermal Engineering, 25, pp. 393-407.

[56] Hajji, A., Worek, W. M., 1991, "Simulation of a Regenerative, Closed-Cycle Adsorption Cooling/ Heating System," Energy, 16, pp. 643-654.

[57] Critoph, R. E., 2001, "Simulation of a Continuous Multiple-Bed Regenerative Adsorption Cycle," International Journal of Refrigeration, 24, pp. 428-437.

[58] Critoph, R. E., 1998, "Forced Convection Adsorption Cycles," Applied Thermal Engineering, 18, pp. 799-807.

[59] Zhang, L. Z., 2000, "Design and Testing of an Automobile Waste Heat Adsorption Cooling System," Applied Thermal Engineering, 20, pp. 103-114.

[60] Sward, B. K., LeVan, M. D., Meunier, F., 2000, "Adsorption Heat Pump Modeling: The Thermal Wave Process with Local Equilibrium," Applied Thermal Engineering, 20, pp. 759-780.

[61] Restuccia, G., Cacciola, G., 1999, "Performances of Adsorption Systems for Ambient Heating and Air Conditioning," International Journal of Refrigeration, 22, pp. 18-26.

[62] VanBenthem, G. H. W., Cacciola, G., Restuccia, G., 1995, "Regenerative Adsorption Heat Pumps: Optimization of the Design," Heat Recovery Systems & CHP, 15, pp. 531-544.

[63] Wang, L. W., Wang, R. Z., Wu, J. Y., Xu, Y. X., Wang, S. G., 2006, "Design Simulation and Performance of a Waste Heat Driven Adsorption Ice Maker for Fishing Boat," Energy, 31, pp. 244-259.

[64] Liu, Y. L., Wang, R. Z., Xia, Z. Z., 2005, "Experimental Performance of a Silica Gel-Water Adsorption Chiller," Applied Thermal Engineering, 25, pp. 359-375.

[65] Lu, Y. Z., Wang, R. Z., Jianzhou, S., Xu, Y. X., Wu, J. Y., 2004, "Practical Experiments on an Adsorption Air Conditioner Powered by Exhausted Heat from a Diesel Locomotive," Applied thermal Engineering, Vol. 24, pp. 1051-1059.

[66] Wang, R. Z., 2001, "Performance Improvement of Adsorption Cooling by Heat and Mass Recovery Operation," International Journal of Refrigeration, 24, pp. 602-611.

[67] Szarzynski, S., Feng, Y., Pons, M., 1997, "Study of Different Internal Vapour Transports for Adsorption Cycles with Heat Regeneration," International Journal of Refrigeration, 20(6), pp. 390-401.

[68] Wang, S., Zhu, D., 2004, "Adsorption Heat Pump Using an Innovative Coupling Refrigeration Cycle", Adsorption (Kluwer Academic Publishers), 10: 47-55.

[69] Rowe, D. M., 1995, "CRC handbook of ThermoElectrics," Boca Raton, FL: CRC Press LLC. ISBN 0-8493-0146-7

[70] Simons, R, E., Ellsworth, M, J., Chu, R, C., 2005. An Assessment of Module Cooling Enhancement With Thermoelectric Cooler. ASME Journal of Heat Transfer. 127, 76-84.

[71] Laird Technologies (2010) Available online: http://www.lairdtech.com/Products/Thermoelectric-Solutions/. Last accessed: 30th June 2010.

[72] Nabi, A., Asias, A., 2005, "A Simple Experimental Technique for the Characterization of the Performance of Thermoelectric-coolers Beyond 100 ^{0}C," 21st IEEE SEMI-THERM Symposium. Digital Object Identifier: 10.1109/STHERM.2005.1412172

[73] Laird Technologies (2010) Available online: http://lairdtech.thomasnet.com/viewitems/thermoelectric-modules-2/thermatec-trade-series-thermoelectric-coolers?&bc=100|3001624|3001688|3001253&forward=1 . Last accessed: 30th June 2010.

[74] Marlow Industries (2010) Available online: http://www.marlow.com/power-generators/ . Last accessed: 30th June 2010.

[75] Cacciola, G., Hajji, A., Maggio, G., Restuccia, G., 1993, "Dynamic Simulation of a Recuperative Adsorption Heat Pump," Energy. Vol 18(11), pp 1125-1137.

[76] Cacciola, G., Restuccia, G.., 1995, "Reversible Adsorption Heat Pump: A Thermodynamic Model," International Journal of Refrigeration, 18(2), pp. 100-106.

[77] Cho, S., Kim, J., 1992, "Modeling of a Silica Gel/Water Adsorption Cooling System," Energy, Vol 17, No 9, pp 829-839.

[78] Hamamoto, Y., Alam, K. C. A., Saha, B. B., Koyama, S., Akisawa, A., Kashiwagi, T., 2006, "Study on Adsorption Refrigeration Cycle Utilizing Activated Carbon Fibers. Part 2. Cycle Performance Evaluation," International Journal of Refrigeration, 29, pp. 315-327.

[79] Qiu, L., Murashov, V., White, M. A., 2000, "Zeolite 4A: Heat Capacity and Thermodynamic Properties," Solid State Sciences, 2, pp. 841-846.

[80] McLinden, M.O., Klein, S., Lemmon, E., Peskin, A., 1998, "NIST Thermodynamic and Transport Properties of Refrigerants and Refrigerant Mixtures Database (REFPROP)," Version 6.0. National Institute of Standards and Technology, Gaithersburg, Maryland, USA.

[81] Coggins, C. Lee., 2007, "Single-and Multiple-Stage Cascaded Vapor Compression Refrigeration for Electronics Cooling", Masters Thesis, Georgia Institute of Technology, Atlanta, http://etd.gatech.edu/theses/available/etd-05082007-184545/unrestricted/coggins_charles_l_200708_mast.pdf Last accesses: 7th July 2010.

[82] Sinha, A., Joshi, Y. K., 2009, "Performance of Thermoelectric Based Regenerative Adsorption Cooling System For Harsh Environment," ASME IMECE Conference, Orlando, FL.

[83] http://www.grace.com/Products/Sylobead/ last accessed 7th August 2010.

[84] http://www.coastalchem.com/PDFs/Grace%20Davison/Sylobead%20514.pdf last accessed 7th August 2010.

[85] http://www.bergquistcompany.com/thermal_materials/gap_pad/gap-pad-5000S35.htm last accessed 7th August 2010.

[86] http://www.heat-transfer-fluid.com/pdf/safetydata/heattransfer/duratherm-g_msds.pdflast accessed 7th August 2010.

[87] Mugnier, D., Goetz, V., 2001, "Energy Storage Comparison of Sorption Systems for Cooling and Refrigeration," Solar Energy, Vol. 71, No. 1, pp. 47-55

[88] Chao, S., Kim, J., 1992, "Modeling of a Silica Gel/Water Adsorption-Cooling System," Energy, Vol. 17, No. 9, pp. 829-839

[89] Zhang, L. Z., Wang, L., 1997, "Performance Estimation of an Adsorption Cooling System for Automobile Waste Heat Recovery," Applied Thermal Engineering, Vol. 17, No. 12, pp. 1127-1139

[90] Chua, H. T., Ng, K. C., Wang, W., Yap, C. Wang, X. L., 2004, "Transient modeling of a two-bed silica gel-water adsorption chiller," International Journal of Heat and Mass transfer, Vol. 47, pp. 659-669

[91] Chua, H. T., Ng, K. C., Malek, A., Kashiwagi, T., Akisawa, A., Saha, B. B., 1999, "Modeling the performance of two-bed, silica gel-water adsorption chillers," International journal of Refrigeration, Vol. 22, pp. 194-204

[92] Alam, K. C. A., Kang, Y. T., Saha, B. B., Akisawa, A., Kashiwagi, T., 2003, "A novel approach to determine optimum switching frequency of a conventional adsorption chiller," Energy, Vol. 28, pp. 1021-1037

[93] Hajji, A., Cacciola, G., Restuccia, G., 1994, "Experimental and Theoretical Study of a Constant Volume Adsorption Process," Energy, Vol. 19, No. 9, pp. 961-965

[94] Hajji, A., Khalloufi, S., 1995, "Theoretical and experimental investigation of a constant-pressure adsorption process," International Journal of Heat and Mass Transfer, Vol. 38, No. 18, pp. 3349-3358

[95] Hajji, A., Khalloufi, S., 1996, "Improving the performance of adsorption heat exchangers using a finned structure," International Journal of Heat and Mass Transfer, Vol. 39, No. 8, pp. 1677-1686

[96] Zhang , L. Z., Wang, L., 1999, "Momentum and heat transfer in the adsorbent of a waste-heat adsorption cooling system," Energy, Vol. 24, pp. 605-624

[97] Sircar, S., Hufton, J. R., 2000, "Why Does the Linear Driving Force Model for Adsorption Kinetics Work?," Adsorption, Vol. 6, pp. 137-147

[98] Chu, R, C., Simons, R, E., 1999. Application of Thermoelectrics to Cooling Electronics: Review and Prospects. Eighteenth International Conference on Thermoelectrics. 270-279. Digital Object Identifier 10.1109/ICT.1999.843385.

[99] Simons, R, E., Ellsworth, M, J., Chu, R, C., 2005. An Assessment of Module Cooling Enhancement With Thermoelectric Cooler. ASME Journal of Heat Transfer. 127, 76-84.

[100] Lakhkar, N., Hossain, M., Agonafer, D., 2008. CFD Modeling of a Thermoelectric Device for Electronics Cooling Applications. ITHERM: 11th Intersociety Conference on Thermal and Thermomechanical Phenomena in Electronic Systems. 889-895. Digital Object Identifier 10.1109/ITHERM.2008.4544360

[101] Vandersande, J.W., Fleurial, J, P., 1996. Thermal Management of Power Electronics Using Thermoelectric Coolers. Fifteenth International Conference on Thermoelectrics. 252-255. Digital Object Identifier 10.1109/ICT.1996.553311

[102] Sahu, V., Joshi, Y, K., Fedorov, A, G., 2009. Hybrid Solid State/Fluidic Cooling for Hot Spot Removal. Nanoscale and Microscale Thermophysical Engineering. 13(3), 135-150.

[103] Moores, K.A., Joshi, Y.K., Miller, G., 1999. Performance Assessment of Thermoelectric Coolers for use in High Temperature Electronics Applications. Eighteenth International Conference on Thermoelectrics. 31-34. Digital Object Identifier 10.1109/ICT.1999.843328.

[104] Nie, Q., Joshi, Y. K., 2008. Reduced Order Modeling of Power Electronics Cabinet With Double-Sided Cooling. ITHERM. Digital Object Identifier: 10.1109/ITHERM.2008.4544266

[105] Suman, S. K., Fedorov, A. G., Joshi, Y. K., 2006. Regenerative Fluid Loop Concept for Performance Enhancement of Adsorption Refrigeration System. ITHERM Conference, Digital Object Identifier: 10.1109/ITHERM.2006.1645420

[106] Fleurial, J. P., Borshchevsky, A., Caillat, T., Ewell, R., 1997. New Materials and Devices for Thermoelectric Applications. Energy Conversion Engineering Conference, IECEC-97. Proceedings of the 32nd Intersociety. 2, 1080-1085. Digital Object Identifier 10.1109/IECEC.1997.661920

[107] Venkatasubramanian, R., Siivola, E., Colpitts, T., O'Quinn, B., 2001. Thin-Film Thermoelectric Devices with High Room-Temperature. Figures of Merit. NATURE |VOL 413 | 11 OCTOBER 2001.

[108] Holman, J. P., "Experimental Methods for Engineers," 7th Edition. Mc-Graw Hill series in Mechanical Engineering. ISBN: 0-07-366055-8.

[109] Treacy, M. J. M., Higgins, J. B., 2001, "Collection of Simulated XRD Powder Patterns for Zeolites," Published by Elsevier on Behalf of International Zeolite Association, Fourth Revised Edition. Available online at http://www.iza-structure.org/databases/books/Collection_4ed.pdf Last visited 13th July 2010.

[110] Wajima, T., Ikegami, Y., 2009, "Synthesis of Crystalline Zeolite-13X from Waste Porcelain using Alkali Fusion," Ceramics International, Vol 35, pp 2983-2986.

[111] Cortes, F. B., Chejne, F., Carrasco-Marin, F., Moreno-Castilla, C., Perez-Cadenas, A. F., 2010, "Water Adsorption on Zeolite 13X: Comparison of the Two Methods Based on Mass Spectrometry and Thermogravimetry," Adsorption, DOI 10.1007/s10450-010-9206-5

[112] Ruthven, D. M., 1984, "Principles of Adsorption and Adsorption Processes," John Wiley and Sons Inc. ISBN 0-471-86606-7

[113] Griesinger, A., Spindler, K., Hahne, E., 1999, "Measurements and Theoretical Modelling of the Effective Thermal Conductivity of Zeolites," International Journal of Heat and Mass Transfer, Vol 42, pp 44363-4374.

[114] Belding, W. A., Delmas, M. P. F., Holeman, W. D., 1996, "Desiccant Aging and its Effects on Desiccant Cooling System Performance," Applied Thermal Engineering, Vol. 16, No. 5, pp. 447-459

[115] Bhatt, M. S., Srinivasan, K., Murthy, M. V. K., Seetharamu, S., 1992, "Thermodynamic Modelling of Absorption-resorption Heating Cycles With Some New Working Pairs," Heat Recovery Systems and CHP, Vol. 12, NO. 3, pp. 225-233.

[116] Chalaev, D. M., Aristov, Y. I., 2006, "Assessment of the Operation of a Low-Temperature Adsorption Refrigerator," Thermal Engineering, Vol. 53, No. 3, pp. 240-244.

[117] Critoph, R. E., Vogel, R., 1986, "Possible adsorption pairs for use in solar cooling," International Journal of Ambient Energy, Vol. 7, No. 4, pp. 183-190